Review

A Comprehensive Review of Piezoelectric PVDF Polymer Fabrications and Characteristics

Nadia Ahbab , Sidra Naz , Tian-Bing Xu * , Shihai Zhang

Posted Date: 2 January 2025

doi: 10.20944/preprints202501.0023.v1

Keywords: Piezoelectric; poly(vinylidene fluoride); Material properties; Fabrication; Characterizations

Review

A Comprehensive Review of Piezoelectric PVDF Polymer Fabrications and Characteristics

Nadia Ahbab [1], Sidra Naz [1], Tian-Bing Xu [1,*] and Shihai Zhang [2]

[1] Department of Mechanical Engineering and Aerospace, Old Dominion University, Norfolk, VA, USA

[2] PolyK Technologies, LLC, 2124 Old Gatesburg Road; State College, PA 16803, USA

* Correspondence: txxu@odu.edu

Abstract: Polyvinylidene fluoride (PVDF) polymer films, renowned for their exceptional piezoelectric, pyroelectric, and ferroelectric properties, offer a versatile platform for the development of cutting-edge micro-scale functional devices, enabling innovative applications in fields ranging from energy harvesting and sensing to medical diagnostics and actuation. This paper offers an in-depth review of the material properties, fabrication methodologies, and characterization of PVDF films. Initially, a comprehensive description of the physical, mechanical, chemical, thermal, electrical, and electromechanical properties is provided. The unique combination of piezoelectric, pyroelectric, and ferroelectric properties, coupled with its excellent chemical resistance and mechanical strength, makes PVDF a highly valuable material for a wide range of applications. Subsequently, the fabrication techniques, phase transitions and achievement methods, their copolymerization and composited that employed to improve and optimize the PVDF properties are elaborated. Enhancing phase transition in PVDF films, especially promoting the high-performance β-phase, can be achieved through various processing techniques, leading to significantly enhanced piezoelectric and pyroelectric properties essential for diverse applications. This concludes the discussion of PVDF material characterization and its associated techniques for thermal, crystal structure, mechanical, electrical, ferroelectric, piezoelectric, electromechanical, and pyroelectric properties, which provide crucial insights into the material properties of PVDF films, directly impacting their performance in applications. By understanding these aspects, researchers and engineers can gain valuable insights into optimizing PVDF-based devices for various applications, including energy harvesting, sensing, and biomedical devices, driving advancements in these fields.

Keywords: piezoelectric; poly(vinsylidene fluoride); material properties; fabrication; characterizations

1. Introduction

Over the past half centry, polymer-based piezoelectric materials [1] have gained significant interest in sensors[2], actuators[3], and energy harvesting[4]. Among these materials, polyvinylidene fluoride (PVDF) and its copolymers have emerged as highly valuable due to their unique combination of properties[5]. PVDF, with the molecular formula $(CH_2\text{-}CF_2)_n$, is a non-reactive thermoplastic known for its exceptional thermal, chemical, elastic, piezoelectric, and pyroelectric properties[6]. It is known for maintaining performance across a wide range of demanding environments, making it a versatile material for various advanced applications[7].

PVDF exhibits multiple crystalline phases, including the α-phase, β-phase, γ-phase, and δ-phase, each with distinct properties[8–9]. The α-phase is the most stable and is characterized by non-polar chains, making it less favorable for piezoelectric applications [10]. In contrast, the β-phase, which is polar and has an all-trans configuration, is highly desirable due to its superior piezoelectric properties[11–12]. The γ-phase[13–14] and δ-phase[15] offer intermediate characteristics, with the γ-phase being partially polar and the δ-phase less common and less studied.

 doi:10.20944/preprints202501.0023.v1

The discovery of piezoelectricity by the Curie brothers in 1880 laid the foundation for the development of numerous piezoelectric materials, including PVDF [16] . Although their discovery was not specific to PVDF, it opened the door to research into various materials exhibiting this property. The piezoelectric properties of PVDF were first recognized in the late 1960s, with significant advancements soon following. In 1969, Kawai[17] demonstrated PVDF's remarkable piezoelectric performance, which was considered superior to other synthetic polymers at that time. This breakthrough spurred extensive research into PVDF and its copolymers, leading to the development of ultrasonic and electroacoustic actuators in the early 1970s [18] .

In 1990s and earlier 2000, droving by U.S. DoD ultrasonic transducer and robostic programs[19–22] as well as the NASA morphing program [23–26], the electroactive properties of various PVDF and its copolymers have been studtied intensively. These historical developments have significantly influenced current research trends, particularly the focus on enhancing the β-phase of PVDF [27–29], which is associated with superior piezoelectric properties. The ability to control the crystalline phase of PVDF through precise processing techniques, such as mechanical stretching [30], annealing[31], and poling[32], has become a central aspect of modern PVDF research. These techniques are crucial for optimizing the material's piezoelectric performance and expanding its application scope, which will be explored in detail in later sections.

PVDF's copolymers, such as Poly (vinylidene fluoride-co-hexafluoropropylene) (Poly (VDF-co-HFP))[33], Poly (vinylidene fluoride-co-trifluoroethylene) (Poly (VDF-co-TrFE)) [34], and Poly (vinylidene fluoride-co-chlorotrifluoroethylene) (Poly (VDF-co-CTFE))[35], further enhance its functionality by offering tailored properties for specific uses. These materials combine flexibility, chemical inertness, and a wide frequency response range, making them ideal for demanding environments such as nuclear power[36] aerospace[37], automotive[38], and biomedical[39], industries.

Recent two decades, motivated by U.S. nano initiative, many researchers have made great efforts on developing PVDF based various nano concopiste materirals. [40] Efforts have been focused on developing nanocomposites[40] by introducing high dielectric constant fillers, such as ceramics, semiconductors, metal particles[41], graphene[42], and carbon nanotubes (CNT)[43], into the PVDF matrix. These nanocomposites have significantly expanded the application range of PVDF, particularly in fields where high performance and durability are crucial, such as aerospace [37], automotive[44], construction[45]. The modification of dielectric properties through nanocomposites has enhanced PVDF's applicability in these sectors by improving its mechanical and electrical characteristics.

Despite having lower piezoelectricity compared to commonly used materials like lead zirconate titanate (PZT)[46] , PVDF and its copolymers offer several advantages, including lightweight, low acoustic impedance, ease of fabrication, and chemical resistance. These benefits contribute to PVDF's broad applicability across diverse industries, including electronics [47], radio engineering, civial inferencestructure healthy moninoring, architecture, and pharmaceuticals.

To ensure polyvinylidene fluoride's (PVDF) optimal performance in a range of applications, it is essential to fully define its structural, electrical, and piezoelectric properties. Differential scanning calorimetry (DSC) [48], Raman spectroscopy [49], Fourier transform infrared spectroscopy (FTIR) [50], and X-ray diffraction (XRD)[51] are among the techniques commonly used to analyze the phase conformation and crystalline structure of PVDF. Scanning electron microscopy (SEM) [52], provides information on its shape and microstructure. Piezoelectric and dielectric properties are assessed using a variety of methods, including dynamic [53] and quasi-static testing [54] for piezoelectric coefficients, dielectric constant tests, and piezoresponse force microscopy (PFM) . Together, these techniques maximize PVDF for complex functional applications. In addition, PVDF and its copolymer not only exhibit excellent ferroelectric properties for sensing, actuation, and transduction applications [19,20,23,25], [55–56], but are also highly chemical resistant and relatively inert with very low surface energy that little can stick to [57–59]. Therefore, PVDF occupied 54% of PV back sheet market share [57]. The low surface energy means that PVDF materials readily can shed dirt and grime

 doi:10.20944/preprints202501.0023.v1

and easily clean off any kind of wet or dry dust/soil for transparency surface coading and other future applications.

Although many review papers on PVDF-based materials have been published [2,7], [60–66], there is a gap on comprehensive review on i) various material properties for device engineering and developers, ii) comprehensive review various characterization methosd for materials scientists, and iii) material property modifications for other resreachers.

This Paper is organize as follow: section 2 highlights the major material properties of PVDF polymers including physical, ssmechanical, chemical, thermal, electrical, and electromechanical properties. Section 3 provides a detailed description of fabrication methods, phase transition techniques including stretching, annealing, and poling used for enhancement of PVDF films. Moreover it provide details about copolymerization of PVDF with various material and its important composits. Section 4 provides PVDF films characterization techniques including FTIR, XRD, SEM, DSC etc. At the end, a summary of the overall paper is described.

2. Materials Properties

Material properties have been continuously investigated by researchers to understand and modify them for improved processing and functional performance. This section outlines the key properties of PVDF shown Figure 1 and compares various processing techniques, discussing their relative advantages and disadvantages in optimizing PVDF's performance. Figures and tables are referenced to support these discussions.

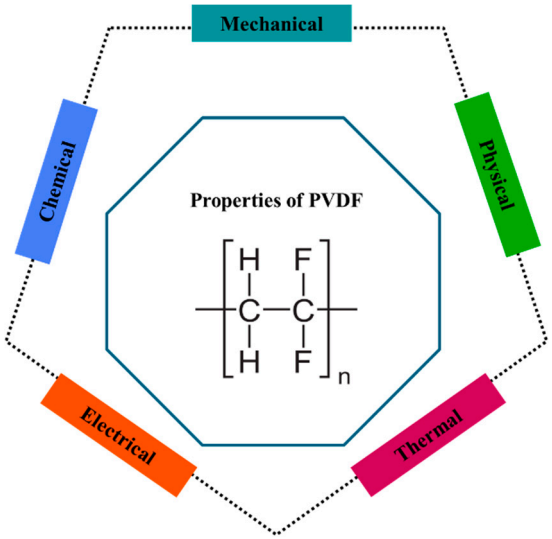

Figure 1. Different properties of PVDF piezoelectric.

2.1. Physical Properties

PVDF is an opaque resin with an extreme melting point (170-180°C), allowing it to tolerate high temperatures without substantial deterioration. Control over its optical properties, such as transparency, haze, and clarity, is crucial for specific applications. The fundamental cause of limited visible-wavelength transmission and significant mist in PVDF is its rough surfaces. It has a density of about 1.78 g/cm which can increase to 1.97 g/cm^3 with β orientation of PVDF to 1.97 g/cm^3, because of a greater level of crystallinity and higher density of packing. PVDF is characterized by its low weight and remarkable flexibility, which allows it to be readily molded into various shapes.

 doi:10.20944/preprints202501.0023.v1

2.1.1. Crystaline Structure of PVDF

In most cases, the primary factor driving variations in the molecular group's crystal structures is a single bond's internal configurations and rotations [30]. As a semi-crystalline piezoelectric polymer, PVDF's structure is determined by the configuration of its chains (gauche and trans) and the orientation of adjacent chains. PVDF can crystallize into nine distinct forms, grouped into five primary phases: alpha (α) [10], beta (β) [67–68], gamma (γ)[13–14], and delta (δ)[15], with the ε-phase [69] being less common corresponding to I, II, III, and IV, corresponding. Among these, the α, β, and γ phases are the most significant for practical applications, each offering distinct thermal, electrical, and mechanical properties. These nine crystal forms can be classified into four classes: I, II, III, and IV, corresponding to alpha (α)[70], beta (β) [71–74], gamma (γ) [75–76], delta (δ) [77] and epsilon (ε) crystal phases [78] . Among these, the α, β, and γ phases are the most significant, while the epsilon (ε) and delta (δ) phases are harder to isolate and are not typically produced through conventional methods. Each crystalline phase has distinct thermal, electrical, and elastic properties, as illustrated in Figure 2.

The α-phase is non-polar and electrically inactive, directly obtained from the molten state, aditionally it is thermodynamically unstable. It features two anti-parallel chains in a TGTG'(Trans-Gauche-Trans-Gauche) configuration[11,79]. In contrast, the β-phase is electroactive, exhibiting strong ferroelectric and piezoelectric behavior[80]. Its all-trans planar zigzag conformation separates most fluorine atoms from hydrogen atoms, resulting in the maximum dipole instant for each unit cell measures 8 $\times 10^{-30}$ cm among all phases. This phase also generates a substantial polarization that occurs naturally due to dipole moment addition[38].

The dipole moments of the γ and δ phases are fewer and weaker compared to the β-phase, but they still possess polar unit cells. The γ-phase, an uncommon state between α and β, has a T3GT3G' configuration with a higher trans fraction. A crucial difference between the α and δ phases lies in the orientation of dipolar moments within the unit cell: in the δ-phase, they are parallel, whereas in the α-phase, they are antiparallel. The δ-phase, characterized by a TGTG' (trans-gauche-trans-gauche) structure, can be transformed into β-phase material through the application of a high external electric field, ranging from (100 to 500 MV/m)[11], [79].

For many PVDF-based piezoelectric applications, it is essential to achieve high electrical conductivity, dielectric permittivity, low dielectric loss, and high breakdown strength. Optimizing the β-phase significantly improves PVDF's dielectric and piezoelectric properties, making it highly effective for a range of applications.

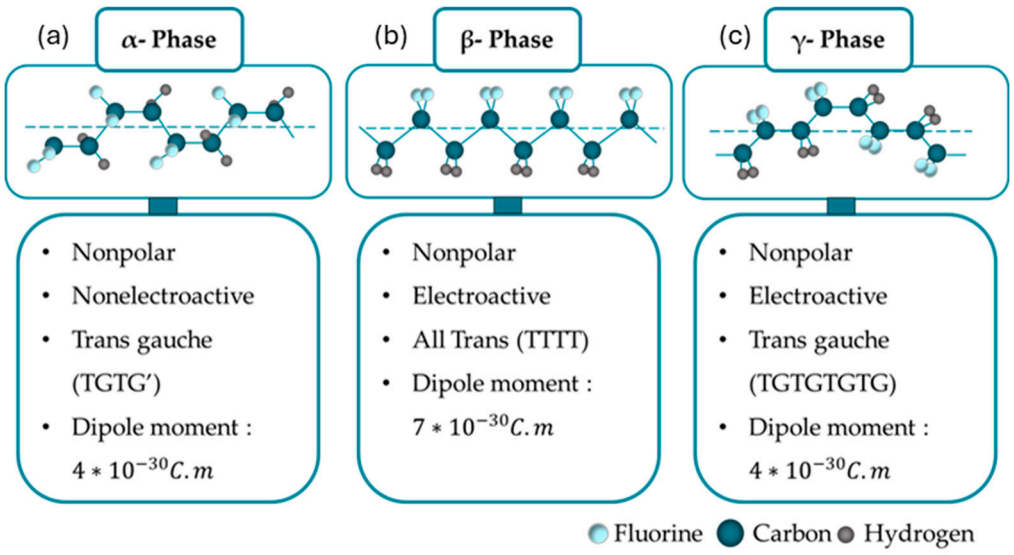

Figure 2. Different phases of PVDF and their properties. (a) α-phase, (b) β-phase, and (c) γ-phase. Redrwed refer to reference [79].

 doi:10.20944/preprints202501.0023.v1

2.2. Mechanical Properties

Polyvinylidene fluoride (PVDF) is a versatile polymer known for its excellent mechanical properties, making it suitable for a wide range of applications. The mechanical properties of PVDF film includes tensile strength, elongation at break, young's modulus, Yield Strength, and, Impact Strength. Tensile strength is the maximum stress of a material that can withstand before breaking under tensile stress. Its units are pascals (Pa) or megapascals (MPa). A higher tensile strength indicates better resistance to breaking or tearing. PVDF exhibits excellent tensile strength, meaning it can withstand significant pulling forces before breaking. This property is crucial for applications requiring high mechanical stress, such as structural components and protective coatings.

Elongation at break is the maximum amount of strain of a material which can withstand before breaking. It is presented in percentage (%). A higher elongation at break indicates better ductility and flexibility. PVDF also demonstrates good elongation at break, indicating its flexibility and ability to deform under stress without fracturing. This characteristic makes it suitable for applications that involve bending or flexing. Young's modulus is another mechanical propertity, which is a measurement of the stiffness of a material. It represents the ratio of stress to strain in the elastic region which units are pascals (Pa) or gigapascals (GPa). A higher young's modulus indicates a stiffer material. Yield strength is the stress at which a material begins to deform plastically. Pascals (Pa) or Megapascals (MPa) are the units of yield strength. A higher yield strength indicates better resistance to plastic deformation.

Impact Strength is the ability of a material to resist sudden impact forces. Its unit is joules per meter (J/m) or foot-pound per inch (ft-lb/in). A higher impact strength indicates better resistance to shock and impact loads. PVDF possesses excellent impact resistance, making it capable of withstanding sudden shocks and impacts. This property is particularly valuable in applications where the material may be subjected to accidental drops or collisions. PVDF exhibits good fatigue resistance, which is meaning it can withstand repeated cycles of stress without experiencing significant degradation. This property is essential for applications that involve continuous or cyclic loading. PVDF also demonstrates excellent creep resistance, indicating its ability to maintain its shape and dimensions over time under constant load. This property is crucial for applications requiring long-term dimensional stability. Besides all these properties PVDF has a high melting point and excellent thermal stability, allowing it to withstand high temperatures without significant degradation. This property makes it suitable for applications in harsh environments. Specific equations for calculating these mechanical properties can be complex and often require experimental data, some fundamental concepts can be expressed mathematically I equations (1-2).

$$\text{Stress } (\sigma) = F/A(\text{Pa}), \quad (1)$$

$$\text{Strain } (\varepsilon) = \Delta L/L_0 \quad (2)$$

Where F symbolize the applied force (Newton), A is the cross-sectional area (m^2), ΔL represents change in length (m),and L_0 is the original length (m). The factors that influence mechanical properties of PVDF includes molecular weight, crystallinity, processing techniques, and post-processing treatments. Higher molecular weight, and crystallinity improves mechanical properties like tensile strength and modulus. Processing techniques like extrusion and molding can influence the final properties. The post processing techniques like stretching and annealing can further enhance the mechanical properties. PVDF is frequently employed to coat the outside surfaces of buildings since it exhibits little to no degradation in mechanical qualities over several decades of outdoor use. Among traditional crystalline polymers, PVDF is particularly notable for its mechanical qualities. It has the greatest impact strength, a significant coefficient of curing, and is ranked second after polyoxymethylene on the basis of the degree of hardness, tensile strength, compressive stress, and flexural stress stiffness[62].The various properties of PVDF are provided in Table 1.

 doi:10.20944/preprints202501.0023.v1

Table 1. List of major properties with parameters of PVDF[81–82].

Properties	Parameters	PVDF example values
Physical	Density (g/cm³)	1.78
	Material color	transparent resin without color
	Water absorption %	0.02 - 0.07
	Refraction Index (N_D)	1.40 - 1.42
	Oxygen Index (%)	42 - 44
Mechanical	Tensile strength @ 23°C (MPa)	35–55
	Hardness, Shore D	50 - 80
	Young's modulus @ 23°C (MPa)	1340–2000
	Permittivity of free space(F/m)	ε_0= 8.854*10^{-12}
	Elastic constant N/m²	C_{11} =2.184*10^9 C_{12}=0.633*10^9
Piezoelectric	Curie temperature 80°C	d_{31} = 20–30
	Strain constant d (10^{-12} C/N)	d_{33} = -30
	Stress constant (10^{-3} mV/N)	g_{33}=335
	Volume resistivity (Ω – cm)	10^{15} -2.0 × 10^{14}
Thermal	Melting Point °C	177
	Defection temperature °C(261 psi)	114–118
	Flammability	V-O
	Thermal expansion coefficient(μm/m-°C)	10^{-4}
	Decomposition Temp (°C)	375
	Thermal Conductivity (W/m - K)	0.144 - 0.2
	Glass transition temperature, °C	−35
	Flammability°C	V-O

2.3. Chemical Properties

A substance's solubility is affected by its chemical and physical characteristics, as well as by external variables like temperature, pressure, and the presence of other chemicals in the solution. PVDF, an organic polymer, follows the "like-dissolves-like" rule, with polarity playing a key role. PVDF is soluble in a few organic solvents, such as dimethylformamide (DMF), dimethyl sulfoxide (DMSO), N-methyl pyrrolidone (NMP), and dimethylacetamide (DMAc), but is generally insoluble in aliphatic compounds, aromatic compounds, chlorine solutions, alcohols, strong acids, halogens, and basic solutions. PVDF copolymers tend to be slightly more soluble due to lower crystallinity[36]. PVDF is recognized for its excellent chemical resistance, making it suitable for harsh environments. However, it reacts negatively with many ketones, esters, and strong alkalis[83]. Over time, the properties of PVDF are weakened by exposure to strong alkaline solutions [84].

For example, NaOH can cause discoloration and brittleness in PVDF membranes. The degradation mechanism involves dehydrofluorination, leading to the formation of carbon-carbon double bonds and polymer chain weakening [85]. Studies have shown that the addition of stress and strain accelerates this degradation process. When exposed to NaOH, PVDF's mechanical strength diminishes, confirmed by various tests and spectroscopic analyses [86]. In addition to NaOH, PVDF's stability has been tested with chemicals like sodium hypochlorite (NaOCl) and potassium hydroxide (KOH) [87]. These studies reveal structural modifications and increased hydrophilicity, resulting in weaker and more flexible membranes after prolonged exposure. Overall, PVDF demonstrates outstanding chemical stability and durability, but careful consideration is required when used with strong alkaline solutions to prevent degradation. Table 2 shows the chemical properties of PVDF.

 doi:10.20944/preprints202501.0023.v1

Table 2. Chemical properties of PVDF[62,81].

Chemical properties of PVDF					
Organic solvent resistance			**Alcohol resistance**		
Chemical	20°C	50°C	Chemical	20 °C	50 °C
Acetone	Not	Not	Benzyl alcohol (pure)	Yes	Yes
Chlorobenzene	Yes	Yes	Methanol	Yes	Yes
Benzene	Yes	Limited	Ethanol (30%)	Yes	Yes
Chloroform	Yes	Yes	Methyl alcohol (10%)	Yes	Yes
Diethylene glycol	Yes	-	Phenol (10%)	Yes	Yes
Cyclohexane	Yes	Yes	Methyl alcohol (pure)	Yes	Yes
Dimethyl formamide	-	-	Propanol	Yes	Yes
Trichloroethane	Yes	Yes	Phenol (100%	Yes	Yes
Diethylamino	Yes	Not	**Resistance to acids and bases**		
Xylol	Yes	yes	Formic acid (10%)	Yes	Yes
Food product resistance			Acetic acid (100%)	Yes	Yes
Glucose	Yes	Not	Acetic acid (10%)	Yes	Yes
Milk	Yes	Yes	Hydrochloric acid	Yes	Yes
Olive oil	Yes	Yes	Sulfuric acid (10%)	Yes	Yes
Wine	Yes	Yes	Lactic acid	Yes	Limited
Vinegar	Yes	Limited	Nitric acid (10%)	Yes	Yes
Resistance to oils and fats			Nitric acid (Conc.)	Limited	Limited
Coconut oil	Yes	Yes	Hydrogen peroxide (90%)	Yes	-
Butyl acetate	Yes	Limited	Sulfuric acid (90%)	Yes	Yes
Mineral oils	Yes	Yes	Sulfuric acid (fuming/monohydrate)	Not	Not
Pine oil	Yes	Yes	Trichlorofluoromethane	Yes	Yes
Paraffin oil	Yes	Yes	Tetrahydrofuran	Limited	Not

2.4. Thermal Properties

Thermal stability in polymers refers to their ability to resist heat and maintain properties like strength, durability, and flexibility. Two key parameters influence PVDF's thermal stability: the glass transition temperature (T_g) and the melting temperature (T_m). PVDF has a T_g between -20°C and 60°C, making it a rubbery polymer above 0°C. Melting temperatures are between 160°C and 190°C, which is depending processing and phase conditions. Every phase of PVDF have comparable melting temperatures, with slight variations in T_m can indicate various crystalline phases. PVDF has excellent thermal stability, withstanding temperatures ranging from -30 to 170°C. Its temperature of thermal degradation also remains constant, ranging from 400 to 450 °C, regardless of the crystalline phase, quantity of crystallinity, and manufacturing technique. Most data suggest that the Curie temperature (T_c) of PVDF, where it loses spontaneous polarization, is between 195°C and 197°C. PVDF's low thermal conductivity makes it ideal for insulation, and its low coefficient of linear thermal expansion ensures minimal dimensional changes under different temperatures [88].

2.5. The Electroactive Properties of the PVDF

PVDF is notable for its exceptional piezoelectricity, which refers to its capability to produce an electric charge when a mechanical stress or force appled, as well as generating mechanical stress whenever an electrical filed is applied. Figure 3 shows a Heckman diagram representing the interrelationship between the mechanical, thermal and electrical properties of materials.

 doi:10.20944/preprints202501.0023.v1

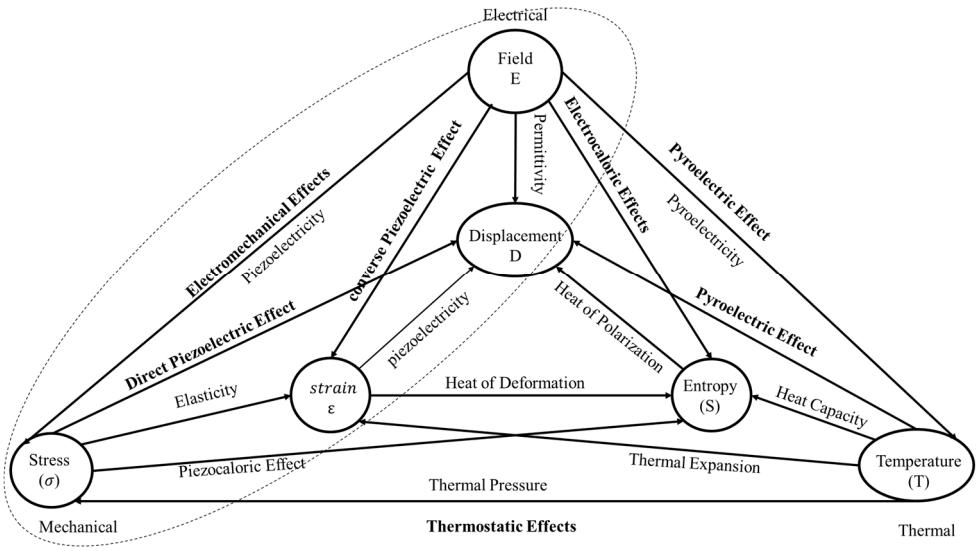

Figure 3. A Heckman diagram. Redrwed, refer to reference [89].

2.5.1. Ferroelectric Effect

PVDF's ferroelectricity is caused by dipole moments, shown in Figure 4, inside its molecular structure, which are mainly induced by strongly electronegative fluorine atoms as shown in the β-phase in Figure 2(b). These dipoles align in response to an electric field, allowing the material to create a hysteresis loop, which is essential for ferroelectric activity. PVDF's ferroelectric properties, discovered in 1974[90], enhance its piezoelectricity by allowing it to keep polarization long after the electric field is removed. However, as-manufactured PVDF films, particularly those formed from melt or solution, lack ferroelectricity because the dipole moments cancel due to their crystal structure. Additional approaches, such as mechanical stretching or the usage of copolymers like P(VDF-TrFE), are necessary to induce ferroelectricity [91]. These techniques enhance dipole alignment, resulting in ferroelectric behavior. PVDF demonstrate a shift in phase and transition temperature with an applied electric field, similar to ferromagnetic materials [92]. When heated over the T_c, the material transitions from the ferroelectric β-phase to the paraelectric α-phase. Below this temperature, PVDF maintains spontaneous polarization [93].

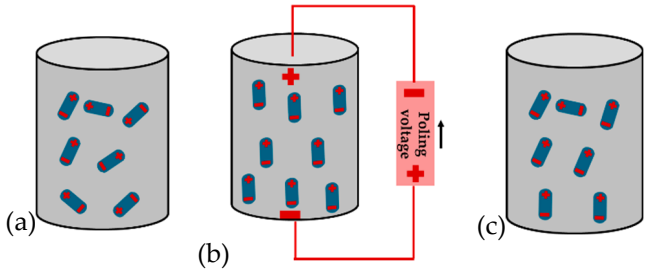

Figure 4. Poling of a ferroelectric. (a) The material initially has a random arrangement of domains. (b) Application of an electric field at elevated temperature aligns domains with the field. (c) Once cooled to room temperature the field is removed and a remnant polarisation and strain is observed. The poled material is piezoelectric.

2.5.1.1. Dielectric Properties

The energy dissipation in PVDF, also known as the dielectric loss (tanδ)[20]. It describes how energy is lost in dielectric materials under an electric field. A loss factor is defined as

$$\tan\delta = \frac{\varepsilon''}{\varepsilon'} \quad (3)$$

 doi:10.20944/preprints202501.0023.v1

Where ε' is the real part of the dielectric constant, and ε″ is the imaginary part representing energy loss. For PVDF, the dielectric loss is influenced by frequency and nanofiller presence, typically ranging from 0.04 to 0.11 depending on the sample [94].

2.5.1.2. Piezoelectric EFFECT

Expression "piezoelectricity" refers to a property of a material to convert intrinsic elasticity into dielectric energy if it is exposed to an external pressure[95], [96], [97]. In PVDF, this effect can be quantified through several important constants such as the piezoelectric strain constant (d_{ij}), the piezoelectric voltage constant (g_{ij}), and the electromechanical coupling coefficient (k_{ij})[98], which together characterize the efficiency and sensitivity of PVDF's piezoelectric response to mechanical stress/deformation. The piezoelectric charge constant (d_{ij}) is a key parameter that describes the relation between mechanical stress and electric polarization.

Direct Piezoelectric Effect: A piezoelectric material produces an electric charge on its surface when mechanical force is applied to it. This charge may be gathered and used to a number of things, including sensors, transducers, and and energy harvesters [99], [100], [101].

$$D = d\sigma + \varepsilon^{\sigma} E \tag{4}$$

where D is the dielectric displacement in C/m² or N/mV. σ is the stress vector in N/m² and d the piezoelectric coefficient C/N or m/V, $\varepsilon^{\sigma}$is the dielectric permittivity in F/m or N/V². E is the applied electric field in V/ m.

Inverse Piezoelectric Effect: A piezoelectric material undergoes deformation or changes in shape when an electric field is appled to it. Utilizing the material's reaction to an applied voltage to provide precise control is how this quality is exploited in devices like piezoelectric actuators[102], [103], [104]. The inverse piezoelectric effect serves as the basis for the electromechanical actuator of electro-deformation. Figure 5 demonstrates a schematic illustration of the piezoelectric phenomenon [105]. Where δ is the strain, s^E is compliance matrix coefficient, d is piezoelectric coefficient, and E is electric field.

$$\delta = s^E \sigma + dE \tag{5}$$

The piezoelectric coefficient, dielectric permittivity, and elastic compliance matrices aregiven in equarion (6), where the 3-direction is along the poling direction and the 1-direction is along the stretching.

$$\begin{bmatrix} 0 & 0 & 0 & 0 & d_{15} & 0 \\ 0 & 0 & 0 & d_{24} & 0 & 0 \\ d_{31} & d_{32} & d_{33} & 0 & 0 & 0 \end{bmatrix}, \begin{bmatrix} K_{11} & 0 & 0 \\ 0 & K_{22} & 0 \\ 0 & 0 & K_{33} \end{bmatrix}, \begin{bmatrix} s_{11} & s_{12} & s_{13} & 0 & 0 & 0 \\ s_{12} & s_{22} & s_{23} & 0 & 0 & 0 \\ s_{13} & s_{23} & s_{33} & 0 & 0 & 0 \\ 0 & 0 & 0 & s_{44} & 0 & 0 \\ 0 & 0 & 0 & 0 & s_{55} & 0 \\ 0 & 0 & 0 & 0 & 0 & s_{66} \end{bmatrix}, \tag{6}$$

Figure 5 shows a schematic representation of direction index of electromechanical constants in poled piezoelectric in various modes including longitudinal, converse, and shear direction[61].

 doi:10.20944/preprints202501.0023.v1

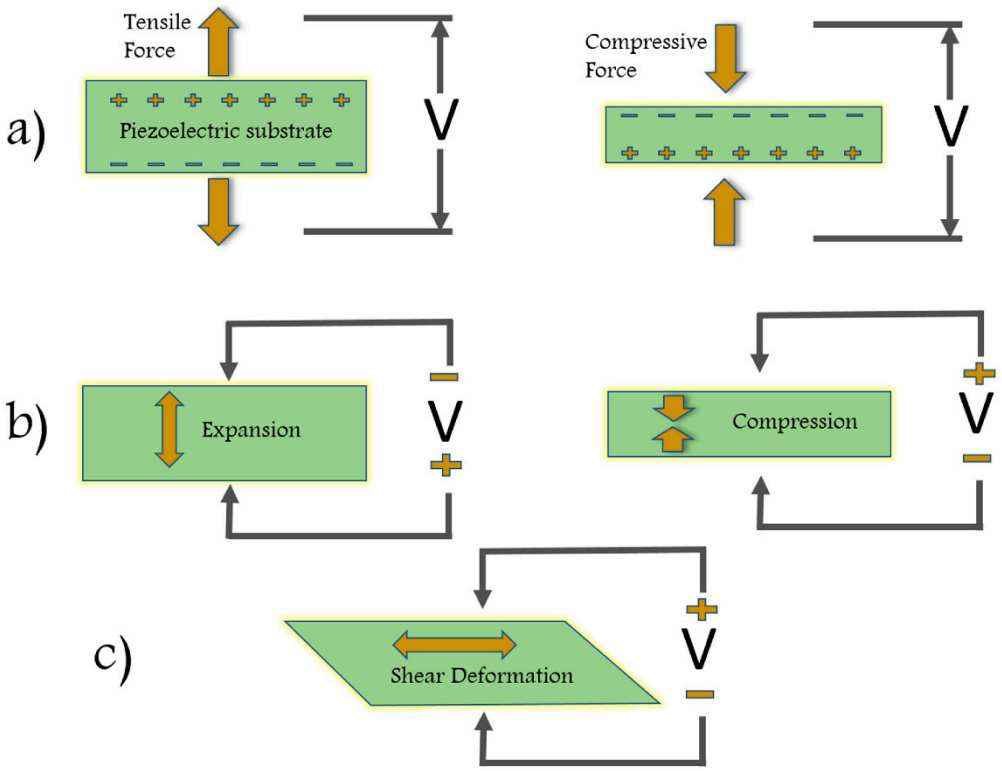

Figure 5. Schematic representation of poling directions in PVDF material (a) direct piezoelectric effec (b) converse piezoelectric effect, (c) shear deformation [61] .

Piezoelectric Strain Const.ant (dij): The general relationship between the applied stress (σ) and the electric polarization (P) is given by[66]:

$$P = d\sigma \tag{7}$$

In this equation, d is the piezoelectric strain constant, which describes the amount of electric charge is generated per unit of applied mechanical stress[106].

The piezoelectric coefficients ($d$ij) form a matrix that expresses the behavior of the material in different directions. The matrix form for the piezoelectric coefficients is represented as [107].

$$d_{ij} = \begin{bmatrix} 0 & 0 & 0 & 0 & d_{15} & 0 \\ 0 & 0 & 0 & d_{24} & 0 & 0 \\ d_{31} & d_{32} & d_{33} & 0 & 0 & 0 \end{bmatrix} \tag{8}$$

Where d_{31}, d_{32} and d_{33} represent the piezoelectric strain constants in different directions, while d_{24} and d_{15} are shear piezoelectric strain constants.

For PVDF, the relationship is expressed as[108]:

$$d_{ij} = \frac{\mathrm{Q_i}}{A_i} / \frac{F_j}{A_j} \tag{9}$$

Where Q_i is the electrical charge generated, A_i is the area over which the charge is measured, F_j is the mechanical force applied, and A_j is the area over which the force is applied. In PVDF, the most commonly measured coefficient is d_{33} , which describes the charge generated along the thickness of the material when subjected to stress in the same direction[12].

$$d_{33} = \mathrm{Q_{sample}} \,/\, \mathrm{F_{dynamic}} \tag{10}$$

Where Q_{sample} is the generated charge, and $F_{dynamic}$ is the applied force.

Another typical piezoelectric coefficient is the transverse mode (d_{31}), where mechanical stress is applied at a right angle to the polarization direction.

Piezoelectric Voltage Constant (g_{ij}): The piezoelectric voltage constant (g) represents the electric field generated per unit of applied mechanical stress [109]. This is crucial in sensing and energy harvesting applications. The equation for the electric field E generated by an applied stress σ is:

 doi:10.20944/preprints202501.0023.v1

$$E = g_{33}\sigma \tag{11}$$

Simplifying this relationship with mechanical stress σ and the Young's modulus Y[109]:

$$V = g_{33}\varepsilon YL \tag{12}$$

Where V is the generated voltage, ε epsilonε is the strain, Y is Young's modulus of the material, and L is the length of the material. Experimental values for PVDF films have shown voltage responses ranging from 5 to 30 mV during mechanical stretching.

The relationship between the piezoelectric charge (d) and voltage (g) coefficients is given by [109]:

$$d_{33} = g_{33}/\varepsilon_{33}^{T} \tag{13}$$

The dielectric constant ε of piezoelectric materials is another key parameter that determines how a material stores electrical energy in the presence of an electric field.

The piezoelectric d_{31} coefficient of PVDF can be calculated by .

$$d_{31} = \varepsilon_r . \varepsilon_0 . g_{31} \tag{14}$$

Where ε_0 is the vacuum permittivity with value of $8.854 \times 10^{-12}\, C/Vm$ and ε_r is the relative permittivity of the material.

Electromechanical Coupling Coefficient (k_{ij}): The electromechanical coupling coefficient is used to directly assess the efficiency of energy conversion in materials [110]. Consequently, the coupling factor k is defined as a direct or inverse function of the piezoelectric effect, based on the following relationships:

$$K^2 = \frac{store\ electrical\ energy}{input\ mechanical\ energy} = \frac{d_{33}^2}{S_{33}^{E}\varepsilon_0\varepsilon_{33}^{T}} \tag{15}$$

$$K^2 = \frac{stored\ mechanical\ energy}{input\ electrical\ energy} \tag{16}$$

Here, S_{33}^{E}represents mechanical compliance at a constant electric field, and ε_{33}^{T} is the dielectric constant.

2.5.4. Pyroelectric Effect

While the piezoelectric effect involves generating charge in response to applied mechanical stress, the pyroelectric effect involves generating charge due to changes in temperature [111–112]. This effect arises from the spontaneous polarization in PVDF's molecular structure, primarily in its β-phase, where dipoles align along the polymer chains. When the temperature changes, the polarization also changes, resulting in a measurable surface electric charge. This property is especially useful in applications such as infrared sensors, thermal detectors, and energy harvesting devices [113]. Pyroelectricity in PVDF is often enhanced by processes like stretching, which align the dipoles more effectively, increasing the material's sensitivity to temperature variations. The pyroelectric effect and its different steps are shown in Figure 6.

The pyroelectric coefficient, denoted as p_3, represents the charge generated per unit area per degree of temperature change and can be expressed as equation (17).

$$p_3(eff) = \left(\frac{\partial p_s}{\partial T}\right)_s \frac{d_{33}^{T}\,\alpha_3^{s}}{s_{33}^{s}} = \left(\frac{I}{A}\right)\left(\frac{\partial T}{\partial t}\right)^{-1} \tag{17}$$

Where P is the polarization, T is the temperature, d_{33} is the piezoelectric constant, α^s is the thermal expansion coefficient, and $\frac{\partial T}{\partial t}$ represents the rate of temperature change.

 doi:10.20944/preprints202501.0023.v1

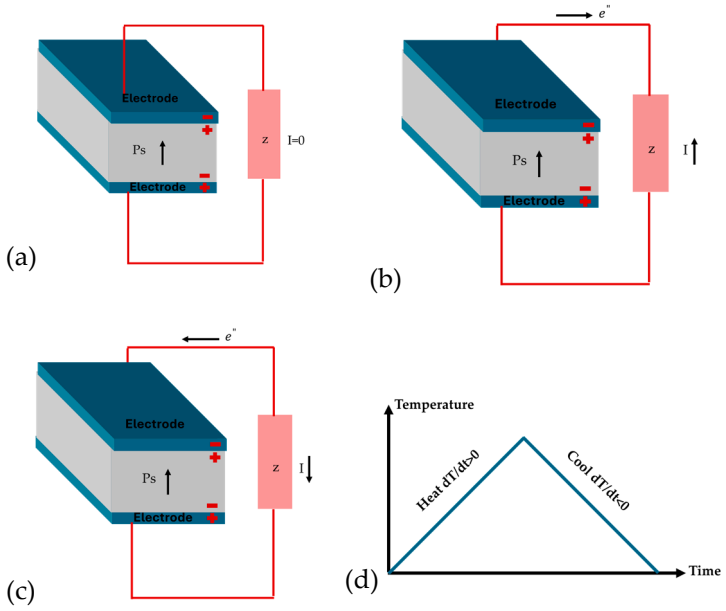

Figure 6. The pyroelectric effect; (a) polarised material and corresponding surface charge (b) cooling leads to increase of polarisation leading to current reversal, (c) heating leads to a decrease in polarisation and free surface charge for current generation (d) applied thermal cycle.

3. Enhancement of PVDF Properties Through Optimized Preparation Methods

The structure of PVDF directly influences its characteristics. For example, in certain fields, PVDF is used for different purposes, such as film, fiber or complex shapes with different thicknesses to meet the needs of different industries. The dielectric permittivity and electrical conductivity of PVDF are known to rise with an increase in the β-phase content. To improve other properties of PVDF, it can be formed into two fibers or layers. Morover, PVDF with piezoelectric characteristics can be achieved through straightforward material modifications, such as phase transitions [114], or by using advanced processing technologies [64]. In addition, achieving the desired properties involves the use of PVDF copolymers[115]. Figure 7 shows different methods of improving PVDF properties. Many researchers have also improved various properties of PVDF, especially piezoelectricity, by blending with polymers or adding fillers [116]. In addition, different grades of PVDF, such as high molecular weight PVDF or low molecular weight PVDF, play a crucial role in achieving certain goals.

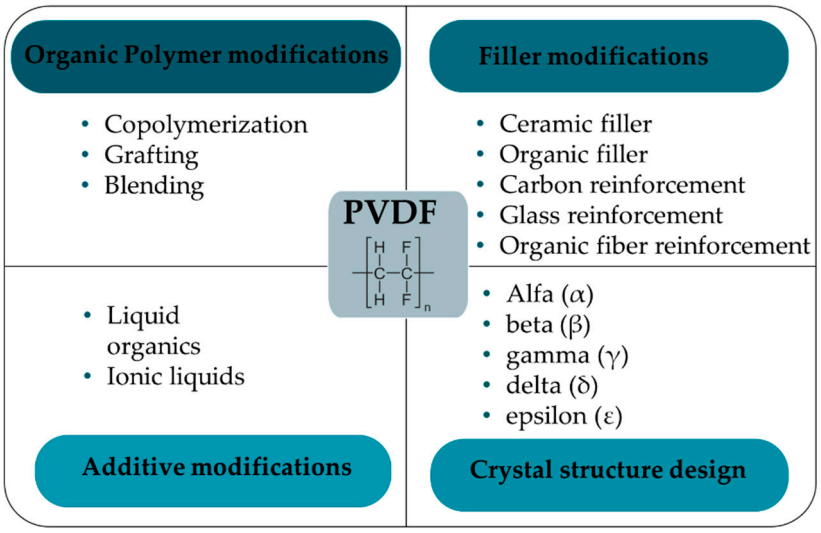

Figure 7. Different methods of improving PVDF properties.

 doi:10.20944/preprints202501.0023.v1

3.1. PVDF Film Fabrication Methods

The manufacturing process plays a crucial role in shaping PVDF's diverse features, including it s superior dielectric and piezoelectric properties. PVDF can be fabricated using a variety of techniques to create a two- or β-phase material. The hot pressing method, 3D printing, spin coating, electrospinning, and solution casting, are examples of common techniques. These methods frequently result in Langmuir–Blodgett films, which are nanostructured solid films formed at the liquid–gas interface. Solvent casting techniques, like electrospinning, solvent evaporation, and spin coating, however, have been receiving increased attention as a result of the need for films with nanoscale thicknesses in numerous applications.

3.1.1. Solution Casting

One common method for producing PVDF and its copolymer-based films is solution casting as shown in Figure 8, which can obtain excellent films with better mechanical, optical, and physical characteristics through the unform in-plane distributions. Certain organic solvents, including DMF[117], methyl ethyl ketone (MEK) [118], dimethyl sulfoxide (DMSO)[119], acetone [120], N,N-dimethylacetamide (DMAc)[121] and 1, 3-dioxolane (DXL) [122], can dissolve PVDF and its copolymers.

The dissolution process usually takes place at room temperature but sometimes, require higher temperature (<70°C) [123]. One popular technique for enhancing dissolution is using ultrasonication aid mixing technology. In most cases, the ultrasonication operation time is less than 30 minutes, but it can vary case by case and range from a few minutes to three hours[121]. Stirring, as compared to ultrasonication, is typically done for longer than 30 minutes. After evaporation, the fully mixed PVDF/organic solution is placed over an Al substrate or glass to create the first films [121]. Evaporation can occur in vacuum chambers or in the air, with temperatures ranging between 50°C and 120°C and glass [123]. A schematic representation of the solution casting technique PVDFpreparation process is shown in Figure 8.

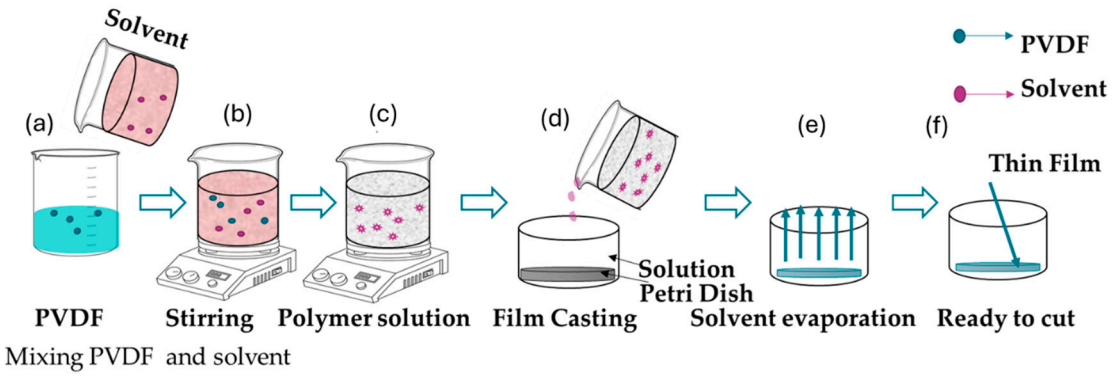

Figure 8. Solution casting process for PVDF films.

3.1.2. Solution Coating

Another commonly employed method for creating composite membranes is solution coating. This method, illustrated in Figure 9, creates composite membranes by applying a thin layer of chosen later polymer solution over a porous substrate. Since a selective coating layer can regulate them, care should be taken beforehand to ensure that the substrate's degree of porosity is larger than the membrane resistance. A low boiling point solvent, which is insoluble with the coating solvent and can lessen invasion, is applied to the substrate prior to the coating process. To create a coated membrane, the solvent is further evaporated. Solution coating's primary benefits are its ease of fabrication—it can produce homogenous coatings over huge areas at low temperatures [124–127].

 doi:10.20944/preprints202501.0023.v1

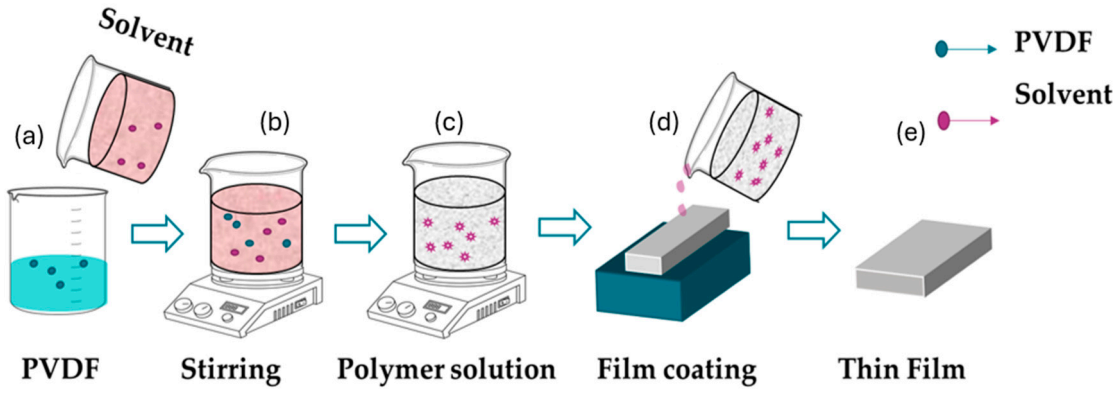

Figure 9. Solution coating processing for PVDF films.

3.1.3. Spin Coating

Spin-coating method shown in Figure 10, is used to prepare thin film, it is a cost-effective and time-efficient method for processing uniform polymer films from a dilute solution on a planar substrate [31]. This method is suitable for producing smooth polymer coatings for microelectronic applications. Researchers have successfully prepared nanoscale films of crystalline phase PVDF using this technique. Key factors like humidity and rotation speed can measure the surface roughness and phase content of thin films[128]. Additionally, the thickness of the films depends on the solvent solution's properties and the spin speed. However, the thin films are pure non-poled alpha phases of PVDF, necessitating further polarization for piezoelectric response [115,129].

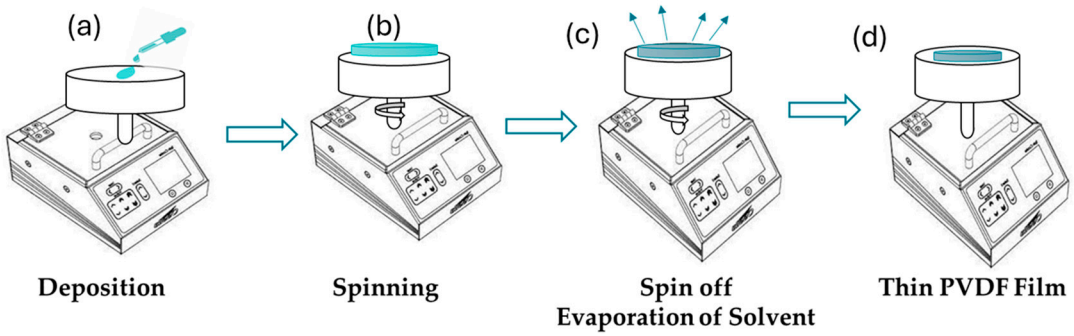

Figure 10. Spin coating for PVDF films.

3.1.4. Hot Pressing Method

The fabrication of PVDF films using hot pressing begins with the preparation of PVDF powder or pellets. Figure 11(a) shows the hot pressing method of PVDF while Figure 11(b) shows the example of hot pressing equipment. The material is melted under controlled conditions, typically at temperatures ranging from 150°C to over 200°C[130], ensuring complete melting without decomposition. High pressures, often between 5 and 40 MPa[131] are applied to compress the material, eliminating voids and enhancing density. Following the application of heat and pressure, the films are cooled in a controlled manner, solidifying the polymer into the desired crystalline phases. Additional treatments such as stretching or electrical poling can be applied to optimize the material's piezoelectric properties[130].

Hot pressing is recognized for its ability to improve the crystalline phases of PVDF, especially the transition from the α-phase to the β-phase, which is critical for piezoelectric applications [132]. The technique is particularly advantageous for its ability to produce dense films with high β-phase content, superior dielectric properties, and improved mechanical performance. For instance, studies

 doi:10.20944/preprints202501.0023.v1

have demonstrated that varying the hot press temperature influences the crystallite size of PVDF films. At temperatures around 170°C, the crystallite size significantly increases, enhancing the β-phase content and resulting in films with superior piezoelectric and dielectric properties. Specifically, crystallite size has been observed to grow from 7.2 nm to 20.54 nm with increased pressing temperature [133].

Hot-pressed PVDF films also exhibit exceptional dielectric properties. Films processed at 150°C have been reported to achieve high energy densities (19.24 J/cm³) coupled with efficiencies of 68.99%. Additionally, their breakdown strength of 1189 kV/cm and dielectric loss as low as 0.04 make them highly suitable for high-performance energy storage applicationss [134]. The temperature and pressure applied during hot pressing play a critical role in determining the crystallinity and phase composition of the films. Rapid cooling post-pressing has been shown to promote β-phase retention, further enhancing the material's functional properties. Comparative studies highlight the superiority of hot pressing over other fabrication methods, such as solvent casting. Hot pressing provides more controlled thermal and mechanical treatment, yielding films with higher β-phase content and fewer defects. For instance, the uniform application of pressure and heat during hot pressing results in films with enhanced thermal stability and superior dielectric and mechanical properties compared to films produced through other techniques [135].

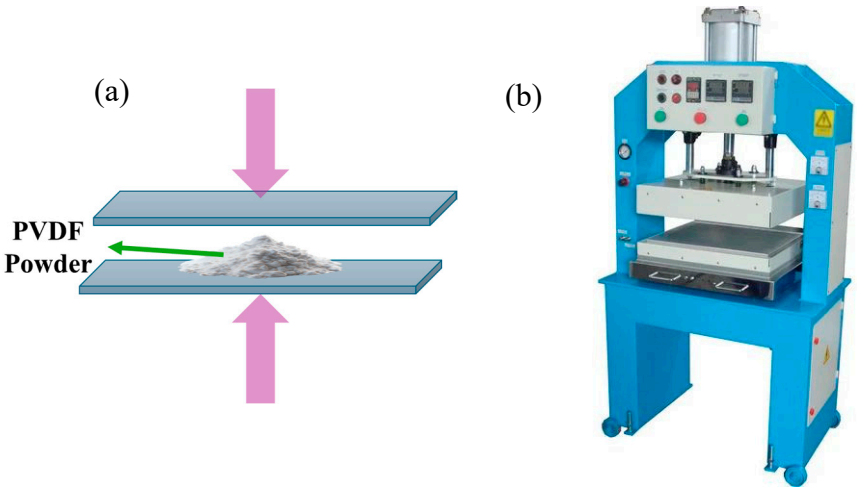

Figure 11. (a) Hot pressing method for PVDF, (b) Equipment use for Hot pressing.

3.1.5. Electrospinning

Electro-spinning is a popular technique for creating PVDF fiber-based films, particularly ultrathin films shown in Figure 12. This method involves the solution preparation, electrostatic field application, jet formation, jet stretching, and solvent evaporation.

The electrospinning of PVDF films is a multifaceted approach that includes the application of a high voltage to a polymer solution, resulting in the formation of a thin jet that dries into nanofibers upon interaction with a collector. The technique utilizes the electrostatic forces produced between the charged polymer solution and the grounded collector, leading to the creation of fibers with diameters from nanometers to micrometers. The fundamental concept is in the interaction of surface tension, electrostatic repulsion, and solvent evaporation, which together dictate the jet's path and fiber development.

Electrospinning has advantages over alternative techniques, as it causes PVDF molecular chains to elongate uni-axially along the fiber axis, resulting in the formation of the β-phase [136]. PVDF films can exhibit piezoelectricity without post-poling, as polymer jet elongation and whipping allow poling to occur during the electrospinning process. Electric forces can complete the poling and stretching process in electrospinning [137]. PVDF membranes with appropriate crystallinity can be created by applying heat treatment in or afterward the electrospinning procedure. Cross-linked

 doi:10.20944/preprints202501.0023.v1

membranes with ideal mechanical characteristics may be created by adjusting the heating procedure during or after the electrospinning[138]. Research has also explored the combination of hot press and electrospinning, with final products obtained by compressing dried electrospun PVDF/SMG membranes[6]. The primary variables in the electro-spinning process include applied voltage, needle-collector distance, and flow rate [139].

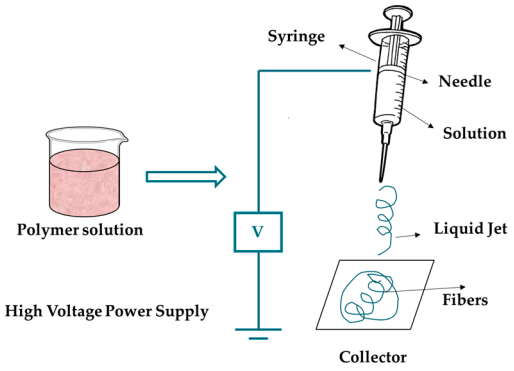

Figure 12. Diagram of Electrospinning for PVDF films.

3.1.6. 3D Printing

Using additive manufacturing, or 3D printing, is another important method in the preparation of PVDF-based piezoelectric materials shown in Figure 13. This technique allows for the creation of precise shapes through layer-by-layer deposition. Fused deposition modeling (FDM) stands out among various methods for its affordability and user-friendliness[140]. PVDF samples in various forms can be produced using FDM by increasing the nozzle temperature beyond the material's melting point. While FDM can induce some β-phase formation through stress, it isn't sufficient to generate a high β-phase content (>50%)[141].

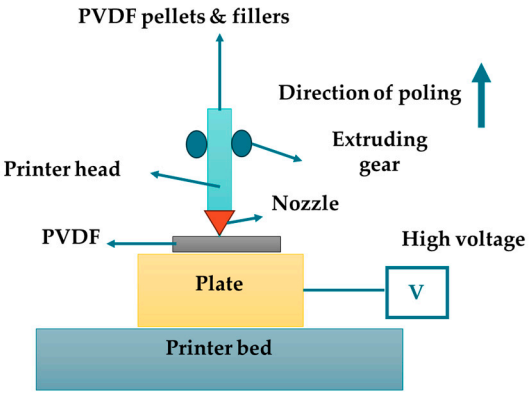

Figure 13. A 3D printing mechanism for PVDF films.

Researchers aim to enhance the β-phase content by optimizing printing parameters, utilizing P(VDF-TrFE) with high ferroelectric phase content, and incorporating additives. After achieving high β-phase content, post-processing poling is necessary to align the dipoles for macroscopic piezoelectricityor example, an "integrated 3D printing and corona poling process" (IPC) was developed by Sebastian *et al* [142], enhancing the β-phase content to 56.8%. Similarly, the electric-poling-assisted additive manufacturing (EPAM) process, developed by[143], employs mechanical stretching and electrical poling to convert α-phase PVDF to β-phase. Although these methods increase β-phase content, achieving higher piezoelectric properties remains a challenge. ubstituting PVDF with P(VDF-TrFE) proves effective, as demonstrated by [144] who achieved 85.8% crystallinity

 doi:10.20944/preprints202501.0023.v1

and a d_{33} value of -18 pC N^{-1} with in situ polarized P(VDF-TrFE). Multi-layered or specially shaped designs can further enhance piezoelectricity, as demonstrated by Yuan et al., whose six-layer P(VDF-TrFE) device exhibited a high d_{33} of -130 pC N^{-1} [145]. In conclusion, FDM and other 3D printing techniques hold great promise for producing high-precision, cost-effective PVDF-based piezoelectric materials, with ongoing research aimed at increasing β-phase content. Table 3 shows the different fabrication methods along with their advantages, disadvantages

Table 3. Different fabrication methods along with their advantages, disadvantages and parameters of PVDF[66].

Method	Advantages	Disadvantages	Common Prameter
Solution Casting	▪ Simple and cost-effective process. ▪ Ability to control film thickness. . ▪ Good control over morphology and properties. .	▫ Solvent selection can be critical. ▫ Limited scalability due to solvent evaporation. ▫ May require post-treatment steps.	Concentration: 10-20 wt% Temperature: 25-80°C
Hot pressing	▪ Improved Crystallinity ▪ Enhanced Mechanical Properties ▪ Reduced Porosity ▪ Faster Processing	▫ Potential for Degradation ▫ Equipment Cost ▫ Limited Control over Film Thickness	-
Electrospinning	▪ High surface area and porosity in the resulting nanofibrous structure. . ▪ Versatile for producing various fiber diameters and architectures. . ▪ Potential for fiber alignment. .	▫ Requires specialized equipment and high voltage power supply. ▫ Limited control over fiber alignment and morphology. ▫ Difficulty in scaling up.	Voltage: 10-30 kV Flow rate: 0.5-2 mL/h
Spin Coating	▪ Uniform and smooth film formation. ▪ Suitable for small-scale and research applications. ▪ Can achieve controlled film thickness.	▫ Limited scalability due to the size of the spinning apparatus. ▫ Solvent evaporation can lead to uneven film formation. ▫ Difficult to achieve thickness control for thicker films.	Speed: 1000-5000 rpm Time: 30-60 s
Solution Coating	▪ Versatile and compatible with various substrates. ▪ Allows for precise control over deposition technique. ▪ Suitable for different scales and applications.	▫ May require optimization for achieving uniform film thickness. ▫ Solvent selection and drying conditions can affect film properties. May require additional post-treatment steps.	Concentration: 5-15 wt% Temperature: 25-60°C
3D Printing	▪ Enables fabrication of intricate 3D structures. ▪ Design flexibility and customization. ▪ Reduced material waste compared to traditional methods.	▫ Limited range of printable materials. .Limited mechanical properties compared to conventionally processed materials. ▫ May require post-processing steps for improved properties.	Layer height: 0.1-0.4 mm Speed: 10-100 mm/s

There have also been reports of other techniques, such as tape casting, template, and phase separation; however, because of drawbacks like irregularity, they are not covered here. of the synthesis processes' costs, complexity, and forms[146].

 doi:10.20944/preprints202501.0023.v1

3.2. Phase Transition and Achievement Methods

Stretching, annealing, and poling the polymer in strong electric fields are common phase transition processes of PVDF crystals, as shown in Figure 14. Processing the solution with polar solvents at a crystallization temperature below 70 °C provides the β-phase, whereas processing at temperatures over 110 °C mostly produces the α-phase. Recognizing and controlling the phase transition is essential for adjusting PVDF`s properties for specific applications. Additionally, these methods works well for producing films with a thickness of several micrometers. However, a major drawback of the phase transition is that it rarely occurs, leaving about 20% of the α-phase in the material after adapting to the β-phase PVDF [147].

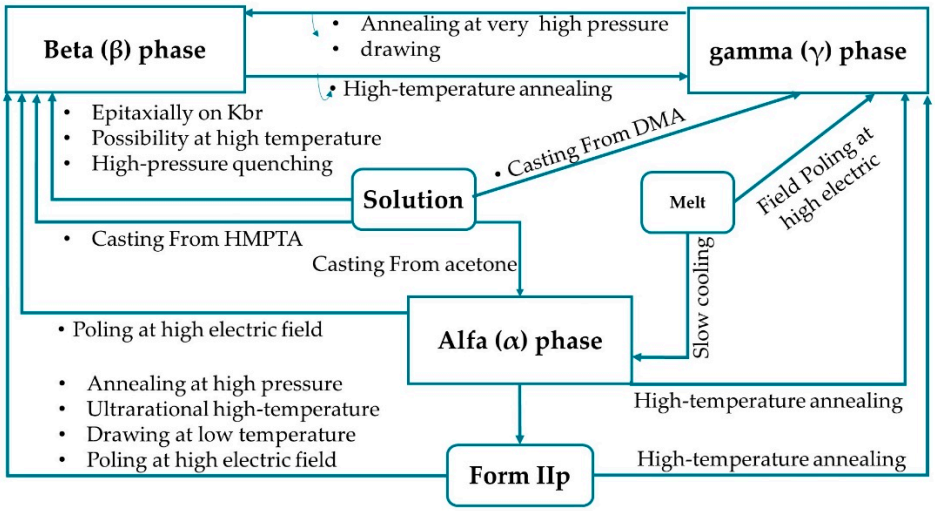

Figure 14. The PVDF polymer's crystalline phase transformation diagram[148].

3.2.1. Stretching

Kawai first described the possibility of a piezoelectric effect in early 1969 on a stretched and poled PVDF film. After that numerous studies have investigated the effect of stretching criteria on PVDF piezoelectricity. These criteria includes temperature stretching , stretching rate, stretching ratio, and stretching direction which need to be considered carefully[30]. It is generally known that ferroelectric β crystals may grow in PVDF under the right stretching circumstances, greatly boosting the material's piezoelectricity when attempting to follow electric poling. Without electric poling, even 100% β phase PVDF films exhibit no piezoelectric activity[149]. The influence of stretching temperature on the composition of the β phase in PVDF was examined in the majority of investigations using FTIR [130]. One of the key factors influencing the crystalline phase of PVDF is stretching temperature. The ideal temperature range to cause β crystals to form varies depending on the original PVDF films' composition and processing parameters. Some highlighted studies based on strectching temperature was reported in these articles[150,151].

Figure 15 displays the scattering intensity profiles from 2 dimensional wide angle X-ray (2D-WAXS) patterns in the meridional direction, based on strain at 60°C and 140°C [150]. According to the published data, the profiles of PVDF prior to stretching at both temperatures exhibit three distinctive peaks that are attributed to the (100), (020), and (110) diffractions of a-form PVDF.One without stretching at various temperatures, it is deduced that the PVDF sample's a-form crystal is predominant. The findings show that the scattering curves evolve similarly during deformation at the two temperatures.

 doi:10.20944/preprints202501.0023.v1

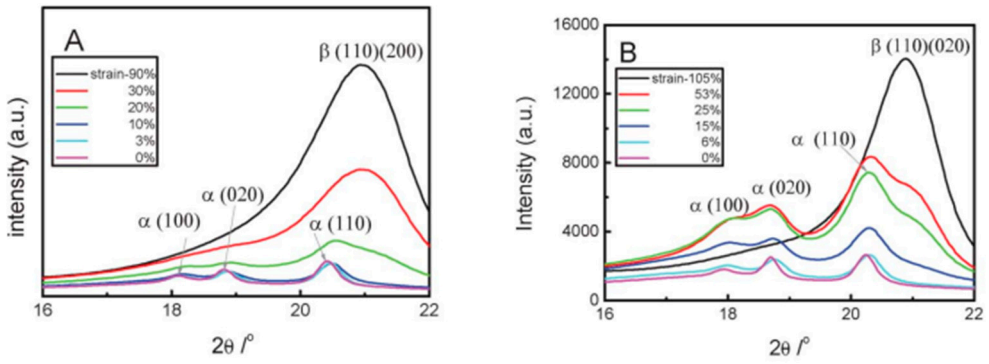

Figure 15. Phase transition by temperature stretching method. 1D WAXS profiles during stretching at: (A) 60°C, (B)140°C [150].

Another crucial factor influencing the formation of the β phase in PVDF, as seen in Figure 16, is the stretching ratio. According to certain studies, it even promoted the production of β crystals in PVDF more effectively than temperature [130]. In a PVDF film, the α phase eventually changed into the β phase by increasing the stretching ratio [152]. The reason for this was that the increased stretching ratio may aid in aligning the polymer chains, favoring crystallization into the all-trans conformation's more compact β phase.

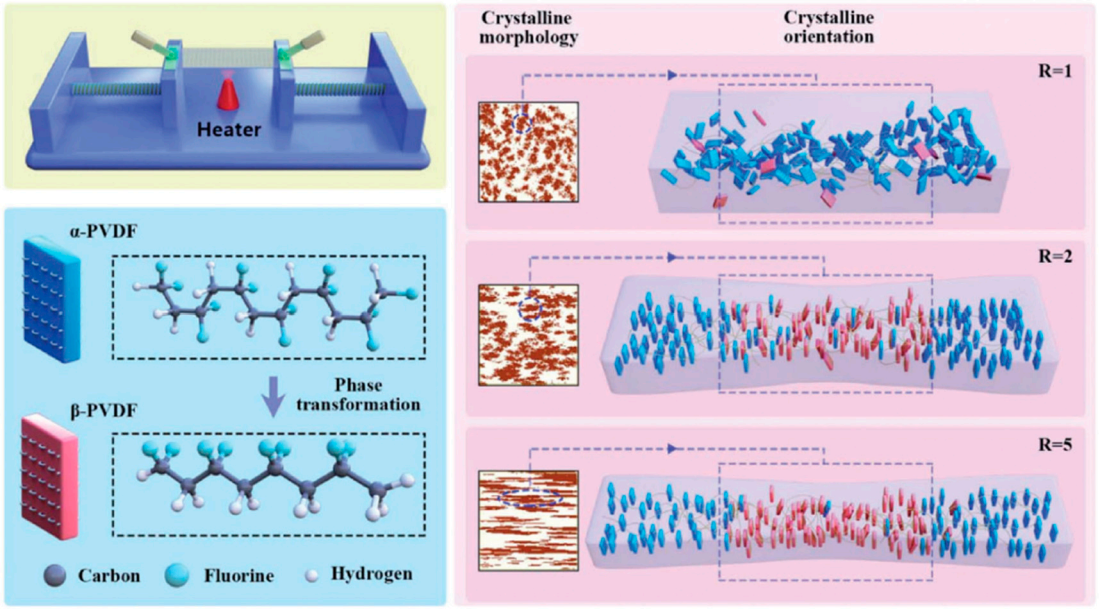

Figure 16. Diagrammatic representation of PVDF films' uniaxial stretching process and structure formation phase change, crystalline orientation, and crystalline shape as the stretch ratio increases[153].

Figure 17a_1 displays the crystalline phase conversion in the PVDF films as determined by FTIR spectroscopy. The PVDF films showed phase transformation from the α to β phase as the stretch ratio increased [153]. This was demonstrated by the α phase's characteristic absorption bands at 764 and 975 cm^{-1} becoming weaker and the β phase's characteristic absorption band at 840 cm^{-1} simultaneously becoming stronger. Additional phase content quantification is shown in Figure. 17(a_2), which demonstrates that when the films were stretched to a ratio of 5, the β phase content grew significantly and subsequently somewhat declined. R = 3 yielded the highest value of 88.18% β phase content. Figure 17b_1 displays the stretched PVDF films' DSC thermographs as a function of temperature, whereas Figure 17(b_2)displays the matching melting temperatures (Tm) and crystallinity values determined from DSC. The PVDF films' crystalline structural characterisation utilizing 1D

 doi:10.20944/preprints202501.0023.v1

WAXD(wide angle X-ray diffraction) profiles is shown in Figure. 17(c1). Figure. 17(c2)provides a detailed analysis of the change tendency of 2θ and crystallite size derived from the (110)/(200)β-PVDF peaks with increasing stretch ratio. The results show that when the stretch ratio increased from R = 1 to R = 5, the crystallite size reduced from 6.51 nm to 3.86 nm and 2θ decreased from 21.03° to 20.63° [153].

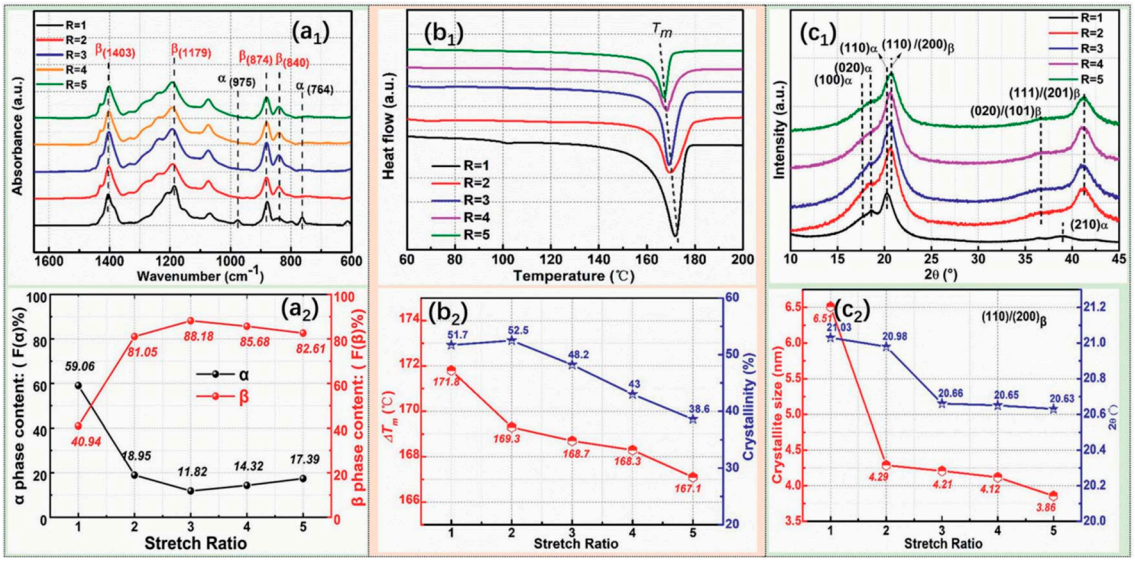

Figure 17. Various stretching conditions of PVDF films for structure evolution. (a1) FTIR spectra, (a2) PVDF films' phase composition changes when the stretch ratio rises, (b1) DSC traces, (b2) Crystallinity and melting temperatures in relation to stretch ratios, (c1) 1D WAXD patterns, (c2) The (110)/(200)β phase's crystallite size and 2θ as a function of stretch ratio, determined by 1D XRD[153].

The efficiency of the phase transition between the nonpolar *α* phase towards the polar *β* phase is also significantly influenced by the stretching direction. Biaxial stretching can provide homogeneous thicknesses for PVDF films while enhancing isotropic piezoelectricity in comparison to uniaxial stretching. In contrast to uniaxially oriented films, the polarized biaxially oriented poly(vinylidene fluoride) (BOPVDF) films demonstrated balanced piezoelectric activity in the film plane, which in turn led to a greater piezoelectric coefficient, according to a research by Mohammadi et al. [154]. Biaxial stretching is simpler to generate *β* crystals than uniaxial stretching, according to Ting et al. [110]. Figure 18 shows the experimental setup consist of two-direction planar stretching machine, which measured 1100 x 1000 x 250 mm, stretched the PVDF thin films uniaxially and biaxially at varying temperatures and stretch ratios. Figure 19 shows the test setup for measurement of piezoelectric coefficient of bixial stretching of PVDF films [110].

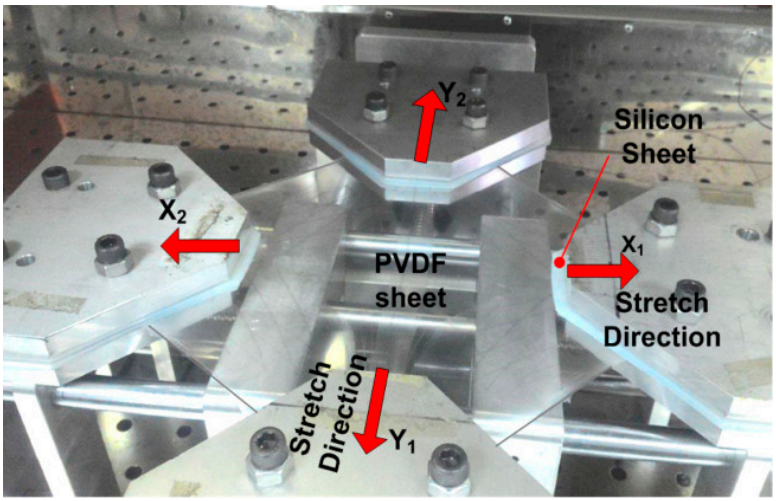

Preprints.org (www.preprints.org) | NOT PEER-REVIEWED | Posted: 2 January 2025 doi:10.20944/preprints202501.0023.v1

Figure 18. Experiment setup biaxial stretching of PVDF [110].

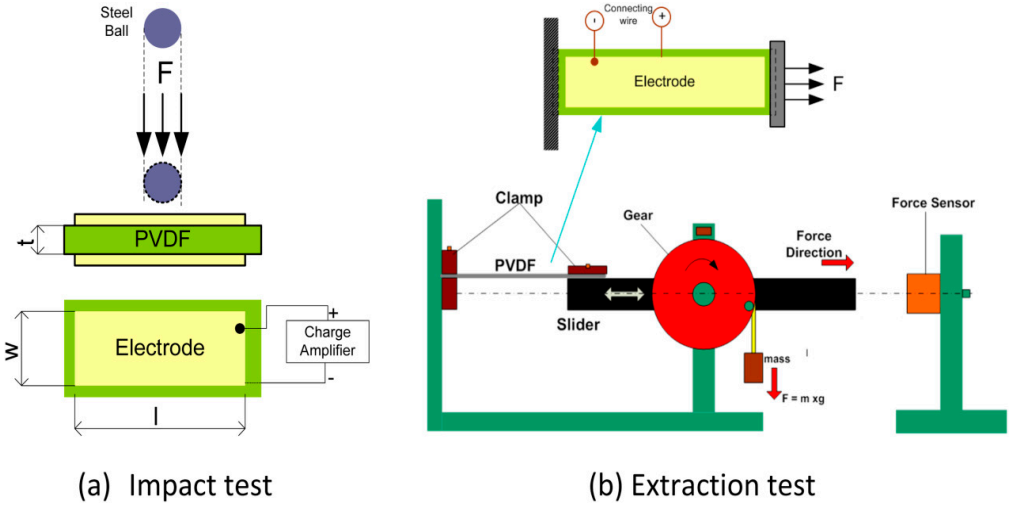

Figure 19. Test setup for measurement of piezoelectric coefficient (a) d_{33}, (b) d_{31} [110].

The FTIR findings of uniaxial stretching with a stretch ratio of R = 5, and biaxial stretching with stretch ratios of R =(2x2), R=(3x3), and R= (4x4) at various temperatures are shown in Figure 20. An arrow designates the absorption band characteristics of each phase in the FTIR spectra, making it simple to identify α phase and β phase. The FTIR spectra of the PVDF samples that were uniaxially stretched are shown in Figure 20(a). The FTIR spectra of the biaxially stretched PVDF samples are shown in Figure 20(b–d). It is evident that several of the α phase and β phase absorption peaks in biaxial stretching differ from those in uniaxial stretching. The absorption peaks of a phase at 763 cm^{-1} grow as the temperature rises in both uniaxial and biaxial stretching, whereas the β phase at 840 cm^{-1} decreases, suggesting that there is less transition from α phase into β phase [110].

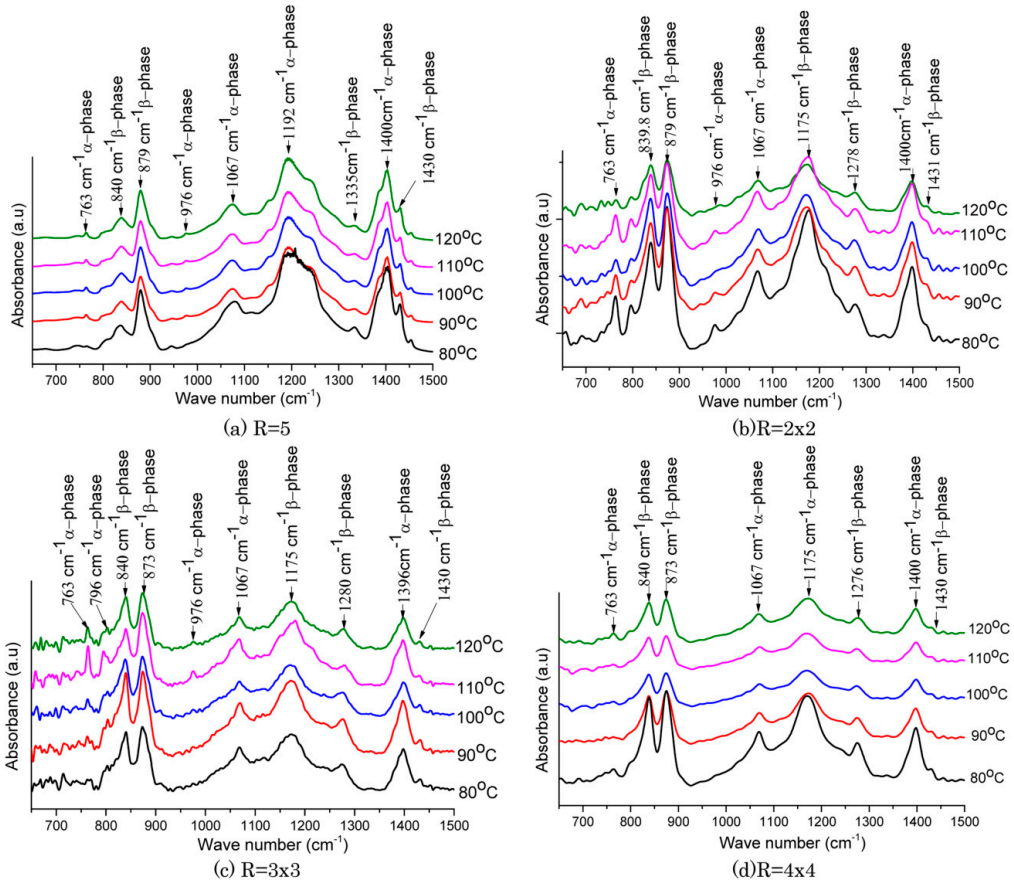

 doi:10.20944/preprints202501.0023.v1

Figure 20. FTIR spectra of stretched PVDF (a) uniaxial, (b–d) biaxial[110].

In conclusion, mechanical stretching is a viable method for causing PVDF films to undergo a phase transition from α to β. Piezoelectric coefficients often increase with the amount of the β phase. It is very desirable to appropriately adjust the stretching parameters in order to enhance the content of β crystals.[12].

3.2.2. Annealing

PVDF-based polymers' piezoelectricity is frequently increased by thermal annealing[128]. Two important factors that affect piezoelectricity during annealing are temperature and time [155–156]. The annealing temperature is usually adjusted between the Curie temperature (T_c) and the melting temperature (T_m) when polymers exhibit considerable chain mobility when in their paraelectric phase [157]. Since Tc is greater than Tm for PVDF at ambient pressure, annealing is a common method for P(VDF-TrFE) film to alter the crystalline structure. Spherical thickness and degree of crystallinity are often improved by longer annealing times[158–159]. Due to enhanced molecular mobility that causes dipole depolarization, annealing can occasionally result in a decrease in piezoelectric coefficients [160]. Annealing can realign and reorient crystalline phases in electrospun fibers, increasing their piezoelectric coefficient and overall dipole moment[161], [162] . Furthermore, the rate at which the materials cools after annealing plays a significant role in the β phase formation. When the annealed PVDF is cooled rapidly, the amount of β phase increases.

3.3. Poling

In semicrystalline materials, poling is essential for realigning molecular dipoles and reorienting crystallites to maximize the piezoelectric effect. By inducing β crystal formation in PVDF-based polymers, this technique achieves macroscopic polarization and piezoelectricity by aligning ferroelectric domains [163]. The most popular methods are contact poling[164], In-situ polarization,[165] and corona poling[166]. Using asymmetric electrodes at high voltage, corona poling produces a uniform electric field that increases the content of β crystals [167]. However, corona poling can introduce conductive charge carriers and reduce crystallinity[12]. Contact poling, often used for preparing piezoelectric PVDF films, is influenced by parameters such as electric field, time, and temperature [168]. Higher electric fields induce more β phase content, but exceeding PVDF's breakdown strength can cause early failure. DC (~106 V/m) at elevated temperatures (~393 K) poling is preferred over AC due to higher breakdown strength [169], [170]. Film thickness should be controlled to achieve high poling fields [12]. Poling time should be optimized to avoid structural defects [166]. Structure between T_c and T_m is effectively changed by the ideal poling temperature, which is typically between 20 and 120 °C. On the other hand, there are certain practical and cost-effectiveness limitations with electrical poling.

Figure 21 shows the schematic diagram of in-situ polarization used for PVDF films [165]. Figure 22 shows the piezoelectric coefficient of PVDF films across various polarization voltages [165]. Figure 23 shows the XRD graphs of PVDF copolymer achieved bu in-situ polarization method, after poling, where A, B, C curves represents poled, annealed and dried process respectively [9]. Figure 24 shows the example of corona poling schematic setup diagram. Figure 25 represent the examples of XRD pattern and FTIR spectra results of PVDF obtained after cornon polarization process. Figure 25 (a) shows XRD patterns and Figure 25 (b) demonistrate compared FTIR spectra of PVDF, where (a) curve represents received PVDF films, (b) curve shows the stretched PVDF while (c) curve indicates a stretched and poled PVDF [166]. Table 4 represents the PVDF polymer's crystalline phase transformation methods along their adavantages and disadvantages.

 doi:10.20944/preprints202501.0023.v1

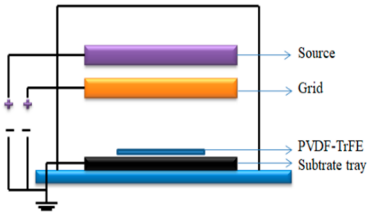

Figure 21. Schematic diagram of in-situ polarization for PVDF film[165].

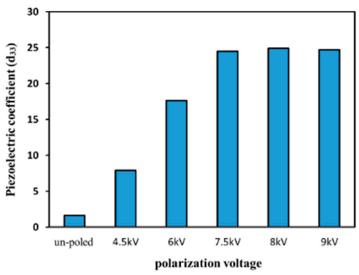

Figure 22. Piezoelectric coefficient corresponding to different polarization voltage [165].

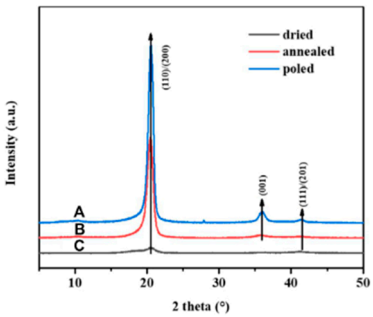

Figure 23. XRD patterns of PVDF-TrFE films after poling [9].

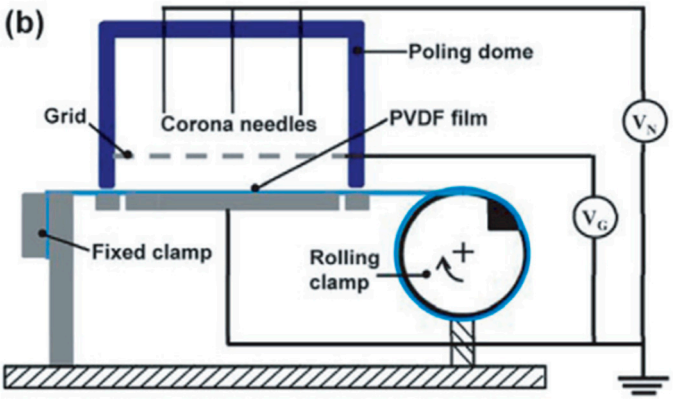

Figure 24. schematic of setup for stretching and corona poling experiment [166].

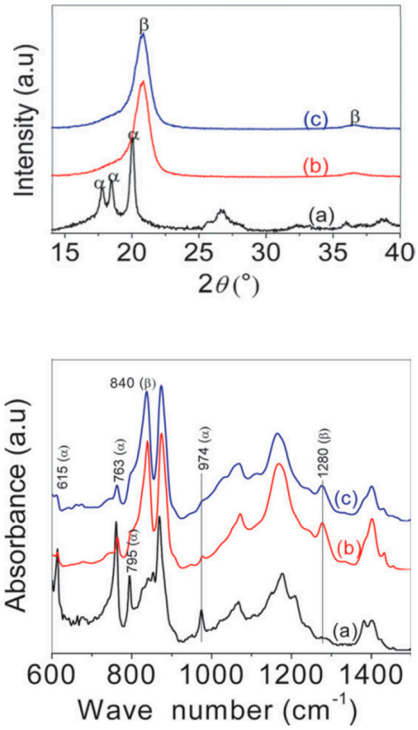

Figure 25. (a) XRD patterns of PVDF after corona polarization, (b) FTIR spectra of PVDF [166].

Table 4. The PVDF polymer's crystalline phase transformation methods along their adavantages and disadvantages.

Methods	Advantages	Disadvantages
Stretching[68], [171]	▪ Increased crystallinity ▪ Improved alignment of polymer chains ▪ Enhanced piezoelectric and mechanical properties ▪ Highly reproducible	▫ Potential material degradation ▫ Introduction of defects or stress concentration
Annealing Treatment [155], [161]	▪ Improved molecular alignment ▪ Increased crystallinity ▪ Enhanced thermal and mechanical properties.	▫ Long processing times ▫ Potential for material degradation ▫ Limited control over phase morphology

 doi:10.20944/preprints202501.0023.v1

Poling [9], [172]	▪ Enhanced piezoelectric properties. . ▪ Improved alignment of dipoles within the polymer ▪ Increased electroactive response ▪ High d33 coefficient and No requirement for one end structure of the material	▫ Risk of electrical breakdown. . ▫ High voltage requirement ▫ Potential for sample damage or degradation.

3.4. Copolymerization of PVDF

Copolymerization allows the modulation of intramolecular and intermolecular forces, enabling changes in properties like melting point, glass transition temperature, crystallinity, stability, elasticity, permeability, and chemical reactivity over a wide temperature range. The electroactive phase that could be achieved with Combining PVDF with trifluoroethylene (TrFE), hexafluoropropylene (HEP), chlorotrifluoroethylene (CTFE), or other polymer, modified for specific applications[33,173]. Table 5 shows the Advantages and applications of PVDF copolymers. Figure 26 shows the various PVDF copolymers chemical compositions.

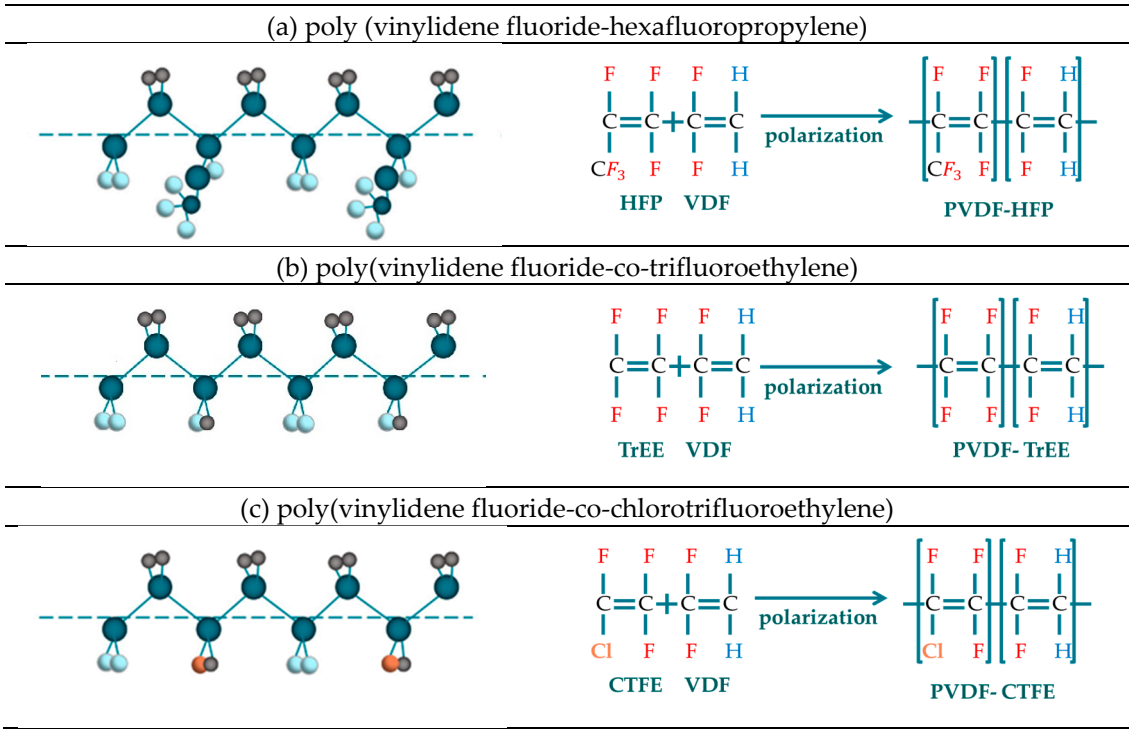

Figure 26. PVDF Co-Polymers (a) poly (vinylidene fluoride-hexafluoropropylene), (b) poly(vinylidene fluoride-co-trifluoroethylene), (c) poly(vinylidene fluoride-co-chlorotrifluoroethylene).

3.4.1. P(VDF-co-HFP)

One widely used PVDF co-polymer is poly (vinylidene fluoride-hexafluoropropylene), formed by polymerizing VDF (vinylidene fluoride) with HFP (hexafluoropropylene). The incorporation of bulky CF_3 groups from HFP significantly reduces crystallinity, adversely affecting the material's piezoelectric properties. However, in comparison to pure PVDF, flexibility increases significantly also can enhanced ferroelectric properties [174]. The addition of HFP results in an increase in fluorine content, which also improves hydrophobicity[175]. While its pyroelectric coefficient is higher, the piezoelectric co-efficient (d_{31}) is reportedly comparable to that of PVDF [176]. The high piezoelectric response makes P(VDF-co-HFP) suitable for applications in flexible energy harvesters, converting mechanical energy from vibrations and human motion into electrical energy. Due to its excellent ferroelectric properties, it is used in sensors and actuators that require materials with high sensitivity and flexibility.

 doi:10.20944/preprints202501.0023.v1

3.4.2. P(VDF-co-TrFE)

poly(vinylidene fluoride-co-trifluoroethylene) (PVDF-TrFE) is a PVDF copolymer synthesized by polymerizing VDF and TrFE. It has higher crystallinity and a preferred orientation, enhancing the electromechanical coupling factor [177]. The addition of TrFE facilitates the formation of the β-phase, allowing polarization without stretching. PVDF-TrFE exhibits a lower Curie temperature due to reduced interactions between units and dipole moments [122]. Its characteristic peak shifts to 19.9° and has a rod-like grain shape in the FTIR spectrum [34]. The introduction of TrFE improves the flexibility and mechanical strength of the polymer, making it suitable for dynamic applications additionally is used in the fabrication of flexible electronic devices, including wearable sensors and flexible displays, due to its high dielectric and piezoelectric properties.

3.4.3. P(VDF-co-CTFE)

High flexibility, electromechanical response, elongation, and superior cold resistance are characteristics of P(VDF-co-CTFE), a semi-crystalline polymer with a lower degree of crystallinity than PVDF [35]. Its higher piezoelectric constant and the presence of Cl and F elements enhance safety and improve mechanical properties [178]. Its C-Cl bond offers an active site for modification, making it a promising membrane material.additionally CTFE enhances the polymer's thermal stability and ferroelectric properties, making it more suitable for high-temperature applications is ideal for sensors and devices that operate in high-temperature environments, such as industrial monitoring equipment Its excellent piezoelectric properties make it suitable for biomedical devices that require precise sensing and actuation, such as medical implants and diagnostic equipment [179].

Table 5. Advantages and applications of PVDF copolymers.

Polymer	Advantage	Applications
PVDF	▪ High degree of crystallinity ▪ Excellent mechanical properties ▪ Chemical resistance.	▪ Sensors actuators ▪ Energy generation ▪ Energy storage ▪ Microfluids ▪ Biomedical
Poly (VDF-co-TrFE)	▪ Directly crystallizes from melt into electroactive phases ▪ Modified crystallinity ▪ High piezoelectric constant ▪ Thermal hysteresis, high electric output ▪ Sensitivity, Flexibility	▪ Sensors actuators ▪ Energy generation ▪ Energy storage ▪ Environmental monitoring and remediation ▪ Microfluids ▪ Biomedical applications
Poly (VDF-co-HFP)	▪ Chemically inert ▪ lower crystallinity due to bulky CF3 groups ▪ High d_{31} piezoelectric constant	▪ Energy storage ▪ Environmental monitoring and remediation
Poly (VDF-co-CTFE)	▪ Optimized piezoelectric properties ▪ High electric-energy density. ▪ High electrostrictive strain response ▪ High dielectric constant ▪ Hroader ferroelectric hysteresis loops	▪ Energy storage

3.5. PVDF Composites

PVDF Composites due to the intriguing qualities of PVDF, there is a great deal of interest in this material, which has led to its combination with certain fillers to create high-performance, multifunctional PVDF-based composites with unique morphologies and physicochemical characteristics. PVDF-based composites, then, are the outcome of combining one or two different

 doi:10.20944/preprints202501.0023.v1

fillers with complimentary qualities to enhance certain particular traits or to introduce new ones, such magnetic or electrical conductivity.

3.5.1. Fillers

According to reports [180], there are PVDF composites with over 30 distinct fillers. In order to decrease the amount of filler and improve functionality, it has been popular recently to build PVDF composites by adding several fillers with complimentary qualities [180]. Magnetic nanoparticles (CoFe2O4 or Fe3O4) [181], carbon nanotubes (CNTs)[182], ceramic particles like barium titanate (BaTiO3) [183], zinc oxide (ZnO) [184–185], titanium dioxide (TiO2)[186] , zeolite, or clays [187] are among the most representative and frequently used fillers in PVDF and its copolymers-based composites. Figure 27 shows the effect of various nanofillers on PVDF properties and their applications. These fillers also encourage the development of a wide range of multifunctional composite materials. PVDF composites are intriguing due to the fact that the final properties may be precisely controlled by appropriate filler size, shape, and content selection, as well as through filler and polymer interaction, dispersion, interface, and processing conditions[188].

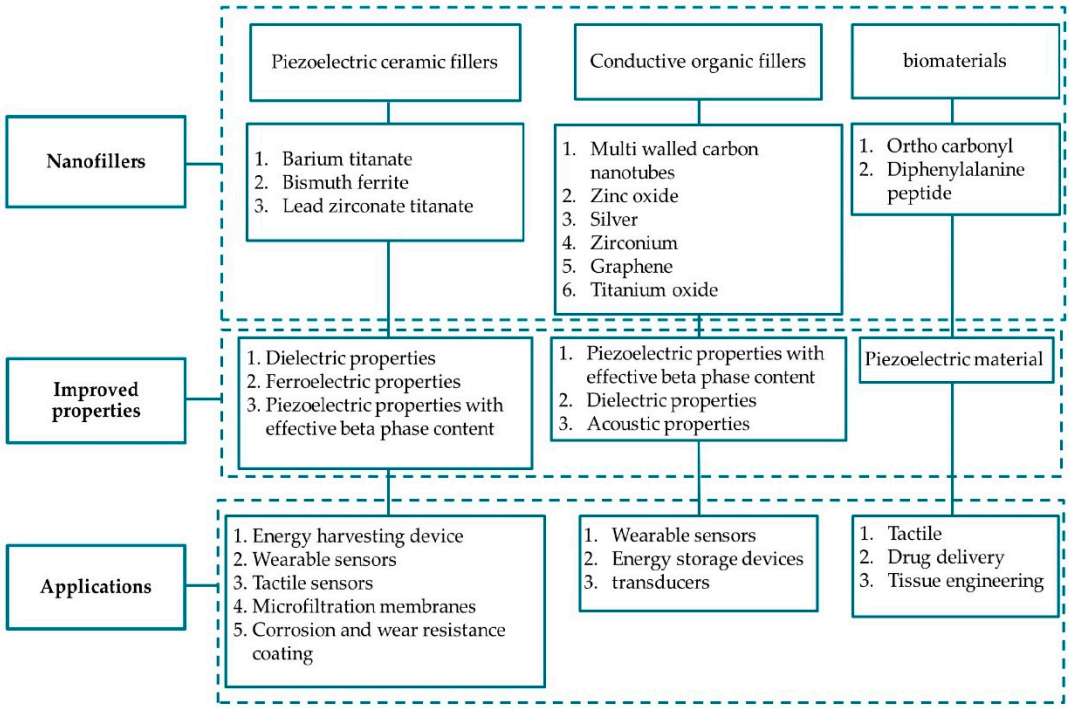

Figure 27. Effect of various nanofillers on PVDF properties and their applications.

3.5.2. Enhanced Piezoelectric Properties by PVDF Blend with Polymers.

PVDF and its copolymers are often blended with various polymers to enhance their properties. The classifications of thermoplastics blending are given in Figure 28. Common blends include poly(methyl methacrylate) (PMMA) [189] ,poly(o-methoxyaniline) (POMA), poly(aniline) (PANI)[190], poly(L-lactic acid) (PLLA) [191] poly(ethylene terephthalate) (PET) [192] , poly(vinyl chloride) (PVC) [193], poly(ethylene oxide) (PEO) [194],poly(vinyl alcohol) (PVA) [195], poly(carbonate) (PC)[196] and poly(amide 11) (PA11)[197]. These blends better processability, induce certain crystalline phases, and adjust electrical and optical properties.

Preprints.org (www.preprints.org) | NOT PEER-REVIEWED | Posted: 2 January 2025 doi:10.20944/preprints202501.0023.v1

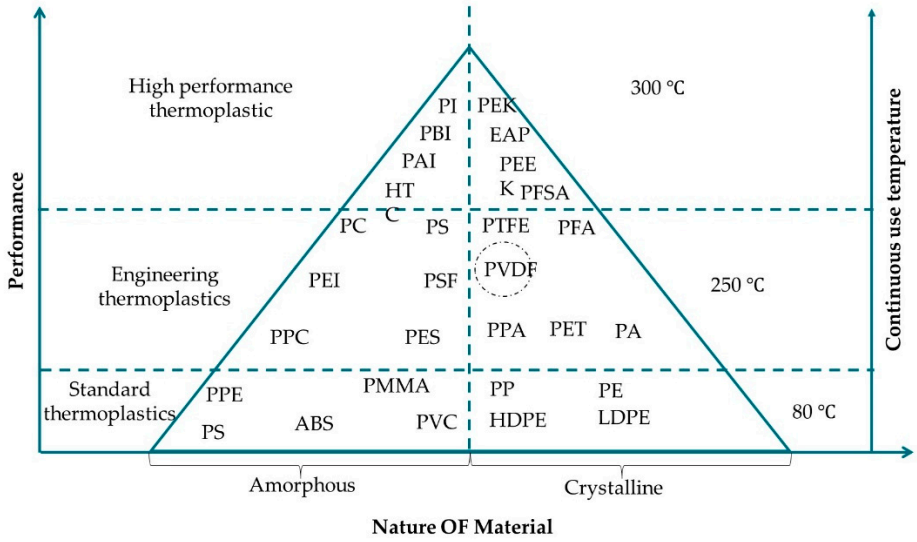

Figure 28. The classification of thermoplastics blending criteria [198].

The PVDF/PMMA blend stands out, as it promotes β-phase formation and enhances the piezoelectric effect [199]. This blend is used in optical applications [200] , Li-ion battery separators [201], wettability switching [202] , pyroelectric applications, and protective coatings. Another notable blind/mixture is PVDF/PLLA, combining two piezoelectric polymers for energy harvesting mechanisms. PVDF is also blended alongside conductive polymers like polypyrrole (PPy)[203], PANI[204], and PEDOT[205], making it ideal for probes in actuators, sensors, and medical applications. For improved dielectric flexibility and strength, PVDF is blended with poly(VDF-ter-TrFE-ter-CFE), suitable for dielectrics and energy storage owing its enhanced dielectric breakdown strength and modulus of elasticity[205]. Nowadays, PVDF blends alongside various ILs have been established, offering tunability for applications ranging from biomedicine to store energy [206]. These blends enhance processability, induce specific crystalline phases, and fine-tune optical and electrical properties. Table 6 shows advantages and applications of PVDF blend with polymers.

Table 6. Advantages and applications of PVDF blend with polymers.

PVDF blend with polymers	Advantage	Applications	Ref
PVDF/PMMA	promotes the formation of the β-phase	• Optical applications • pyroelectric application • as a coating	[207], [208]
PLLA/PVDF	Improved biodegradability	• energy harvesting devices	[209], [210]
PVDF/ ILs	-	• biomedicine to energy storage	[211], [212]

4. Material Property Characterizations and Techniques

Several characterisation methods, such as differential scanning calorimetry (DSC), Fourier transform infrared (FTIR) spectroscopy, and X-ray diffraction (XRD), have been widely used to measure the phase composition and comprehend the features of PVDF. Measurements of polarity switching are then employed to determine the material's overall polarization. Additionally, Raman spectroscopy has been used more recently. This section will focus on the methods used to characterize the mechanical, electrical, thermal, structural, and electromechanical characteristics as well as how they affect PVDF.

The characterization methods for comprehending PVDF's fundamental properties are compiled in Figure 29 [213]. The complete crystallinity capability, which includes all non-amorphous phases

 doi:10.20944/preprints202501.0023.v1

that can be achieved by DSC is demonstrated by Figure 29(a) . Figure 29(b) illustrates how FTIR, XRD, and Raman spectroscopy investigations contribute to determining the relative quantities of the crystalline phases. While Figure 29(c) shows the P-E hysteresis for net polarization after poling process. Table 7 represents the popular techniques for characterizing PVDF, detailing its material, thermal, and electrical properties.

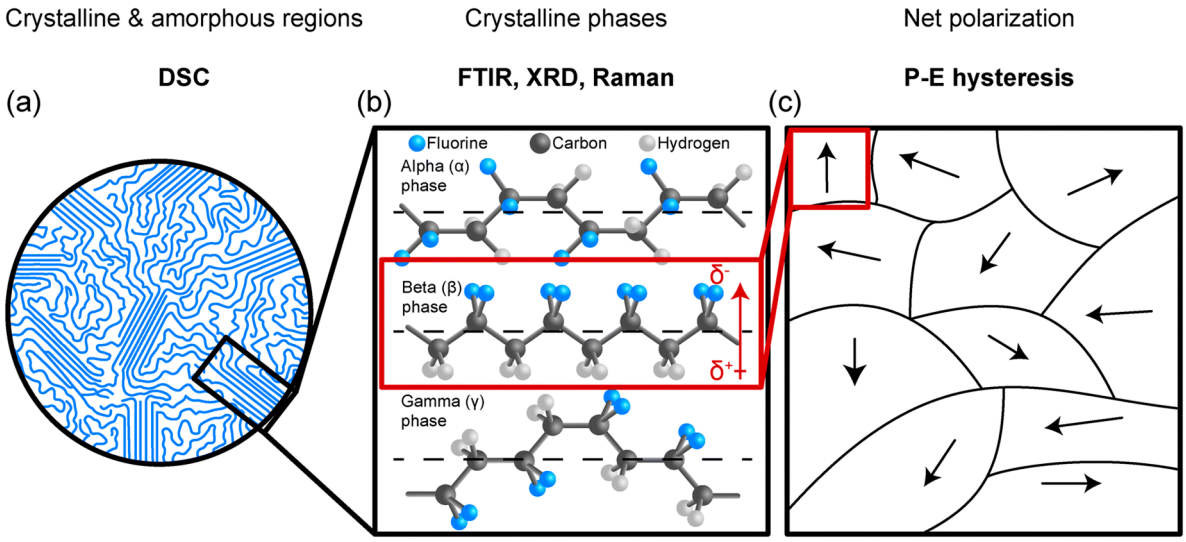

Figure 29. Different methods used for PVDF characterization a) Crystalline and amorphous regions-DSC b) Crystallin phases – FTIR,XRD,Raman c) Net polarization P-E hysteresis [213].

Table 7. The characterizations methods for various properties of PVDF.

Properties	Characterization methods	Determining parameters
Thermal characterization	Differential Scanning Calorimetry (DSC)	Melting point, Glass transition temperature, Crystallization temperature.
	Thermogravimetric Analysis (TGA)	Thermal stability, Degradation behavior.
Structural characterization	X-ray Diffraction (XRD)	Crystal phases (α, β, γ), Crystallinity percentage.
	Fourier Transform Infrared Spectroscopy (FTIR)	Characteristic peaks of various crystal phases.
Mechanical characterization	Universal testing machine(UTM)	Tensile strength, Young's modulus, Elongation at break.
	Dynamic Mechanical Analysis (DMA)	Viscoelastic behavior,
Electrical characterization	Dielectric Spectroscopy	Dielectric constant, Loss tangent over frequency.
	Conductivity Measurements	Electrical conductivity.
Dielectric	Impedance Analyzer	Dielectric constant, Loss tangent as a function of frequency.

 doi:10.20944/preprints202501.0023.v1

Ferroelectric characterization	Ferroelectric Loop Tracer	Polarization-electric field (P-E) hysteresis loops.
	Switching Spectroscopy	Domain switching dynamics.
Electromechanical characterization	Strain Gauge	Strain generated by electric field.
	Laser Interferometry	Displacement due to electric field.
Piezoelectric characterization	d_{33} Meter	Piezoelectric charge coefficient (d_{33}).
	Piezo response Force Microscopy (PFM)	Piezoelectric domains, Piezoelectric coefficients.
Pyroelectric characterization	Pyroelectric Current Meter	Pyroelectric current caused by temperature variation.
	Electrocaloric Effect Measurements	Temperature change induced by electric field.

4.1. Thermal Characterization

For thermal characterizations the two basic equipment's are commonly used, the Differential Scanning Calorimetry (DSC), and Thermogravimetric Analysis (TGA). DSC measures the heat flow associated with phase transitions, such as melting and crystallization. It can be used to determine the crystallization temperature, melting temperature, and degree of crystallinity of PVDF. Figure 30 displays an example of available DSC equipment that measures the temperatures and heat flows related to a material's thermal transitions. In research, assurance of quality, and industrial applications, DSC is frequently used for material inquiry, selection, comparison, and end-use evaluation of performance. Properties measured by TA Instruments' DSC techniques include glass transitions, "cold" crystallization, phase changes, melting, crystallization, product stability, cure / cure kinetics, and oxidative stability. TGA measures the weight loss of a sample as a function of temperature. It can be used to determine the thermal stability of PVDF and identify potential degradation processes, examples of available TGA equipments is shown in Figure 31 [214].

Figure 30. Thermal analysis apparatus Differential Scanning Calorimeters, Discovery DSC 250 (www.tainstruments.com).

Figure 31. Thermogravimetric instrument for high temperature and high-pressure thermogravimetric analysis. Discovery HP TGA – High Pressure TGA (www.tainstruments.com).

An example of illustration of PVDF engineering stress-strain curves under uniaxial tensile deformation at various temperatures is shown in Figure 32 [150] . The yield point is shown by red arrows, the long period's greatest value by green arrows, the start of the α–β transition by blue

 doi:10.20944/preprints202501.0023.v1

arrows, and the moment at which the long period turns stable and low after reaching its maximum by cyan arrows. The fact that the phase change starts at almost the same strain at all temperatures is a striking phenomena. The beginning of the α–β transition occurs at the PVDF's orientational turning point. Figure 33 shows the temperature dependent yield stress and yield strain [150]. It can be seen that the yield strains remains same while yield stress value decreases with the increase of temoerature.

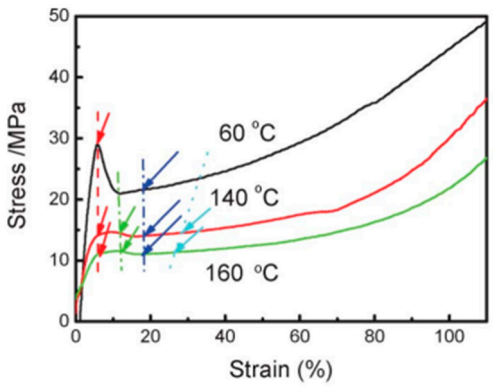

Figure 32. PVDF's engineering stress-strain curves at various temperatures under uniaxial tensile deformation [150].

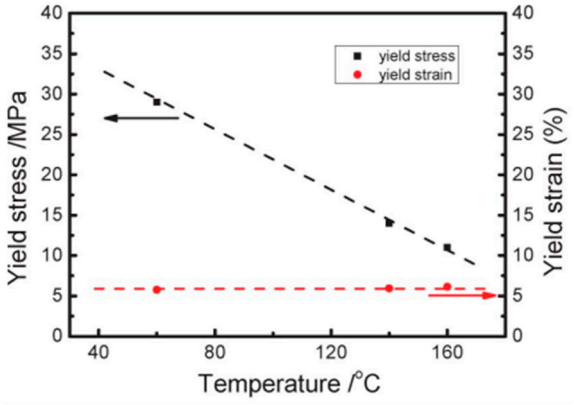

Figure 33. Yield stress and yield strain at verious temperatures[150].

4.2. Structural Characterization

For structural characterization most commonly two techniques are used FTIR Spectroscopy, and XRD. The XRD technique is used to determine the phase composition, and crystal structure of PVDF. It can help identify the presence of distinct crystalline phases, such as α, β, γ, and δ. The FTIR Spectroscopy is utilized to recognize the functional groups exhibit in PVDF. It can also be employed to study the degree of crystallinity and the alignment of polymer chains. The examples of FTIR Spectrometers instrument and XRD device used for structural characterization are shown in Figure 34 [214], [215–216].

Figure 34. FTIR Spectrometers: a) Nicolet™ iS50 FTIR Spectrometer https://www.thermofisher.com/ ,.

b) Vertex80 model (Bruker Instruments, Germany).

 doi:10.20944/preprints202501.0023.v1

The example of crystalline structural characterisation using FTIR and WAXD (wide-angle X-ray diffraction) for BOPVDF (biaxially oriented poly(vinylidene fluoride)) is displayed in Figure. 35 [214]. Where the 2D WAXD patterns were used to create the one-dimensional (1D) WAXD profiles at room temperature as seen in Figure. 35(a). The machine direction (MD) is vertical, and the X-ray beam is transverse direction (TD). It also labels the main reflections for the α and β crystals where only the β crystal reflections (310)β, (110/200) β, (001)β, (220)β, (201)β, (221)β, and (311)β, were found for the strongly poled BOPVDF film. The FTIR spectra analysis for the poled and fresh BOPVDF films in the transmission mode are displayed in Figure 35(b), where the α and β crystals' absorption bands are designated. According to this analysis, all α crystals were changed into β crystals by the high-field electric poling, while the overall crystallinity remained unchanged. This is confirmed by the FTIR measurement, which showed that all of the α absorption bands were vanished. Following lengthy unipolar poling at 650 MV/m, the BOPVDF film effectively produced pure β-phase crystals, according to the WAXD and FTIR data.

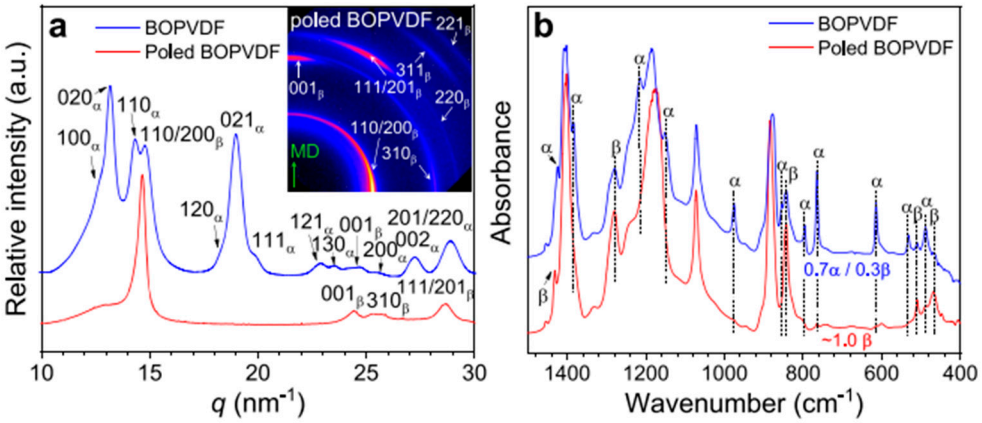

Figure 35. Structural characterization by WAXD and FTIR. (a) BOPVDF films at room temperature are profiled using 1D WAXD, (b) The FTIR spectra analysis for the poled and fresh BOPVDF films in the transmission mode [214].

4.3. Mechanical Characterization

4.3.1. Tensile Testing

Tensile Strength measures PVDF's resistance to stress, while Young's Modulus reflects its rigidity. Both are typically evaluated through tensile testing using a Universal Testing Machine (UTM), where sample thickness and internal stress conditioning are vital for accuracy. Figures 36 and 37 shows the examples of commercially available UTMs for tensil testing.

 doi:10.20944/preprints202501.0023.v1

Figure 36. Nano mechanical testing system Hysteron TI Premier II(www.Bruker.com).

Figure 37. The Model 5965 UTM are designed to perform tensile, compression etc (www.instron.com).

Figure 38 pictorially demonstrates the example of experimental setup for tensile and flexural tests. The apparatus consists of UTM by Tinius Olsen H25KT, Video extensometer Tinius Olsen VEM 300, embedded vision system ADLINK EOS-1200, CCD camera Allied Vision Manta G-146B, and computer machine. UTM is used to carry out experiments at room temperature, where different load cells according to requirements can install during testing procedure. Video extensometer is utilized for strain analysis. The tripod-mounted monochrome CCD camera, which has an optics-correctable lens, is placed in front of the machine, 300 mm away from the specimen. Horizon, a Tinius Olsen program, is used to interpret data and control machines remotely[217].

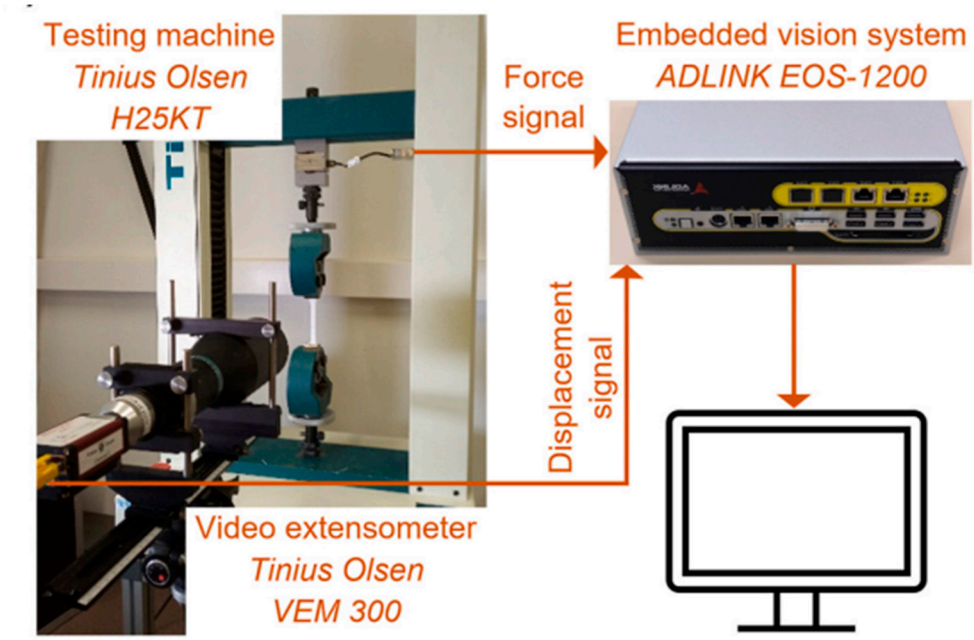

Figure 38. Tensile strength testing Experimental setup [217].

Farusil et al. [217] used this apparatus for tensile and flexural testing, where the specimens were clamped using wedge grips with hooked jaws, which were subjected to uniaxial tensile loading at 1

 doi:10.20944/preprints202501.0023.v1

mm/ min rate. A custom-made guide provided precise longitudinal alignment of the clamped specimens with the machine vertical axis. The displacements is observed with the video extensometer. Load forces and displacements were measured till specimen break. Tensile strength was calculated by dividing the value of peak force by the cross-sectional area of the specimen. Figure 39 shows the tensile stress verses tensil strain calculated for various patteren structures of PVDF homopolymer and PVDF copolymer specimens.

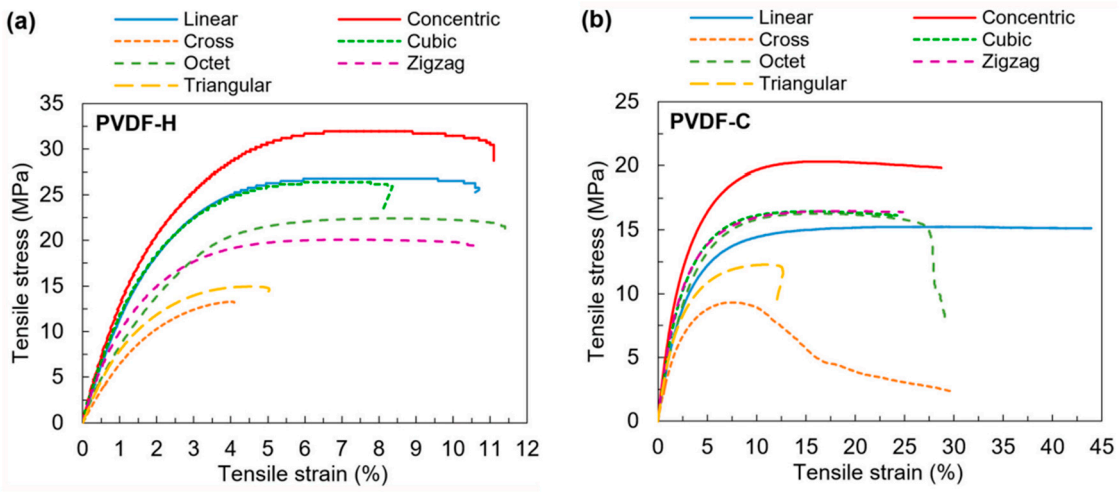

Figure 39. Tensile Stress verses tensil strain curves of specimens printed with various crystalline patterns by using (a) PVDF-homopolymer and (b) PVDF-copolymer [217].

In order to determine the compression modulus shown in Figure 40(a) in the normal direction of the BOPVDF sheet, a Nano Indent experiment was carried out using a Nano Indenter G200 (Agilent Technologies, USA) at a constant strain rate of 0.05 s^{-1} with a maximal indentation width of 1 μm [214]. The Young's modulus of the BOPVDF film shown in Figure 40(b) was determined using tensile tests on a UTM (Model 5965, Instron Instruments, USA), in both the machine direction and the transverse direction. The highest values of k3j (j = 1, 2, and 3) are also shown [214].

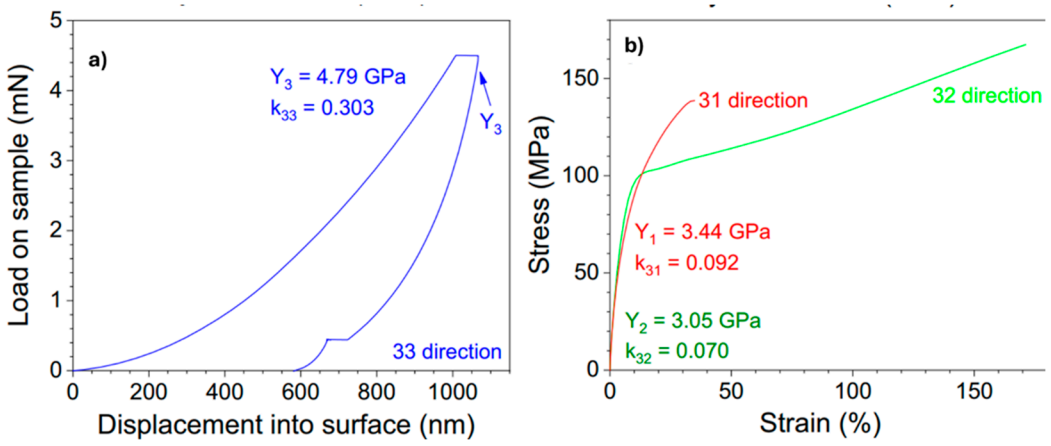

Figure 40. Tensil test for highly poled PVDF film (a) Compression modulus (Y3) is obtained by nanoindentation, (b) tensile moduli (Y1 and Y2) are obtained from the stress-strain curves [214].

The example of elastic modulus graph versus temperature for PVDF film is shown in Figure 41. Where elastic modulus was tested in order to calculate the elastic energy density, a crucial characteristic for many transducers. Furthermore, it displays the data for the stretched film exposed to 60 Mrad radiation at 95 °C along the drawing direction and the unstretched film exposed to 60

 doi:10.20944/preprints202501.0023.v1

Mrad radiation at 120 °C. It shows that the stretched film's elastic modulus Y along the drawing direction is significantly greater than the unstretched film's. The stretched film's modulus is 1.3 GPa at room temperature (around 20 °C), but the unstretched film's modulus is 0.4 GPa [218].

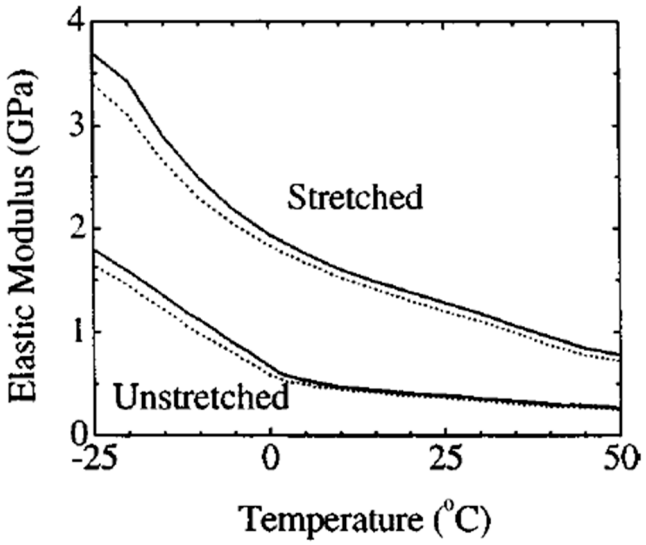

Figure 41. The elastic modulus for both stretched and unstretched materials as a function of temperature. The data recorded at 1 and 10 Hz are represented by the dots and solid lines, respectively[218].

4.4. Electrical Characterization

The dielectric constant measures PVDF's ability to store electrical energy, essential for energy storage applications. Impedance analyzers or LCR meters are used to measure it across frequencies, with PVDF placed between electrodes in a controlled electric field. Uniform electrode deposition (e.g., silver or aluminum) and controlled sample thickness are crucial for accuracy. Dielectric spectroscopy is used to study the dielectric properties of PVDF, such as permittivity and dielectric loss. These properties are important for applications like energy storage and insulation. Figure 42 shows the dielectric test system consist of a test fixture for temperature chamber and material charge device [55]. This turnkey dielectric test device measures the dielectric constant/loss (impedance) in relation to frequency and temperature. Figure 43 shows the example of dielectric constant with respect to temperature in range of -25 to 100˚C for PVDF-TrFE-CFE. It can bee seen that value of dielectric constant increases as rising of temperature due to the molecular motion and phase transition effect. As the temperature increases, the molecular motion enhance the dipole orientation due to applied electric field, which produce higher dielectric constant of PVDF. PVDF features a variety of crystalline phases, including α, β, γ, and others. Phase transitions brought on by temperature have the potential to drastically change the dielectric constant. Therefore, the dielectric constant is significantly rise as a result of transitions to the strongly polar β phase.

 doi:10.20944/preprints202501.0023.v1

Figure 42. Dielectric test system a test fixture along with dielectric material charge system[55].

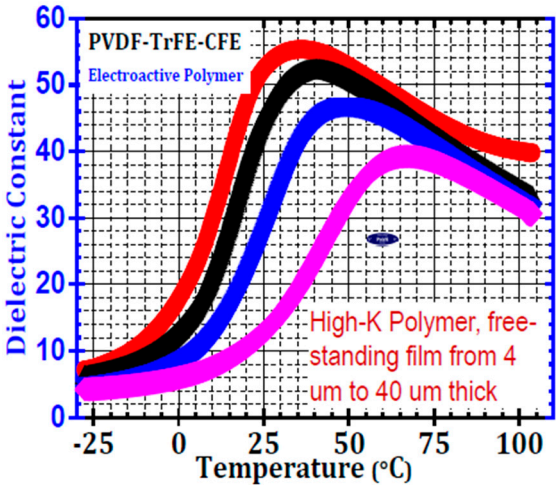

Figure 43. Dielectric constant for various temperature of PVDF-TrFE-CFE [55].

4.4.1. Ferroelectricity

Polyvinylidene fluoride (PVDF) is a fascinating material known for its unique ferroelectric properties. To understand these properties, we often visualize them using a polarization vs. electric field (P-E) loop. A P-E loop is a graphical representation of how a material's polarization (electric dipole moment per unit volume) changes in response to an applied electric field. It's a bit like a hysteresis loop, showing how the material "remembers" its past state even after the external stimulus (electric field) is removed. The high voltage dielectric and polarization loop test system, depicted in Figure 44, is an example of a commercially available fully automated test system that enables consumers to measure the dielectric breakdown strength, consequently provide the charge-discharge efficiency, energy density, and obtain the polarization loop of ferroelectric and dielectric materials. (www.piezopvdf.com) Another highlighted instrument utilized [214] for P-E loop measurement is a Premiere II ferroelectric tester (Radiant Technologies, Inc., Albuquerque, NM) shown in Figure 45.

Preprints.org (www.preprints.org) | NOT PEER-REVIEWED | Posted: 2 January 2025 doi:10.20944/preprints202501.0023.v1

Figure 44. Dielectric Material Charge Measurement System [55].

Figure 45. Premier II Ferroelectric Test System (Radiant technology) www.ferrodevices.com.

Figure 46 shows the P-E loop for commercial piezoelectric PVDF polymer, when subjected to an increasing electric field, exhibits a characteristic P-E loop (www.piezopvdf.com).As an electric field is applied, Initially, the dipoles in PVDF are randomly oriented. These dipoles start to align with the field, leading to an increase in polarization. At a certain field strength, most of the dipoles are aligned, and the polarization reaches a saturation point. When the electric field is reduced to zero, the dipoles don't completely return to their random orientation. A certain amount of polarization, known as remnant polarization (Pr), persists. To completely reverse the polarization, a reverse electric field, called the coercive field (Ec), must be applied. Hysteresis Loop: The loop formed by the polarization changes as the electric field is cycled is known as the hysteresis loop. The area enclosed by this loop represents the energy loss during each cycle.

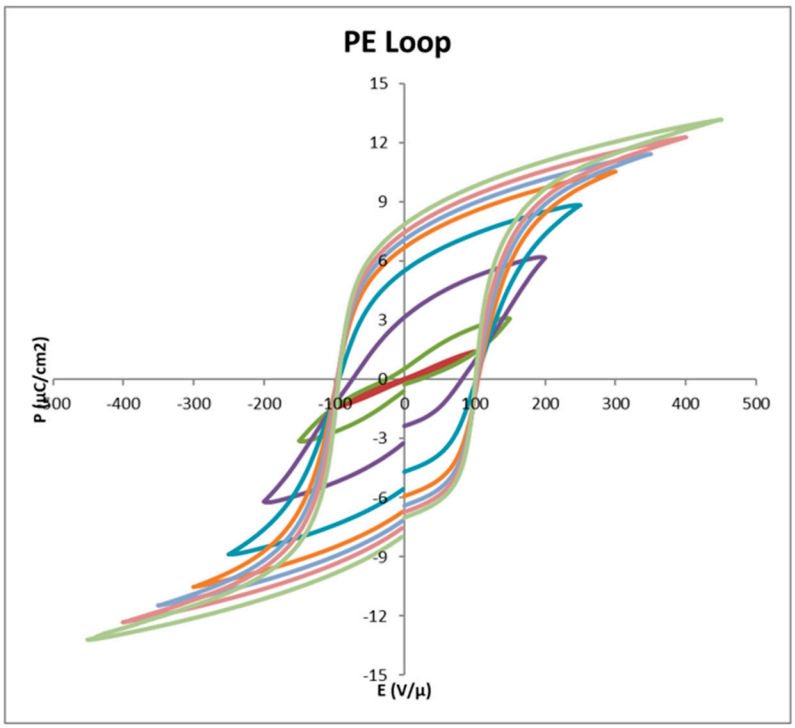

Figure 46. P-E loop for commercial piezoelectric PVDF polymer provided by PolyK Technologies [55].

4.5. Electromechanical Properties

PVDF (Polyvinylidene Fluoride) is a versatile polymer known for its unique electromechanical properties. Its capability to produce electrical energy from mechanical energy and vice versa makes

 doi:10.20944/preprints202501.0023.v1

it a significant material for various applications, including sensors, actuators, and energy harvesting devices. To characterize these properties, several techniques are employed:

4.5.1. Piezoelectric Coefficient by Direct Methods

To perform the piezoelectric coefficient characterization of PVDF, researchers utilized many techniques and equipment's. The most popular procedures at the moment are the quasi-static, dynamic, Interferometric, static, and acoustic testing methods.

The commercially available highlighted equipment's includes "Berlincourt Quasi Static d_{33} meter" (www.piezopvdf.com) shown in Figure 47, and "Radiant's Thin Film Piezoelectric Test Bundle" (www.ferrodevices.com) shown in Figure 48. The characterization can be done by either direct or converse piezoelectric effects methods.

Figure 47. Berlincourt Quasi Static d_{33} meter[55].

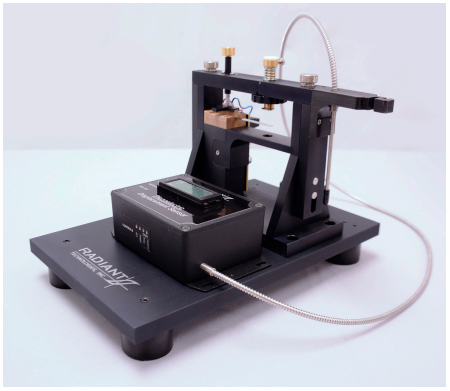

Figure 48. Radiant's Thin Film Piezoelectric Test Bundle www.ferrodevices.com.

Quasi-Static Method

The main setup for the quasi-static method of evaluating PVDF piezoelectric properties is shown in Figure 49. The operational principle of this basic berlincourt d_{33} meter consist of multiple steps, initially piezoelectric sample is mounted onto the meter's probe and properly clamped, and a small oscillating force is applied to the sample through the probe. The electrical charge produced by the piezoelectric effect is then measured by the meter's sensitive electronics. The d_{33} coefficient is calculated by dividing the measured charge by the applied force. This method includes gradually increasing mechanical stress on the material and measuring the consequent electrical displacement. Several studies have focused on different measuring methods to investigate how fabrication methods influence the piezoelectric coefficient d_{33} of PVDF. For example, Satthiyaraju et al.[160] employed the quasi-static method to measure the d_{33} of annealed PVDF nanofibers, demonstrating that annealing significantly improved the piezoelectric performance by enhancing both the d_{33} coefficient and the β-phase content.

The quasi-static method used equations (18-19) to characterize the piezoelectric properties of PVDF film [108].

$$Q = d_{33} A \sigma \quad (18)$$

$$d_{33} = Q_{sample} / F_{Dynamic} \quad (19)$$

where Q is the accumulated charge, d_{33} is the piezoelectric coefficient, A is the sensing area, and σ is the applied stress.

 doi:10.20944/preprints202501.0023.v1

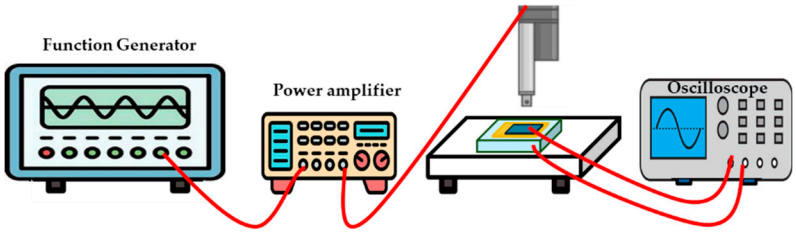

Figure 49. Setup of quasistatic measurement for PVDF films.

Hang et al. developed an equipment phase sensitive d_{33} meter and utilized the direct piezoelectric effect for characterization of PVDF in 1993 [219]. This high sensitivity, phase sensitive d_{33} meter system was used to measure d_{33} value of 1pC/N at phase angle 0.05°and its schematic diagram for complete setup is shown in Figure 50. However, its operational principle was based on basic berlincourt d_{33} meter.

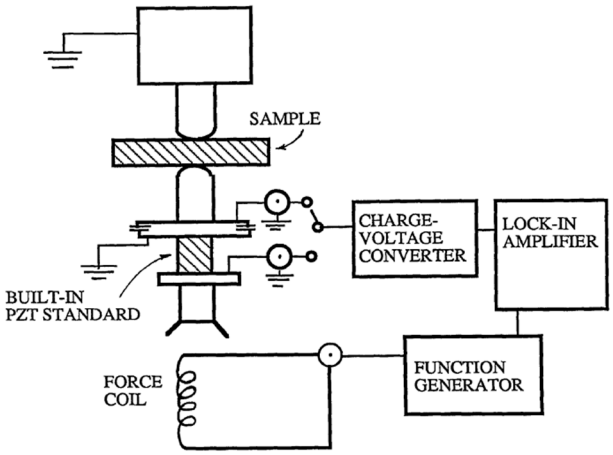

Figure 50. A schematic diagram of high sensitivity, phase sensitive d_{33} meter system [219].

Dynamic Method

The dynamic method, unlike the quasi-static approach, applies a high-frequency force to the material to measure the resulting voltage. The setup involves placing the sample on a mass connected to an exciter providing sinusoidal acceleration shown in Figure 51. This configuration evaluates the piezoelectric coefficient by varying parameters like frequency and amplitude, making it suitable for sensor and actuator applications. Dynamic methods are divided into cyclic loading and vibration modal techniques, which utilize the transient effect of PVDF to generate regular electrical signals[220]. The dynamic method is governed by the relationship between the applied stress (σ), the generated electric field (E), and the frequency of the applied force (f). The piezoelectric charge constant (dij) and voltage response (gij) can be expressed in equations (20-21).

$$d_{ij} = \frac{Q}{\sigma} \tag{20}$$

$$g_{ij} = \frac{E}{\sigma} \tag{21}$$

Where, Q is the charge generated by the material, σ is the applied oscillatory stress, E is the electric field generated in response to the applied stress, d_{ij} represents the piezoelectric charge constant, and g_{ij}represents the voltage response.

Preprints.org (www.preprints.org) | NOT PEER-REVIEWED | Posted: 2 January 2025 doi:10.20944/preprints202501.0023.v1

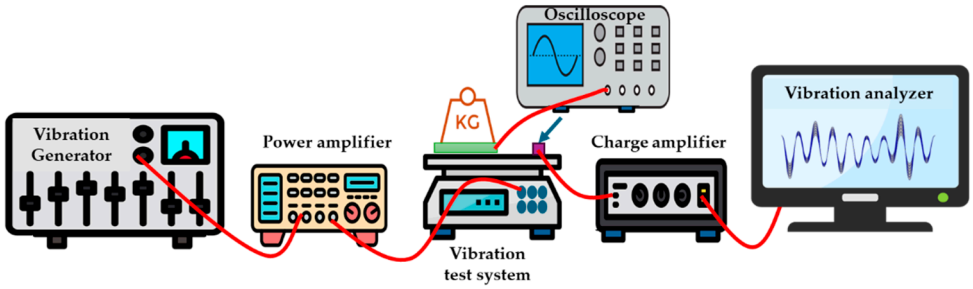

Figure 51. Setup of dynamic measurement method.

In dynamic method, the total pressure *p(t)* shown in equation (22), on the PVDF sample is the sum of a static load P_0 and a dynamic oscillating load $\hat{p}_d \cos(\omega t)$, where m is the mass, A is the sample area, g is gravity, and $g + \hat{a}\cos(\omega t)$ represents sinusoidal acceleration. The piezoelectric coefficient d_{33} is calculated by measuring the voltage response to these forces, which varies with frequency and amplitude. Although dynamic tests typically yield a slightly lower d_{33} value, they provide valuable insights into PVDF's sensor and actuator performance.

$$p(t) = \frac{m}{A}(g + \hat{a}\cos(\omega t)) = p_0 + \hat{p}_d \cos(\omega t) \quad (22)$$

Mrllík et al.[53] used dynamic testing to investigate the piezoelectric properties of PVDF films, focusing on the influence of harmonic oscillations on the material's electric charge response, ultimately demonstrating improved sensitivity in vibration-sensing applications. Aghayari et al.[221] used dynamic testing to assess PVDF's piezoelectric properties under cyclic loading, revealing enhanced electrical performance and stability, making the material suitable for applications in sensor technologies.

Acoustic Method

In the acoustic method, the piezoelectric material acts like a microphone, and its sensitivity is used to determine the piezoelectric coefficient. The method involves placing the sample on a back electrode and subjecting it to sound waves in an anechoic chamber to avoid external noise shown in Figure 52. The sensitivity of the microphone is calculated, which, together with the sample's capacitance and area, allows for the determination of the d_{33} coefficient. Although effective, the need for an anechoic chamber and the associated costs make this method more complex and expensive.

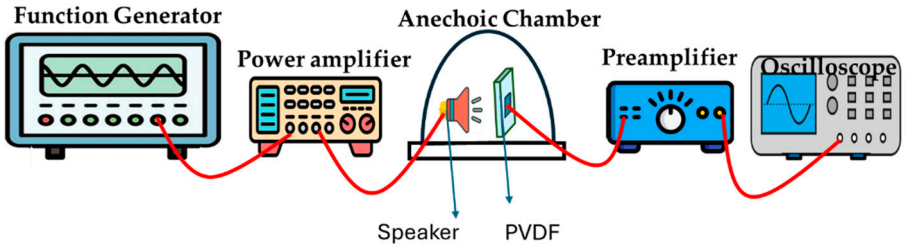

Figure 52. Acoustic method experiment setup.

The primary equation used in the acoustic method is based on the relationship between the sound pressure (P), the piezoelectric charge constant (d), and the resulting electric field (E), and induced strain(S) by the applied pressure as given in equation (23).

$$P = \left(E/_d\right) \times S \quad (23)$$

The acoustic method is particularly useful for measuring the piezoelectric charge constant (d) in applications that involve acoustic stimuli. This method can also be adapted to measure the voltage response of PVDF, which is crucial for understanding the material's performance in acoustic sensor applications. Electric displacement, which represents the charge per unit area generated by the

 doi:10.20944/preprints202501.0023.v1

material in response to sound pressure, can also be measured using the acoustic method. This measurement is critical for designing PVDF-based acoustic sensors.

Figure 53 displays the example of piezoelectric characteristics of PVDF where several piezoelectric coefficients are calculated by direct piezoelectric testing. Figure. 53(a) shows that d_{33} is negative and its absolute value rose as the applied dynamic stress increased. It is evident that a typical $|d_{33}|$ ~18 pC/N is attained below 0.1 MPa. The d_{33} value obtained using a d_{33} piezometer having a static load of 2.5 N is indicated by the red star. Figure 53(b) displays the stress-dependent d_{31} and d_{32} measurements. At 41 MPa, the highest values were d_{31} = 22 pC/N, and at 49 MPa, d_{32} = 18 pC/N [214].

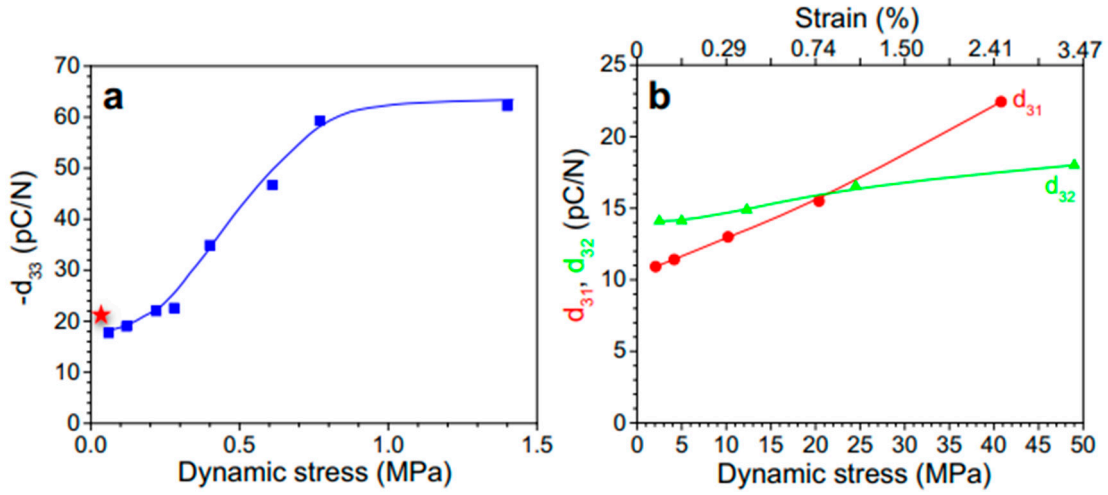

Figure 53. Several piezoelectric coefficients for highly poled BOPVDF film (a) d_{33}, (b) d_{31}, d_{32} as a function of dynamic stress.[214].

4.5.2. Strain Induced by Indirect Piezoelectric Effect

Interferometric Method

The interferometric method untilize laser interferometry based on the inverse piezoelectric effect. Although this method is less commonly used as compared to the quasi-static and dynamic methods, this technique offers high resolution and is effective over a broad frequency range. Figure 54 shows the interferometric basic setup, which involves fixing the sample on a probe table and observing it through a telescope while a laser interferometer measures displacement [222]. By measuring the vibration amplitude of the sample, the coefficient is derived from the ratio of this amplitude to the applied voltage which can be calculated using the following equation (24).

$$d_{33} = \frac{\Delta L}{\Delta F} \tag{24}$$

Where ΔL is the change in the sample's length, L is the original length, and ΔF is the applied force.

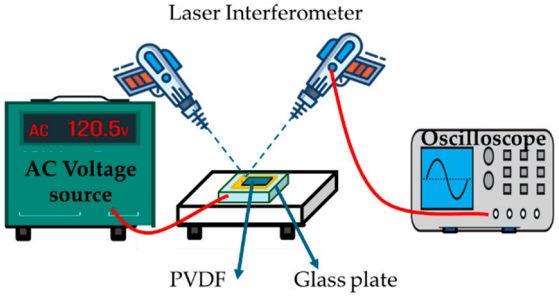

Figure 54. Interferometric method setup.

 doi:10.20944/preprints202501.0023.v1

The interferometric method is particularly effective for accurately measuring the piezoelectric charge constant (*dij*), especially in applications that require high precision. Chen et al.[223] used interferometric techniques to investigate the electromechanical behavior of PVDF-TrFE-FA tetrapolymers, revealing a significant improvement in electroactuation strain at low electric fields, achieving up to -3.3% strain at 50 MV/m. Chen et al.[224] utilized interferometric techniques to investigate the electromechanical properties of PVDF-based polymers, achieving an impressive d_{33} of -1050 pm/V and a coupling factor k_{33} of 88%, demonstrating high electroactuation at low fields. The example of PVDF strain shown in Figure 55 is measured using a dilatometer based on the cantilever beam[225]. The dilatometer is simple to use and can measure the transverse strain response of soft polymer films without requiring the sample to be mechanically constrained throughout a wide strain range. Under various load and temperature conditions, it can measure strain across a rather broad frequency range, from mHz to over 100 Hz.

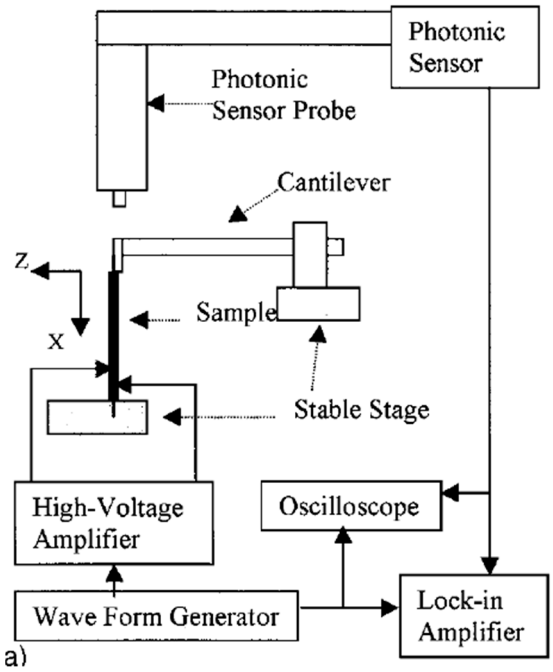

Figure 55. Schematic diagram for PVDF strain measurement setup dilatometer based on the cantilever beam.[225].

The transverse strain of a pure PVDF piezoelectric film at room temperature under various electric fields of 1 Hz is displayed in Figure 56. The frequency dependence of a PVDF piezoelectric film's transverse strain caused by an electric field is seen in Figure 57. The load impact on the electric field that caused the transverse strain response is depicted in Figure 6 for a 65/35 mol% PVDF-TrFE copolymer film that was exposed to radiation at 95 °C with a dose of 60 Mrad at room temperature with an applied electric field of 1 Hz. The relationship between the electric field and strain response for films under various loads is shown in figure 58(a). The relationship between strain response and static load for films at varying electric field strengths is depicted in Figure58 (b).

 doi:10.20944/preprints202501.0023.v1

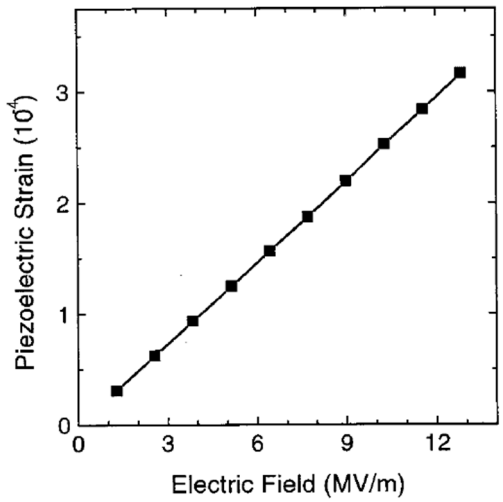

Figure. 56. Pure PVDF piezoelectric film's transverse strain at room temperature under various electric fields of 1 Hz.[225]

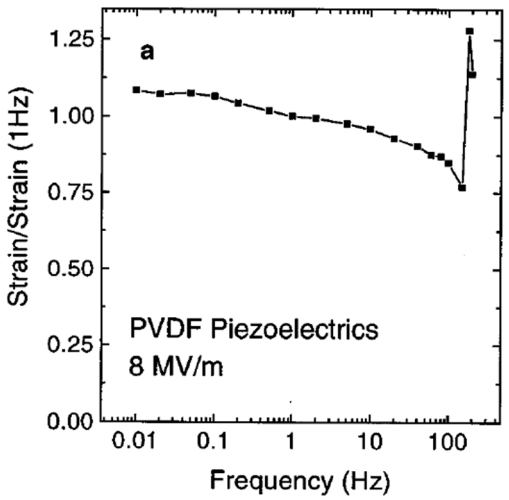

Figure. 57. Frequency dependence of the transverse strain caused by an electric field in a PVDF piezoelectric film.[225]

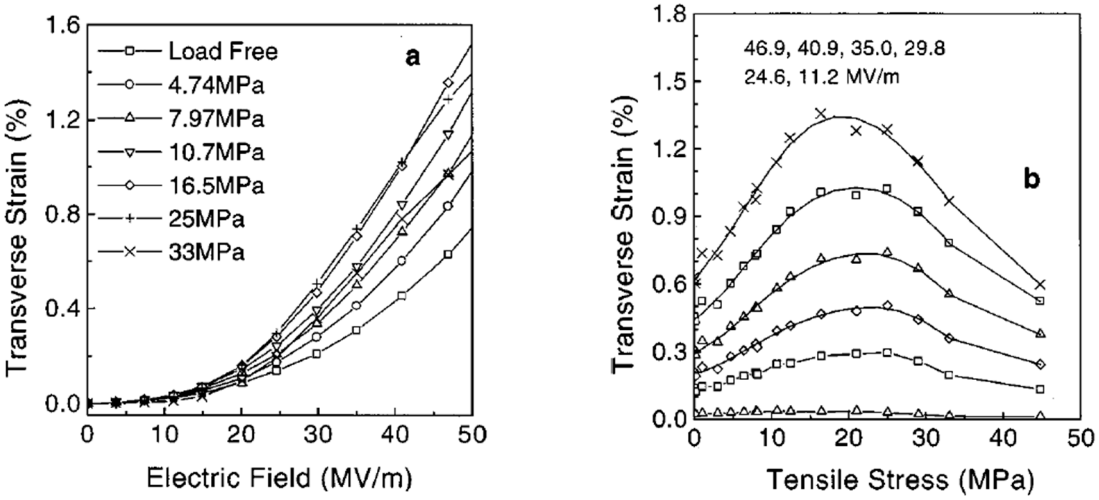

Figure. 58. Load effect on the electric field induced transverse strain response measured for PVDF-TrFE copolymer film, (a) Strain response as function of electric field for films under different loads b). Strain response and static load for films at various electric field strengths[225].

4.5.3. Resonance Methods

The coupling factor of a piezoelectric material may also be obtained using the resonance technique, which involves measuring its electrical impedance as a function of frequency near a specified resonance frequency[226]. The frequency variation of the dielectric properties of the stretched and irradiated P(VDF-TrFE) copolymer is illustrated in Figure 59[227]. The statistics indicate that both the dielectric constant and loss diminish with the application of a DC bias field. A distinct resonance is seen at a frequency range of 20-50 kHz, corresponding to the resonance along the sample's stretching direction. The resonance intensifies with an increase in the DC bias field. Based on the dielectric behavior seen in Figure 59, the sample's impedance and admittance may be computed. The series resonance frequency *fs*, corresponding to the maximal real component (*R*) of the impedance, and the parallel resonance frequency fp, corresponding to the maximal real component (*G*) of the admittance, may be determined from the frequency-dependent values of *R* and *G*. According to the standard procedure (IEEE Standard, 1988):

$$\frac{k_{31}^2}{1-k_{31}^2} = \frac{\pi}{2}\frac{f_p}{f_s}\tan\frac{\pi}{2}\frac{f_p - f_s}{f_s} \tag{25}$$

 doi:10.20944/preprints202501.0023.v1

$$\frac{1}{S_{11}^{E}} = 4\rho f_s l \tag{26}$$

Where S_{11}^{E} represents the elastic compliance in the stretching direction, ρ denotes the density, and l indicates the length in the resonance direction. The electro-mechanical coupling coefficient k_{31} of the specimen under various DC bias fields is computed, as illustrated in Figure 60[227]. The results demonstrate that the coupling factor in the sample remains rather constant across frequencies.

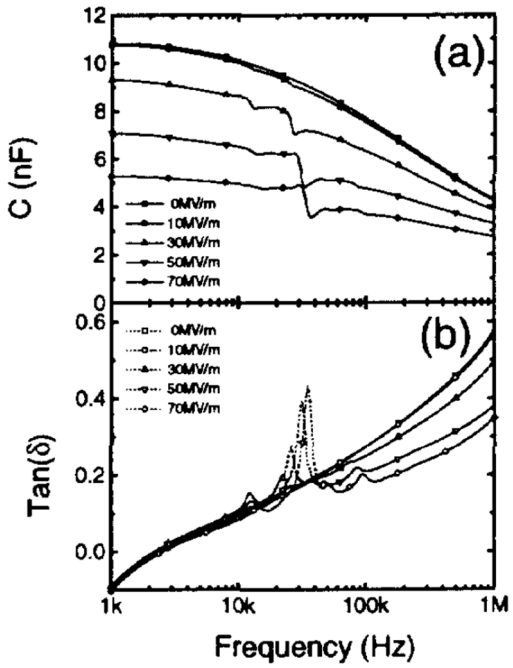

Figure 59 The impedance as a function of frequency (a) the capacitance, and (b) the dielectric loss[227].

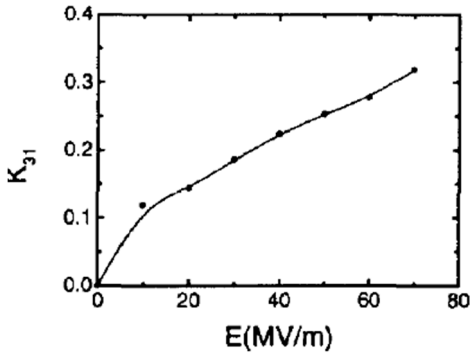

Figure 60 Electromechanical coupling coefficient vs. dc-bias fields for the copolymer[227].

4.6. Pyroelectric Coefficient

The Pyroelectric Coefficient represents the electric charge generated from temperature fluctuations, crucial for thermal detectors and infrared sensors. Measurement methods for the pyroelectric coefficient include direct measurement using a heating source and electrometer to record charge changes, with smooth electrodes ensuring uniform heating. Dynamic measurement can also capture pyroelectric current response under periodic temperature changes. The pyroelectric coefficient (p) can be calculated as p=ΔQA·ΔT ,where ΔQ is the charge generated, A is electrode area, and ΔT is temperature change. Pyroelectric current (I) is given by I=p·A·dTdt , with dT/dt as the temperature change rate. [128,228]. Example of pyroelectric PVDF films is shown in Figures 61 and 62 [128],.

Figure 61 illustrates that the maximum pyroelectric coefficient which is achieved with 1 wt% doping of Graphene-Oxide (GO). GO-doping can significantly enhance the pyroelectric characteristics of PVDF. Figure 62 shows the pyroelectric current for the 1 wt% GO-doping scenario is thrice that of the 2 wt% GO-doping scenario and tenfold that of the scenario without GO-doping. Excessive GO-doping will result in current leakage. High doping concentrations have been shown to reduce the figure of merit (FV) due to a substantial rise in the dielectric constant, resulting in a diminished pyroelectric signal.

 doi:10.20944/preprints202501.0023.v1

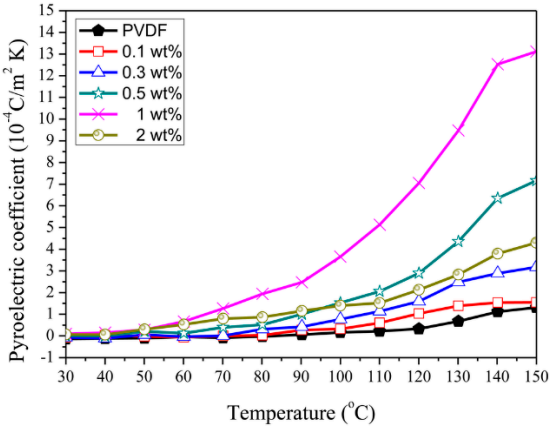

Figure 61 The pyroelectricities of PVDF film with various wt% GO-doping [128].

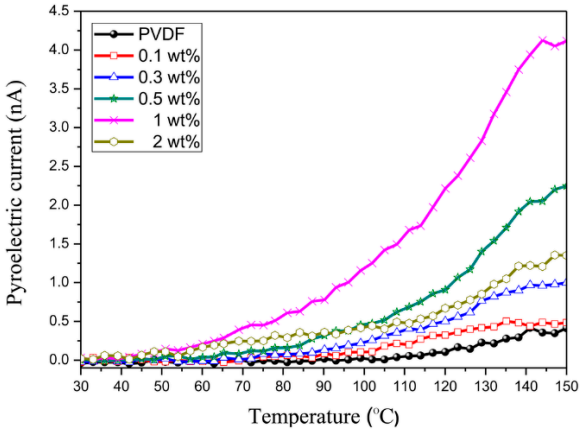

Figure 62 The pyroelectric currents of PVDF film with various wt% GO-doping [128].

5. Summary and Future Pespectives

This paper provides a comprehensive review of PVDF polymer films, their material properties, fabrication methodologies, and characterization methods. The PVDF material properties, including physical, mechanical, chemical, thermal, electrical, electromechanical are described in details. A special focus is given to the PVDF film fabrication methods that includes solution casting and coating, spin coating, hot pressing, electrospinning and 3D printing. Techniques like mechanical stretching, annealing, and electric field poling can enhance phase transition, resulting in improved piezoelectric and pyroelectric properties. Moreover, this article explores the characterization of PVDF material for thermal, structural, mechanical, electrical, and electromechanical properties, using various methods such as FTIR, XRD, DSC, PFM, UTM, TGA, dielectric test systems, ferroelectric test systems, piezoelectric test methods, dynamic measurement methods, electric field induced strain and actuation measurement methods, electromechanical coupling factor measurements, and pyroelectric coefficient measurements, providing insights into its properties and performance in various applications. Understanding these aspects can help optimize PVDF-based devices for energy harvesting, sensing, biomedical applications, radio-electronic devices, architectural coating, printed circuit boards, non-destructive testing, environmental monitoring, and manymore, driving advancements in these fields.

Although various new PVDF-based copolymer and terpolymers as well as nanocomposites are developed recently, most of those materials have not been comprehensively characterized for device application. Colaberations among material sienctists, mechanical and electrical energineeriing, and device delvelopers might accelerate the research in this field. In addition, adopt ferroelectric ceramic research methods into PVDF research is another approach.

Considering the lengths of this paper, we do not include the review of PVDF-based devices, such as sensors, actuators, transducers, and energy harvesters. We will provide another comprehensive review on the specific device issue in the near future.

Author Contributions: "Conceptualization, TB.Xu. and S. N; methodology,S. Z. and S.N.; formal analysis, S.N.; investigation, S.N and N.A; resources, TB.Xu.and S. Z.; data curation, N.A, .S.N,and S. Z; writing—original draft preparation, N.A and S.N.; writing—review and editing, TB.Xu.; visualization, S.N and N.A.; supervision, TB.Xu.; project administration, TB.Xu.; funding acquisition, TB.Xu. All authors have read and agreed to the published version of the manuscript.".

Funding: "This research was sponsored by the Office of Naval Research and was accomplished under Grant Number W911NF-23-1-0177".

Data Availability Statement: In this review paper no new data were created.

Conflicts of Interest: The authors declare no conflicts of interest.

 doi:10.20944/preprints202501.0023.v1

References

1. M. Smith and S. Kar-Narayan, "Piezoelectric polymers: theory, challenges and opportunities," *International Materials Reviews*, vol. 67, no. 1, pp. 65–88, Jan. 2022, doi: 10.1080/09506608.2021.1915935.
2. K. S. Ramadan, D. Sameoto, and S. Evoy, "A review of piezoelectric polymers as functional materials for electromechanical transducers," *Smart Mater Struct*, vol. 23, no. 3, p. 033001, Mar. 2014, doi: 10.1088/0964-1726/23/3/033001.
3. X. Gao *et al.*, "Piezoelectric Actuators and Motors: Materials, Designs, and Applications," *Adv Mater Technol*, vol. 5, no. 1, Jan. 2020, doi: 10.1002/admt.201900716.
4. S. Mishra, L. Unnikrishnan, S. K. Nayak, and S. Mohanty, "Advances in Piezoelectric Polymer Composites for Energy Harvesting Applications: A Systematic Review," *Macromol Mater Eng*, vol. 304, no. 1, Jan. 2019, doi: 10.1002/mame.201800463.
5. P. Ueberschlag, "PVDF piezoelectric polymer," *Sensor Review*, vol. 21, no. 2, pp. 118–126, Jun. 2001, doi: 10.1108/02602280110388315.
6. S. Mohammadpourfazeli, S. Arash, A. Ansari, S. Yang, K. Mallick, and R. Bagherzadeh, "Future prospects and recent developments of polyvinylidene fluoride (PVDF) piezoelectric polymer; fabrication methods, structure, and electro-mechanical properties," *RSC Adv*, vol. 13, no. 1, pp. 370–387, 2023, doi: 10.1039/D2RA06774A.
7. G. Kalimuldina *et al.*, "A Review of Piezoelectric PVDF Film by Electrospinning and Its Applications," *Sensors*, vol. 20, no. 18, p. 5214, Sep. 2020, doi: 10.3390/s20185214.
8. Y. Pei and X. C. Zeng, "Elastic properties of poly(vinyldene fluoride) (PVDF) crystals: A density functional theory study," *J Appl Phys*, vol. 109, no. 9, May 2011, doi: 10.1063/1.3574653.
9. X. Hu, M. You, N. Yi, X. Zhang, and Y. Xiang, "Enhanced Piezoelectric Coefficient of PVDF-TrFE Films via In Situ Polarization," *Front Energy Res*, vol. 9, Aug. 2021, doi: 10.3389/fenrg.2021.621540.
10. S. Barrau *et al.*, "Nanoscale Investigations of α- and γ-Crystal Phases in PVDF-Based Nanocomposites," *ACS Appl Mater Interfaces*, vol. 10, no. 15, pp. 13092–13099, Apr. 2018, doi: 10.1021/acsami.8b02172.
11. A. Gebrekrstos, T. S. Muzata, and S. S. Ray, "Nanoparticle-Enhanced β-Phase Formation in Electroactive PVDF Composites: A Review of Systems for Applications in Energy Harvesting, EMI Shielding, and Membrane Technology," *ACS Appl Nano Mater*, vol. 5, no. 6, pp. 7632–7651, Jun. 2022, doi: 10.1021/acsanm.2c02183.
12. L. Zhang *et al.*, "Recent Progress on Structure Manipulation of Poly(vinylidene fluoride)-Based Ferroelectric Polymers for Enhanced Piezoelectricity and Applications," *Adv Funct Mater*, vol. 33, no. 38, Sep. 2023, doi: 10.1002/adfm.202301302.
13. S. K. Si *et al.*, "*In situ* -grown organo-lead bromide perovskite-induced electroactive γ-phase in aerogel PVDF films: an efficient photoactive material for piezoelectric energy harvesting and photodetector applications," *Nanoscale*, vol. 12, no. 13, pp. 7214–7230, 2020, doi: 10.1039/D0NR00090F.
14. A. C. Lopes, C. Caparros, J. L. Gómez Ribelles, I. C. Neves, and S. Lanceros-Mendez, "Electrical and thermal behavior of γ-phase poly(vinylidene fluoride)/NaY zeolite composites," *Microporous and Mesoporous Materials*, vol. 161, pp. 98–105, Oct. 2012, doi: 10.1016/j.micromeso.2012.05.019.
15. M. Li *et al.*, "Revisiting the δ-phase of poly(vinylidene fluoride) for solution-processed ferroelectric thin films," *Nat Mater*, vol. 12, no. 5, pp. 433–438, May 2013, doi: 10.1038/nmat3577.
16. J. Curie and P. Curie, "Développement par compression de l'électricité polaire dans les cristaux hémièdres à faces inclinées," *Bulletin de la Société minéralogique de France*, vol. 3, no. 4, pp. 90–93, 1880, doi: 10.3406/bulmi.1880.1564.
17. H. Kawai, "The Piezoelectricity of Poly (vinylidene Fluoride)," *Jpn J Appl Phys*, vol. 8, no. 7, p. 975, Jul. 1969, doi: 10.1143/JJAP.8.975.
18. "M. TAMURA, Y. T, O. T, and Y. T, 'ELECTROACOUSTIC TRANSDUCERS WITH PIEZOELECTRIC HIGH POLYMER FILMS.,' ELECTROACOUSTIC TRANSDUCERS WITH PIEZOELECTRIC HIGH POLYMER FILMS., 1975".
19. ZhongYang Cheng, Tian-Bing Xu, Qiming Zhang, R. Meyer, D. Van Tol, and J. Hughes, "Design, fabrication, and performance of a flextensional transducer based on electrostrictive polyvinylidene

fluoride-trifluoroethylene copolymer," *IEEE Trans Ultrason Ferroelectr Freq Control*, vol. 49, no. 9, pp. 1312–1320, Sep. 2002, doi: 10.1109/TUFFC.2002.1041548.

20. T.-B. Xu, Z.-Y. Cheng, and Q. M. Zhang, "High-performance micromachined unimorph actuators based on electrostrictive poly(vinylidene fluoride–trifluoroethylene) copolymer," *Appl Phys Lett*, vol. 80, no. 6, pp. 1082–1084, Feb. 2002, doi: 10.1063/1.1448661.
21. Z.-Y. Cheng, V. Bharti, T.-B. Xu, H. Xu, T. Mai, and Q. M. Zhang, "Electrostrictive poly(vinylidene fluoride-trifluoroethylene) copolymers," *Sens Actuators A Phys*, vol. 90, no. 1–2, pp. 138–147, May 2001, doi: 10.1016/S0924-4247(01)00496-4.
22. Q. M. Zhang, V. Bharti, and X. Zhao, "Giant Electrostriction and Relaxor Ferroelectric Behavior in Electron-Irradiated Poly(vinylidene fluoride-trifluoroethylene) Copolymer," *Science (1979)*, vol. 280, no. 5372, pp. 2101–2104, Jun. 1998, doi: 10.1126/science.280.5372.2101.
23. T.-B. Xu and J. Su, "Development, characterization, and theoretical evaluation of electroactive polymer-based micropump diaphragm," *Sens Actuators A Phys*, vol. 121, no. 1, pp. 267–274, May 2005, doi: 10.1016/j.sna.2005.01.020.
24. J. Su, T.-B. Xu, S. Zhang, T. R. Shrout, and Q. Zhang, "An electroactive polymer-ceramic hybrid actuation system for enhanced electromechanical performance," *Appl Phys Lett*, vol. 85, no. 6, pp. 1045–1047, Aug. 2004, doi: 10.1063/1.1779341.
25. T.-B. Xu and J. Su, "Theoretical modeling of electroactive polymer-ceramic hybrid actuation systems," *J Appl Phys*, vol. 97, no. 3, Feb. 2005, doi: 10.1063/1.1844616.
26. J. S. O. Z. Harrison, "Piezoelectric Polymers," 2001. [Online]. Available: http://www.sti.nasa.gov
27. G. Zhu, Z. Zeng, L. Zhang, and X. Yan, "Piezoelectricity in β-phase PVDF crystals: A molecular simulation study," *Comput Mater Sci*, vol. 44, no. 2, pp. 224–229, Dec. 2008, doi: 10.1016/j.commatsci.2008.03.016.
28. A. Lund, C. Gustafsson, H. Bertilsson, and R. W. Rychwalski, "Enhancement of β phase crystals formation with the use of nanofillers in PVDF films and fibres," *Compos Sci Technol*, vol. 71, no. 2, pp. 222–229, Jan. 2011, doi: 10.1016/j.compscitech.2010.11.014.
29. Z. He, F. Rault, M. Lewandowski, E. Mohsenzadeh, and F. Salaün, "Electrospun PVDF Nanofibers for Piezoelectric Applications: A Review of the Influence of Electrospinning Parameters on the β Phase and Crystallinity Enhancement," *Polymers (Basel)*, vol. 13, no. 2, p. 174, Jan. 2021, doi: 10.3390/polym13020174.
30. P. Sajkiewicz, A. Wasiak, and Z. Gocłowski, "Phase transitions during stretching of poly(vinylidene fluoride)," *Eur Polym J*, vol. 35, no. 3, pp. 423–429, Mar. 1999, doi: 10.1016/S0014-3057(98)00136-0.
31. S. J. Kang *et al.*, "Spin cast ferroelectric beta poly(vinylidene fluoride) thin films via rapid thermal annealing," *Appl Phys Lett*, vol. 92, no. 1, Jan. 2008, doi: 10.1063/1.2830701.
32. Z. Jin, D. Lei, Y. Wang, L. Wu, and N. Hu, "Influences of poling temperature and elongation ratio on PVDF-HFP piezoelectric films," *Nanotechnol Rev*, vol. 10, no. 1, pp. 1009–1017, Aug. 2021, doi: 10.1515/ntrev-2021-0070.
33. C. Boyer, B. Ameduri, B. Boutevin, W. R. Dolbier, R. Winter, and G. Gard, "Radical Terpolymerization of 1,1,2-Trifluoro-2-pentafluorosulfanylethylene and Pentafluorosulfanylethylene in the Presence of Vinylidene Fluoride and Hexafluoropropylene by Iodine Transfer Polymerization," *Macromolecules*, vol. 41, no. 4, pp. 1254–1263, Feb. 2008, doi: 10.1021/ma071907l.
34. D. Mao, B. E., and M. A., "Ferroelectric Properties and Polarization Switching Kinetic of Poly (vinylidene fluoride-trifluoroethylene) Copolymer," in *Ferroelectrics - Physical Effects*, InTech, 2011. doi: 10.5772/17147.
35. Y. W. Kim, J. K. Choi, J. T. Park, and J. H. Kim, "Proton conducting poly(vinylidene fluoride-co-chlorotrifluoroethylene) graft copolymer electrolyte membranes," *J Memb Sci*, vol. 313, no. 1–2, pp. 315–322, Apr. 2008, doi: 10.1016/j.memsci.2008.01.015.
36. B. Ameduri, "From Vinylidene Fluoride (VDF) to the Applications of VDF-Containing Polymers and Copolymers: Recent Developments and Future Trends," *Chem Rev*, vol. 109, no. 12, pp. 6632–6686, Dec. 2009, doi: 10.1021/cr800187m.
37. N. Ahbab and T.-B. Xu, "Multifunctional Polyvinylidene Fluoride (PVDF)-Based Polymer, Copolymer, and Compo-Sites for Aerospace Applications: A Comprehensive Technical Review," in *ASME 2024 Aerospace Structures, Structural Dynamics, and Materials Conference*, American Society of Mechanical Engineers, Apr. 2024. doi: 10.1115/SSDM2024-121357.

 doi:10.20944/preprints202501.0023.v1

38. J. G. Drobny, "Fluoropolymers in automotive applications," *Polym Adv Technol*, vol. 18, no. 2, pp. 117–121, Feb. 2007, doi: 10.1002/pat.807.
39. C. M. Costa *et al.*, "Smart and Multifunctional Materials Based on Electroactive Poly(vinylidene fluoride): Recent Advances and Opportunities in Sensors, Actuators, Energy, Environmental, and Biomedical Applications," *Chem Rev*, vol. 123, no. 19, pp. 11392–11487, Oct. 2023, doi: 10.1021/acs.chemrev.3c00196.
40. C.-W. Tang, B. Li, L. Sun, B. Lively, and W.-H. Zhong, "The effects of nanofillers, stretching and recrystallization on microstructure, phase transformation and dielectric properties in PVDF nanocomposites," *Eur Polym J*, vol. 48, no. 6, pp. 1062–1072, Jun. 2012, doi: 10.1016/j.eurpolymj.2012.04.002.
41. Z. Chen, Y. Shen, N. Xi, and X. Tan, "Integrated sensing for ionic polymer–metal composite actuators using PVDF thin films," *Smart Mater Struct*, vol. 16, no. 2, pp. S262–S271, Apr. 2007, doi: 10.1088/0964-1726/16/2/S10.
42. Md. Ataur Rahman and G.-S. Chung, "Synthesis of PVDF-graphene nanocomposites and their properties," *J Alloys Compd*, vol. 581, pp. 724–730, Dec. 2013, doi: 10.1016/j.jallcom.2013.07.118.
43. E. Kabir, M. Khatun, L. Nasrin, M. J. Raihan, and M. Rahman, "Pure β -phase formation in polyvinylidene fluoride (PVDF)-carbon nanotube composites," *J Phys D Appl Phys*, vol. 50, no. 16, p. 163002, Apr. 2017, doi: 10.1088/1361-6463/aa5f85.
44. D. A. van den Ende, H. J. van de Wiel, W. A. Groen, and S. van der Zwaag, "Direct strain energy harvesting in automobile tires using piezoelectric PZT–polymer composites," *Smart Mater Struct*, vol. 21, no. 1, p. 015011, Jan. 2012, doi: 10.1088/0964-1726/21/1/015011.
45. X.-H. Yin, J.-W. Jian, C. Yang, T. Lei, and T. Cheng, "Piezoelectric Performance of PVDF Composites for Transportation Engineering: A Multi-Scale Simulation Study," in *Volume 3: Advanced Materials: Design, Processing, Characterization, and Applications*, American Society of Mechanical Engineers, Nov. 2020. doi: 10.1115/IMECE2020-24549.
46. D. Vatansever, R. L. Hadimani, T. Shah, and E. Siores, "An investigation of energy harvesting from renewable sources with PVDF and PZT," *Smart Mater Struct*, vol. 20, no. 5, p. 055019, May 2011, doi: 10.1088/0964-1726/20/5/055019.
47. W. Xia and Z. Zhang, "PVDF-based dielectric polymers and their applications in electronic materials," *IET Nanodielectrics*, vol. 1, no. 1, pp. 17–31, Apr. 2018, doi: 10.1049/iet-nde.2018.0001.
48. S. Lanceros-Méndez, J. F. Mano, A. M. Costa, and V. H. Schmidt, "FTIR AND DSC STUDIES OF MECHANICALLY DEFORMED β-PVDF FILMS," *Journal of Macromolecular Science, Part B*, vol. 40, no. 3–4, pp. 517–527, May 2001, doi: 10.1081/MB-100106174.
49. D. Chapron *et al.*, "In-situ Raman monitoring of the poly(vinylidene fluoride) crystalline structure during a melt-spinning process," *Journal of Raman Spectroscopy*, vol. 52, no. 5, pp. 1073–1079, May 2021, doi: 10.1002/jrs.6081.
50. L. Wu *et al.*, "Recent advances in the preparation of PVDF-based piezoelectric materials," *Nanotechnol Rev*, vol. 11, no. 1, pp. 1386–1407, Mar. 2022, doi: 10.1515/ntrev-2022-0082.
51. S. Lan, J. Feng, Y. Xiong, S. Tian, S. Liu, and L. Kong, "Performance and Mechanism of Piezo-Catalytic Degradation of 4-Chlorophenol: Finding of Effective Piezo-Dechlorination," *Environ Sci Technol*, vol. 51, no. 11, pp. 6560–6569, Jun. 2017, doi: 10.1021/acs.est.6b06426.
52. B.-X. Cheng *et al.*, "A review of microphase separation of polyurethane: Characterization and applications," *Polym Test*, vol. 107, p. 107489, Mar. 2022, doi: 10.1016/j.polymertesting.2022.107489.
53. M. Mrlík *et al.*, "Comparative Study of PVDF Sheets and Their Sensitivity to Mechanical Vibrations: The Role of Dimensions, Molecular Weight, Stretching and Poling," *Nanomaterials*, vol. 11, no. 7, p. 1637, Jun. 2021, doi: 10.3390/nano11071637.
54. C. Ravikumar and V. Markevicius, "Development of Ultrasound Piezoelectric Transducer-Based Measurement of the Piezoelectric Coefficient and Comparison with Existing Methods," *Processes*, vol. 11, no. 8, p. 2432, Aug. 2023, doi: 10.3390/pr11082432.
55. https://piezopvdf.com/, "PolyK piezoelectric PVDF."
56. Tian-Bing Xu and Ji Su, "Design, modeling, fabrication, and performances of bridge-type high-performance electroactive polymer micromachined actuators," *Journal of Microelectromechanical Systems*, vol. 14, no. 3, pp. 539–547, Jun. 2005, doi: 10.1109/JMEMS.2005.844744.

 doi:10.20944/preprints202501.0023.v1

57. Shravan Chunduri, "PVDF Rules Backsheet Market ," Nov. 2020. Accessed: Dec. 27, 2024. [Online]. Available: http://taiyangnews.info/technology/a-review-backsheet-components/
58. [58]; Jiaxin Jason Ge Gregory S . O ' Brien, "Photovoltaic Module Using PVDF Based Flexible Glazing Film," May 01, 2018
59. I. PVPS Task 13, "Task 13 Performance, Operation and Reliability of Photovoltaic Systems," Apr. 2021. [Online]. Available: www.iea-pvps.org
60. F. Qi, L. Xu, Y. He, H. Yan, and H. Liu, "PVDF-Based Flexible Piezoelectric Tactile Sensors: Review," *Crystal Research and Technology*, vol. 58, no. 10, Oct. 2023, doi: 10.1002/crat.202300119.
61. K. K. Sappati and S. Bhadra, "Piezoelectric Polymer and Paper Substrates: A Review," *Sensors*, vol. 18, no. 11, p. 3605, Oct. 2018, doi: 10.3390/s18113605.
62. R. Dallaev, T. Pisarenko, D. Sobola, F. Orudzhev, S. Ramazanov, and T. Trčka, "Brief Review of PVDF Properties and Applications Potential," *Polymers (Basel)*, vol. 14, no. 22, p. 4793, Nov. 2022, doi: 10.3390/polym14224793.
63. V. O. C. Concha *et al.*, "Properties, characterization and biomedical applications of polyvinylidene fluoride (PVDF): a review," *J Mater Sci*, vol. 59, no. 31, pp. 14185–14204, Aug. 2024, doi: 10.1007/s10853-024-10046-3.
64. G. Kang and Y. Cao, "Application and modification of poly(vinylidene fluoride) (PVDF) membranes – A review," *J Memb Sci*, vol. 463, pp. 145–165, Aug. 2014, doi: 10.1016/j.memsci.2014.03.055.
65. M. Golda-Cepa, K. Engvall, M. Hakkarainen, and A. Kotarba, "Recent progress on parylene C polymer for biomedical applications: A review," *Prog Org Coat*, vol. 140, p. 105493, Mar. 2020, doi: 10.1016/j.porgcoat.2019.105493.
66. D. M. Nivedhitha and S. Jeyanthi, "Polyvinylidene fluoride, an advanced futuristic smart polymer material: A comprehensive review," *Polym Adv Technol*, vol. 34, no. 2, pp. 474–505, Feb. 2023, doi: 10.1002/pat.5914.
67. S. S. Chauhan, U. M. Bhatt, P. Gautam, S. Thote, M. M. Joglekar, and S. K. Manhas, "Fabrication and modeling of β-phase PVDF-TrFE based flexible piezoelectric energy harvester," *Sens Actuators A Phys*, vol. 304, p. 111879, Apr. 2020, doi: 10.1016/j.sna.2020.111879.
68. V. Sencadas, R. Gregorio, and S. Lanceros-Méndez, "α to β Phase Transformation and Microestructural Changes of PVDF Films Induced by Uniaxial Stretch," *Journal of Macromolecular Science, Part B*, vol. 48, no. 3, pp. 514–525, May 2009, doi: 10.1080/00222340902837527.
69. A. J. Lovinger, "Poly(Vinylidene Fluoride)," in *Developments in Crystalline Polymers—1*, Dordrecht: Springer Netherlands, 1982, pp. 195–273. doi: 10.1007/978-94-009-7343-5_5.
70. S. Barrau *et al.*, "Nanoscale Investigations of α- And γ-Crystal Phases in PVDF-Based Nanocomposites," *ACS Appl Mater Interfaces*, vol. 10, no. 15, pp. 13092–13099, Apr. 2018, doi: 10.1021/acsami.8b02172.
71. S. S. Chauhan, U. M. Bhatt, P. Gautam, S. Thote, M. M. Joglekar, and S. K. Manhas, "Fabrication and modeling of β-phase PVDF-TrFE based flexible piezoelectric energy harvester," Apr. 01, 2020, *Elsevier B.V.* doi: 10.1016/j.sna.2020.111879.
72. H. H. Singh, S. Singh, and N. Khare, "Enhanced β-phase in PVDF polymer nanocomposite and its application for nanogenerator," *Polym Adv Technol*, vol. 29, no. 1, pp. 143–150, Jan. 2018, doi: 10.1002/pat.4096.
73. E. Kar, N. Bose, S. Das, N. Mukherjee, and S. Mukherjee, "Enhancement of electroactive β phase crystallization and dielectric constant of PVDF by incorporating GeO2 and SiO2 nanoparticles," *Physical Chemistry Chemical Physics*, vol. 17, no. 35, pp. 22784–22798, Jul. 2015, doi: 10.1039/c5cp03975d.
74. V. Sencadas, R. Gregorio, and S. Lanceros-Méndez, "α to β phase transformation and microestructural changes of PVDF films induced by uniaxial stretch," *Journal of Macromolecular Science, Part B: Physics*, vol. 48, no. 3, pp. 514–525, May 2009, doi: 10.1080/00222340902837527.
75. S. K. Si *et al.*, "In situ -grown organo-lead bromide perovskite-induced electroactive γ-phase in aerogel PVDF films: An efficient photoactive material for piezoelectric energy harvesting and photodetector applications," *Nanoscale*, vol. 12, no. 13, pp. 7214–7230, Apr. 2020, doi: 10.1039/d0nr00090f.
76. A. C. Lopes, C. Caparros, J. L. Gómez Ribelles, I. C. Neves, and S. Lanceros-Mendez, "Electrical and thermal behavior of γ-phase poly(vinylidene fluoride)/NaY zeolite composites," *Microporous and Mesoporous Materials*, vol. 161, pp. 98–105, Oct. 2012, doi: 10.1016/j.micromeso.2012.05.019.

77. M. Li *et al.*, "Revisiting the δ-phase of poly(vinylidene fluoride) for solution-processed ferroelectric thin films," *Nature Materials 2013 12:5*, vol. 12, no. 5, pp. 433–438, Mar. 2013, doi: 10.1038/nmat3577.
78. A. J. Lovinger, "POLY(VINYLIDENE FLUORIDE)," 1982.
79. M. Fortunato *et al.*, "Phase Inversion in PVDF Films with Enhanced Piezoresponse Through Spin-Coating and Quenching," *Polymers (Basel)*, vol. 11, no. 7, p. 1096, Jun. 2019, doi: 10.3390/polym11071096.
80. L. Zhang *et al.*, "Recent Progress on Structure Manipulation of Poly(vinylidene fluoride)-Based Ferroelectric Polymers for Enhanced Piezoelectricity and Applications," *Adv Funct Mater*, vol. 33, no. 38, Sep. 2023, doi: 10.1002/adfm.202301302.
81. P. Saxena and P. Shukla, "A comprehensive review on fundamental properties and applications of poly(vinylidene fluoride) (PVDF)," *Adv Compos Hybrid Mater*, vol. 4, no. 1, pp. 8–26, Mar. 2021, doi: 10.1007/s42114-021-00217-0.
82. H. S. TZOU, H.-J. LEE, and S. M. ARNOLD, "Smart Materials, Precision Sensors/Actuators, Smart Structures, and Structronic Systems," *Mechanics of Advanced Materials and Structures*, vol. 11, no. 4–5, pp. 367–393, Jul. 2004, doi: 10.1080/15376490490451552.
83. N. Awanis Hashim, Y. Liu, and K. Li, "Stability of PVDF hollow fibre membranes in sodium hydroxide aqueous solution," *Chem Eng Sci*, vol. 66, no. 8, pp. 1565–1575, Apr. 2011, doi: 10.1016/j.ces.2010.12.019.
84. D. Hou, J. Wang, D. Qu, Z. Luan, and X. Ren, "Fabrication and characterization of hydrophobic PVDF hollow fiber membranes for desalination through direct contact membrane distillation," *Sep Purif Technol*, vol. 69, no. 1, pp. 78–86, Sep. 2009, doi: 10.1016/j.seppur.2009.06.026.
85. H. Shinohara, "Fluorination of polyhydrofluoroethylenes. II. Formation of perfluoroalkyl carboxylic acids on the surface region of poly(vinylidene fluoride) film by oxyfluorination, fluorination, and hydrolysis," *Journal of Polymer Science: Polymer Chemistry Edition*, vol. 17, no. 5, pp. 1543–1556, May 1979, doi: 10.1002/pol.1979.170170526.
86. M. Wegener, W. Küunstler, and R. Gerhard-Multhaupt, "Poling Behavior and Optical Absorption of Partially Dehydrofluorinated and Uniaxially Stretched Polyvinylidene Fluoride," *Ferroelectrics*, vol. 336, no. 1, pp. 3–8, Jul. 2006, doi: 10.1080/00150190600694761.
87. V. Puspitasari, A. Granville, P. Le-Clech, and V. Chen, "Cleaning and ageing effect of sodium hypochlorite on polyvinylidene fluoride (PVDF) membrane," *Sep Purif Technol*, vol. 72, no. 3, pp. 301–308, May 2010, doi: 10.1016/j.seppur.2010.03.001.
88. I. Jung, Y.-H. Shin, S. Kim, J. Choi, and C.-Y. Kang, "Flexible piezoelectric polymer-based energy harvesting system for roadway applications," *Appl Energy*, vol. 197, pp. 222–229, Jul. 2017, doi: 10.1016/j.apenergy.2017.04.020.
89. M. de Jong, W. Chen, H. Geerlings, M. Asta, and K. A. Persson, "A database to enable discovery and design of piezoelectric materials," *Sci Data*, vol. 2, no. 1, p. 150053, Sep. 2015, doi: 10.1038/sdata.2015.53.
90. T. Furukawa, "Ferroelectric properties of vinylidene fluoride copolymers," *Phase Transitions*, vol. 18, no. 3–4, pp. 143–211, Aug. 1989, doi: 10.1080/01411598908206863.
91. R. C. G. Naber, K. Asadi, P. W. M. Blom, D. M. de Leeuw, and B. de Boer, "Organic Nonvolatile Memory Devices Based on Ferroelectricity," *Advanced Materials*, vol. 22, no. 9, pp. 933–945, Mar. 2010, doi: 10.1002/adma.200900759.
92. A. M. G. M. E. Lines, *Principles and Applications of Ferroelectrics and Related Materials*. 2001. Accessed: Sep. 25, 2024. [Online]. Available: https://books.google.com/books/about/Principles_and_Applications_of_Ferroelec.html?id=p6ruJH8C84kC
93. C. Wan and C. R. Bowen, "Multiscale-structuring of polyvinylidene fluoride for energy harvesting: the impact of molecular-, micro- and macro-structure," *J Mater Chem A Mater*, vol. 5, no. 7, pp. 3091–3128, 2017, doi: 10.1039/C6TA09590A.
94. V. Cauda, S. Stassi, K. Bejtka, and G. Canavese, "Nanoconfinement: an Effective Way to Enhance PVDF Piezoelectric Properties," *ACS Appl Mater Interfaces*, vol. 5, no. 13, pp. 6430–6437, Jul. 2013, doi: 10.1021/am4016878.

95. A. Kausar, C.-Y. Chang, M. A. Z. Raja, A. Zameer, and M. Shoaib, "Novel design of recurrent neural network for the dynamical of nonlinear piezoelectric cantilever mass–beam model," *The European Physical Journal Plus*, vol. 139, no. 1, p. 16, Jan. 2024, doi: 10.1140/epjp/s13360-023-04708-5.
96. A. Kausar, C.-Y. Chang, M. A. Z. Raja, and M. Shoaib, "A novel design of layered recurrent neural networks for fractional order Caputo–Fabrizio stiff electric circuit models," *Modern Physics Letters B*, May 2024, doi: 10.1142/S0217984924503937.
97. A. Zameer, S. Naz, and M. A. Z. Raja, "Parallel differential evolution paradigm for multilayer electromechanical device optimization," *Modern Physics Letters B*, Mar. 2024, doi: 10.1142/S0217984924503123.
98. J. Song, G. Zhao, B. Li, and J. Wang, "Design optimization of PVDF-based piezoelectric energy harvesters," *Heliyon*, vol. 3, no. 9, p. e00377, Sep. 2017, doi: 10.1016/j.heliyon.2017.e00377.
99. S. Naz, M. A. Z. Raja, A. Kausar, A. Zameer, A. Mehmood, and M. Shoaib, "Dynamics of nonlinear cantilever piezoelectric–mechanical system: An intelligent computational approach," *Math Comput Simul*, vol. 196, pp. 88–113, Jun. 2022, doi: 10.1016/j.matcom.2022.01.011.
100. A. Zameer, S. Naz, M. A. Z. Raja, J. Hafeez, and N. Ali, "Neuro-Evolutionary Framework for Design Optimization of Two-Phase Transducer with Genetic Algorithms," *Micromachines (Basel)*, vol. 14, no. 9, p. 1677, Aug. 2023, doi: 10.3390/mi14091677.
101. S. Naz, A. Usman, A. Zameer, K. Muhammad, and M. A. Z. Raja, "Efficient multivariate optimization of an ultrasonic transducer with genetic parallel algorithms," *Waves in Random and Complex Media*, pp. 1–25, Sep. 2023, doi: 10.1080/17455030.2023.2256889.
102. Z. Abdullah, S. Naz, M. A. Z. Raja, and A. Zameer, "Design of wideband tonpilz transducers for underwater SONAR applications with finite element model," *Applied Acoustics*, vol. 183, p. 108293, Dec. 2021, doi: 10.1016/j.apacoust.2021.108293.
103. S. Naz, M. A. Z. Raja, A. Mehmood, A. Zameer, and M. Shoaib, "Neuro-intelligent networks for Bouc–Wen hysteresis model for piezostage actuator," *The European Physical Journal Plus*, vol. 136, no. 4, p. 396, Apr. 2021, doi: 10.1140/epjp/s13360-021-01382-3.
104. S. Naz, M. A. Z. Raja, A. Mehmood, and A. Z. Jaafery, "Intelligent Predictive Solution Dynamics for Dahl Hysteresis Model of Piezoelectric Actuator," *Micromachines (Basel)*, vol. 13, no. 12, p. 2205, Dec. 2022, doi: 10.3390/mi13122205.
105. K. K. Sappati and S. Bhadra, "Piezoelectric polymer and paper substrates: A review," Nov. 01, 2018, *MDPI AG*. doi: 10.3390/s18113605.
106. S. Naz and T.-B. Xu, "A Comprehensive Review of Piezoelectric Ultrasonic Motors: Classifications, Characterization, Fabrication, Applications, and Future Challenges," *Micromachines (Basel)*, vol. 15, no. 9, p. 1170, Sep. 2024, doi: 10.3390/mi15091170.
107. M. G. Cain, Ed., *Characterisation of Ferroelectric Bulk Materials and Thin Films*, vol. 2. in Springer Series in Measurement Science and Technology, vol. 2. Dordrecht: Springer Netherlands, 2014. doi: 10.1007/978-1-4020-9311-1.
108. R. Khajavi and M. Abbasipour, "Piezoelectric PVDF Polymeric Films and Fibers: Polymorphisms, Measurements, and Applications," in *Industrial Applications for Intelligent Polymers and Coatings*, Cham: Springer International Publishing, 2016, pp. 313–336. doi: 10.1007/978-3-319-26893-4_15.
109. C. Chang, V. H. Tran, J. Wang, Y.-K. Fuh, and L. Lin, "Direct-Write Piezoelectric Polymeric Nanogenerator with High Energy Conversion Efficiency," *Nano Lett*, vol. 10, no. 2, pp. 726–731, Feb. 2010, doi: 10.1021/nl9040719.
110. Y. Ting, Suprapto, C. Chiu, and H. Gunawan, "Characteristic analysis of biaxially stretched PVDF thin films," *J Appl Polym Sci*, vol. 135, no. 36, Sep. 2018, doi: 10.1002/app.46677.
111. R. Sagar, S. S. Gaur, and M. S. Gaur, "Effect of BaZrO3 nanoparticles on pyroelectric properties of polyvinylidene fluoride (PVDF)," *J Therm Anal Calorim*, vol. 128, no. 2, pp. 1235–1239, May 2017, doi: 10.1007/s10973-016-5964-y.
112. M. C. Sekhar, E. Veena, N. S. Kumar, K. C. B. Naidu, A. Mallikarjuna, and D. B. Basha, "A Review on Piezoelectric Materials and Their Applications," *Crystal Research and Technology*, vol. 58, no. 2, Feb. 2023, doi: 10.1002/crat.202200130.

113. T.-B. Xu, H. Kang, and Emilie J . Siochi, "PYROELECTRIC SANDWICH THERMAL ENERGY HARVESTERS," US 10 , 147 , 863 B2, Dec. 04, 2018 Accessed: Dec. 28, 2024. [Online]. Available: https://patentimages.storage.googleapis.com/e6/52/2e/7ab65ef12c4790/US10147863.pdf
114. k. Tashiro, "Crystal structure and phase transition of PVDF and related copolymers," *PLASTICS ENGINEERING-NEW YORK*, vol. 28, pp. 63--63, 1995.
115. Z. Yin, B. Tian, Q. Zhu, and C. Duan, "Characterization and Application of PVDF and Its Copolymer Films Prepared by Spin-Coating and Langmuir–Blodgett Method," *Polymers (Basel)*, vol. 11, no. 12, p. 2033, Dec. 2019, doi: 10.3390/polym11122033.
116. L. Ruan, X. Yao, Y. Chang, L. Zhou, G. Qin, and X. Zhang, "Properties and applications of the β phase poly(vinylidene fluoride)," Feb. 26, 2018, *MDPI AG*. doi: 10.3390/polym10030228.
117. L. He *et al.*, "Enhancement of β-crystalline phase of poly(vinylidene fluoride) in the presence of hyperbranched copolymer wrapped multiwalled carbon nanotubes," *J Colloid Interface Sci*, vol. 363, no. 1, pp. 122–128, Nov. 2011, doi: 10.1016/j.jcis.2011.07.042.
118. A. Navid, C. S. Lynch, and L. Pilon, "Purified and porous poly(vinylidene fluoride-trifluoroethylene) thin films for pyroelectric infrared sensing and energy harvesting," *Smart Mater Struct*, vol. 19, no. 5, p. 055006, May 2010, doi: 10.1088/0964-1726/19/5/055006.
119. P. Thomas, K. T. Varughese, K. Dwarakanath, and K. B. R. Varma, "Dielectric properties of Poly(vinylidene fluoride)/CaCu3Ti4O12 composites," *Compos Sci Technol*, vol. 70, no. 3, pp. 539–545, Mar. 2010, doi: 10.1016/j.compscitech.2009.12.014.
120. M. Nasir, H. Matsumoto, M. Minagawa, A. Tanioka, T. Danno, and H. Horibe, "Preparation of PVDF/PMMA Blend Nanofibers by Electrospray Deposition: Effects of Blending Ratio and Humidity," *Polym J*, vol. 41, no. 5, pp. 402–406, 2009, doi: 10.1295/polymj.PJ2008171.
121. S. Yu, W. Zheng, W. Yu, Y. Zhang, Q. Jiang, and Z. Zhao, "Formation Mechanism of β-Phase in PVDF/CNT Composite Prepared by the Sonication Method," *Macromolecules*, vol. 42, no. 22, pp. 8870–8874, Nov. 2009, doi: 10.1021/ma901765j.
122. J. Nunes-Pereira, P. Martins, V. F. Cardoso, C. M. Costa, and S. Lanceros-Méndez, "A green solvent strategy for the development of piezoelectric poly(vinylidene fluoride–trifluoroethylene) films for sensors and actuators applications," *Mater Des*, vol. 104, pp. 183–189, Aug. 2016, doi: 10.1016/j.matdes.2016.05.023.
123. Q. Xia, X. J. Zhao, S. J. Chen, W. Z. Ma, J. Zhang, and X. L. Wang, "Effect of solution-blended poly(styrene-co-acrylonitrile) copolymer on crystallization of poly(vinylidene fluoride)," *Express Polym Lett*, vol. 4, no. 5, pp. 284–291, 2010, doi: 10.3144/expresspolymlett.2010.36.
124. M. Remeika and Y. Qi, "Scalable solution coating of the absorber for perovskite solar cells," *Journal of Energy Chemistry*, vol. 27, no. 4, pp. 1101–1110, Jul. 2018, doi: 10.1016/j.jechem.2017.10.005.
125. B. Fotovvati, N. Namdari, and A. Dehghanghadikolaei, "On Coating Techniques for Surface Protection: A Review," *Journal of Manufacturing and Materials Processing*, vol. 3, no. 1, p. 28, Mar. 2019, doi: 10.3390/jmmp3010028.
126. N. An, H. Liu, Y. Ding, M. Zhang, and Y. Tang, "Preparation and electroactive properties of a PVDF/nano-TiO2 composite film," *Appl Surf Sci*, vol. 257, no. 9, pp. 3831–3835, Feb. 2011, doi: 10.1016/j.apsusc.2010.12.076.
127. F. Mokhtari *et al.*, "Recent progress in electrospun polyvinylidene fluoride (PVDF)-based nanofibers for sustainable energy and environmental applications," *Prog Mater Sci*, vol. 148, p. 101376, Feb. 2025, doi: 10.1016/j.pmatsci.2024.101376.
128. Y.-C. Hu, W.-L. Hsu, Y.-T. Wang, C.-T. Ho, and P.-Z. Chang, "Enhance the Pyroelectricity of Polyvinylidene Fluoride by Graphene-Oxide Doping," *Sensors*, vol. 14, no. 4, pp. 6877–6890, Apr. 2014, doi: 10.3390/s140406877.
129. M. D. Tyona, "A theoritical study on spin coating technique," *Advances in materials Research*, vol. 2, no. 4, pp. 195–208, Dec. 2013, doi: 10.12989/amr.2013.2.4.195.
130. A. Salimi and A. A. Yousefi, "Analysis Method: FTIR studies of β-phase crystal formation in stretched PVDF films," *Polym Test*, vol. 22, no. 6, pp. 699–704, Sep. 2003, doi: 10.1016/S0142-9418(03)00003-5.

131. G. H. Jaffari, M. S. I. Khan, F. Mumtaz, Y. Wang, and N. A. Khan, "Manipulation of crystallization and dielectric relaxation dynamics via hot pressing and copolymerization of PVDF with Hexafluoropropylene," *Journal of Polymer Research*, vol. 30, no. 1, p. 11, Jan. 2023, doi: 10.1007/s10965-022-03395-7.
132. S. Dhumrash, A. Gautam, A. Kumar, N. Jaglan, and P. Uniyal, "Appreciable amelioration in the dielectric and energy storage behavior of the electrospun fluoropolymer PVDF-HFP thick films: Effect of hot-pressing," *J Energy Storage*, vol. 103, p. 114337, Dec. 2024, doi: 10.1016/j.est.2024.114337.
133. A. Hartono, M. Djamal, S. Satira, H. Bahar, Ramli, and E. Sanjaya, "Effect of roll hot press temperature on crystallite size of PVDF film," 2014, pp. 217–220. doi: 10.1063/1.4868785.
134. J. Yuan, H. Chen, and H. Luo, "Enhancing the energy storage performance of PVDF films through optimized hot-pressing temperatures," *Ionics (Kiel)*, vol. 30, no. 9, pp. 5341–5351, Sep. 2024, doi: 10.1007/s11581-024-05692-1.
135. Z.-X. Huang, M.-M. Wang, Y.-H. Feng, and J.-P. Qu, "β-Phase Formation of Polyvinylidene Fluoride *via* Hot Pressing under Cyclic Pulsating Pressure," *Macromolecules*, vol. 53, no. 19, pp. 8494–8501, Oct. 2020, doi: 10.1021/acs.macromol.0c01609.
136. C. M. Wu and M. H. Chou, "Polymorphism, piezoelectricity and sound absorption of electrospun PVDF membranes with and without carbon nanotubes," *Compos Sci Technol*, vol. 127, pp. 127–133, Apr. 2016, doi: 10.1016/j.compscitech.2016.03.001.
137. G. Kalimuldina *et al.*, "A Review of Piezoelectric PVDF Film by Electrospinning and Its Applications," *Sensors*, vol. 20, no. 18, p. 5214, Sep. 2020, doi: 10.3390/s20185214.
138. T. Lei, P. Zhu, X. Cai, L. Yang, and F. Yang, "Electrospinning of PVDF nanofibrous membranes with controllable crystalline phases," *Applied Physics A*, vol. 120, no. 1, pp. 5–10, Jul. 2015, doi: 10.1007/s00339-015-9197-x.
139. B. Zaarour, L. Zhu, and X. Jin, "Controlling the surface structure, mechanical properties, crystallinity, and piezoelectric properties of electrospun PVDF nanofibers by maneuvering molecular weight," *Soft Mater*, vol. 17, no. 2, pp. 181–189, Apr. 2019, doi: 10.1080/1539445X.2019.1582542.
140. S. Cailleaux, N. M. Sanchez-Ballester, Y. A. Gueche, B. Bataille, and I. Soulairol, "Fused Deposition Modeling (FDM), the new asset for the production of tailored medicines," *Journal of Controlled Release*, vol. 330, pp. 821–841, Feb. 2021, doi: 10.1016/j.jconrel.2020.10.056.
141. A. Gheibi, R. Bagherzadeh, A. A. Merati, and M. Latifi, "Electrical power generation from piezoelectric electrospun nanofibers membranes: electrospinning parameters optimization and effect of membranes thickness on output electrical voltage," *Journal of Polymer Research*, vol. 21, no. 11, p. 571, Nov. 2014, doi: 10.1007/s10965-014-0571-8.
142. M. S. Sebastian *et al.*, "Understanding nucleation of the electroactive β-phase of poly(vinylidene fluoride) by nanostructures," *RSC Adv.*, vol. 6, no. 114, pp. 113007–113015, 2016, doi: 10.1039/C6RA24356H.
143. C. Lee and J. A. Tarbutton, "Electric poling-assisted additive manufacturing process for PVDF polymer-based piezoelectric device applications," *Smart Mater Struct*, vol. 23, no. 9, p. 095044, Sep. 2014, doi: 10.1088/0964-1726/23/9/095044.
144. B. Li, F. Zhang, S. Guan, J. Zheng, and C. Xu, "Wearable piezoelectric device assembled by one-step continuous electrospinning," *J Mater Chem C Mater*, vol. 4, no. 29, pp. 6988–6995, 2016, doi: 10.1039/C6TC01696K.
145. J.-E. Lee, Y.-E. Shin, G.-H. Lee, J. Kim, H. Ko, and H. G. Chae, "Polyvinylidene fluoride (PVDF)/cellulose nanocrystal (CNC) nanocomposite fiber and triboelectric textile sensors," *Compos B Eng*, vol. 223, p. 109098, Oct. 2021, doi: 10.1016/j.compositesb.2021.109098.
146. M. El Achaby, F. Z. Arrakhiz, S. Vaudreuil, E. M. Essassi, and A. Qaiss, "Piezoelectric β-polymorph formation and properties enhancement in graphene oxide – PVDF nanocomposite films," *Appl Surf Sci*, vol. 258, no. 19, pp. 7668–7677, Jul. 2012, doi: 10.1016/j.apsusc.2012.04.118.
147. G. Kalimuldina *et al.*, "A review of piezoelectric pvdf film by electrospinning and its applications," Sep. 02, 2020, *MDPI AG*. doi: 10.3390/s20185214.
148. C. Lee and J. A. Tarbutton, "Polyvinylidene fluoride (PVDF) direct printing for sensors and actuators," *The International Journal of Advanced Manufacturing Technology*, vol. 104, no. 5–8, pp. 3155–3162, Oct. 2019, doi: 10.1007/s00170-019-04275-z.

 doi:10.20944/preprints202501.0023.v1

149. L. Li, M. Zhang, M. Rong, and W. Ruan, "Studies on the transformation process of PVDF from α to β phase by stretching," *RSC Adv.*, vol. 4, no. 8, pp. 3938–3943, 2014, doi: 10.1039/C3RA45134H.
150. H. Guo *et al.*, "In-situ synchrotron SAXS and WAXS investigations on deformation and α–β transformation of uniaxial stretched poly(vinylidene fluoride)," *CrystEngComm*, vol. 15, no. 8, p. 1597, 2013, doi: 10.1039/c2ce26578h.
151. Y. Huang *et al.*, "Can Relaxor Ferroelectric Behavior Be Realized for Poly(vinylidene fluoride- *co* -chlorotrifluoroethylene) [P(VDF–CTFE)] Random Copolymers by Inclusion of CTFE Units in PVDF Crystals?," *Macromolecules*, vol. 51, no. 14, pp. 5460–5472, Jul. 2018, doi: 10.1021/acs.macromol.8b01155.
152. A. Gaur, C. Kumar, S. Tiwari, and P. Maiti, "Efficient Energy Harvesting Using Processed Poly(vinylidene fluoride) Nanogenerator," *ACS Appl Energy Mater*, vol. 1, no. 7, pp. 3019–3024, Jul. 2018, doi: 10.1021/acsaem.8b00483.
153. R. Guo *et al.*, "Ultrahigh energy density of poly(vinylidene fluoride) from synergistically improved dielectric constant and withstand voltage by tuning the crystallization behavior," *J Mater Chem A Mater*, vol. 9, no. 48, pp. 27660–27671, 2021, doi: 10.1039/D1TA07680A.
154. B. Mohammadi, A. A. Yousefi, and S. M. Bellah, "Effect of tensile strain rate and elongation on crystalline structure and piezoelectric properties of PVDF thin films," *Polym Test*, vol. 26, no. 1, pp. 42–50, Feb. 2007, doi: 10.1016/j.polymertesting.2006.08.003.
155. M. P. Silva, C. M. Costa, V. Sencadas, A. J. Paleo, and S. Lanceros-Méndez, "Degradation of the dielectric and piezoelectric response of β-poly(vinylidene fluoride) after temperature annealing," *Journal of Polymer Research*, vol. 18, no. 6, pp. 1451–1457, Nov. 2011, doi: 10.1007/s10965-010-9550-x.
156. M. Baniasadi *et al.*, "Correlation of annealing temperature, morphology, and electro-mechanical properties of electrospun piezoelectric nanofibers," *Polymer (Guildf)*, vol. 127, pp. 192–202, Oct. 2017, doi: 10.1016/j.polymer.2017.08.053.
157. Furukawa, Nakajima, and Takahashi, "Factors governing ferroelectric switching characteristics of thin VDF/TrFE copolymer films," *IEEE Transactions on Dielectrics and Electrical Insulation*, vol. 13, no. 5, pp. 1120–1131, Oct. 2006, doi: 10.1109/TDEI.2006.247840.
158. S. Men, Z. Gao, R. Wen, J. Tang, and J. M. Zhang, "Effects of annealing time on physical and mechanical properties of <scp>PVDF</scp> microporous membranes by a melt extrusion-stretching process," *Polym Adv Technol*, vol. 32, no. 6, pp. 2397–2408, Jun. 2021, doi: 10.1002/pat.5268.
159. N. Spampinato, J. Maiz, G. Portale, M. Maglione, G. Hadziioannou, and E. Pavlopoulou, "Enhancing the ferroelectric performance of P(VDF-co-TrFE) through modulation of crystallinity and polymorphism," *Polymer (Guildf)*, vol. 149, pp. 66–72, Aug. 2018, doi: 10.1016/j.polymer.2018.06.072.
160. M. Satthiyaraju and T. Ramesh, "Effect of annealing treatment on PVDF nanofibers for mechanical energy harvesting applications," *Mater Res Express*, vol. 6, no. 10, p. 105366, Sep. 2019, doi: 10.1088/2053-1591/ab4037.
161. M. Baniasadi *et al.*, "Correlation of annealing temperature, morphology, and electro-mechanical properties of electrospun piezoelectric nanofibers," *Polymer (Guildf)*, vol. 127, pp. 192–202, Oct. 2017, doi: 10.1016/j.polymer.2017.08.053.
162. H. Li and S. Lim, "Self-poled and transparent polyvinylidene fluoride- *co* -hexafluoropropylene-based piezoelectric devices for printable and flexible electronics," *Nanoscale*, vol. 15, no. 9, pp. 4581–4590, 2023, doi: 10.1039/D2NR05986J.
163. M. Pusty and P. M. Shirage, "Insights and perspectives on graphene-PVDF based nanocomposite materials for harvesting mechanical energy," *J Alloys Compd*, vol. 904, p. 164060, May 2022, doi: 10.1016/j.jallcom.2022.164060.
164. E. Nilsson, A. Lund, C. Jonasson, C. Johansson, and B. Hagström, "Poling and characterization of piezoelectric polymer fibers for use in textile sensors," *Sens Actuators A Phys*, vol. 201, pp. 477–486, Oct. 2013, doi: 10.1016/j.sna.2013.08.011.
165. M. You, X. Hu, and Y. Xiang, "In-situ polarization enhanced piezoelectric property of polyvinylidene fluoride-trifluoroethylene films," *IOP Conf Ser Earth Environ Sci*, vol. 770, no. 1, p. 012071, May 2021, doi: 10.1088/1755-1315/770/1/012071.

166. S. K. Mahadeva, J. Berring, K. Walus, and B. Stoeber, "Effect of poling time and grid voltage on phase transition and piezoelectricity of poly(vinyledene fluoride) thin films using corona poling," *J Phys D Appl Phys*, vol. 46, no. 28, p. 285305, Jul. 2013, doi: 10.1088/0022-3727/46/28/285305.
167. L. Gasperini, G. Selleri, D. Pegoraro, and D. Fabiani, "Corona poling for polarization of nanofibrous mats: advantages and open issues," in *2022 IEEE Conference on Electrical Insulation and Dielectric Phenomena (CEIDP)*, IEEE, Oct. 2022, pp. 479–482. doi: 10.1109/CEIDP55452.2022.9985267.
168. G. Rui *et al.*, "Giant spontaneous polarization for enhanced ferroelectric properties of biaxially oriented poly(vinylidene fluoride) by mobile oriented amorphous fractions," *J Mater Chem C Mater*, vol. 9, no. 3, pp. 894–907, 2021, doi: 10.1039/D0TC04632A.
169. T. Ju, X. Chen, D. Langhe, M. Ponting, E. Baer, and L. Zhu, "Enhancing breakdown strength and lifetime of multilayer dielectric films by using high temperature polycarbonate skin layers," *Energy Storage Mater*, vol. 45, pp. 494–503, Mar. 2022, doi: 10.1016/j.ensm.2021.12.009.
170. J. Gomes, J. Serrado Nunes, V. Sencadas, and S. Lanceros-Mendez, "Influence of the β-phase content and degree of crystallinity on the piezo- and ferroelectric properties of poly(vinylidene fluoride)," *Smart Mater Struct*, vol. 19, no. 6, p. 065010, Jun. 2010, doi: 10.1088/0964-1726/19/6/065010.
171. Y. Z. Liu *et al.*, "A high-performance soft actuator based on a poly(vinylidene fluoride) piezoelectric bimorph," *Smart Mater Struct*, vol. 28, no. 5, p. 055011, May 2019, doi: 10.1088/1361-665X/ab0844.
172. Y. Li *et al.*, "Investigation on in-situ sprayed, annealed and corona poled PVDF-TrFE coatings for guided wave-based structural health monitoring: From crystallization to piezoelectricity," *Mater Des*, vol. 199, p. 109415, Feb. 2021, doi: 10.1016/j.matdes.2020.109415.
173. C. Boyer and B. Améduri, "Iodine transfer copolymerization of vinylidene fluoride and α-trifluoromethacrylic acid in emulsion process without any surfactants," *J Polym Sci A Polym Chem*, vol. 47, no. 18, pp. 4710–4722, Sep. 2009, doi: 10.1002/pola.23525.
174. S. Abbrent, J. Plestil, D. Hlavata, J. Lindgren, J. Tegenfeldt, and Å. Wendsjö, "Crystallinity and morphology of PVdF–HFP-based gel electrolytes," *Polymer (Guildf)*, vol. 42, no. 4, pp. 1407–1416, Feb. 2001, doi: 10.1016/S0032-3861(00)00517-6.
175. L. Shi, R. Wang, and Y. Cao, "Effect of the rheology of poly(vinylidene fluoride-co-hexafluropropylene) (PVDF–HFP) dope solutions on the formation of microporous hollow fibers used as membrane contactors," *J Memb Sci*, vol. 344, no. 1–2, pp. 112–122, Nov. 2009, doi: 10.1016/j.memsci.2009.07.041.
176. Y. Huan, Y. Liu, Y. Yang, and Y. Wu, "Influence of extrusion, stretching and poling on the structural and piezoelectric properties of poly (vinylidene fluoride-hexafluoropropylene) copolymer films," *J Appl Polym Sci*, vol. 104, no. 2, pp. 858–862, Apr. 2007, doi: 10.1002/app.25603.
177. P. Martins, A. C. Lopes, and S. Lanceros-Mendez, "Electroactive phases of poly(vinylidene fluoride): Determination, processing and applications," *Prog Polym Sci*, vol. 39, no. 4, pp. 683–706, Apr. 2014, doi: 10.1016/j.progpolymsci.2013.07.006.
178. Z. Li, Y. Wang, and Z.-Y. Cheng, "Electromechanical properties of poly(vinylidene-fluoride-chlorotrifluoroethylene) copolymer," *Appl Phys Lett*, vol. 88, no. 6, Feb. 2006, doi: 10.1063/1.2170425.
179. F. Guan, Z. Yuan, E. W. Shu, and L. Zhu, "Fast discharge speed in poly(vinylidene fluoride) graft copolymer dielectric films achieved by confined ferroelectricity," *Appl Phys Lett*, vol. 94, no. 5, Feb. 2009, doi: 10.1063/1.3079332.
180. A. Mooti *et al.*, "Magnetic and high-dielectric-constant nanoparticle polymer tri-composites for sensor applications," *J Mater Sci*, vol. 55, no. 34, pp. 16234–16246, Dec. 2020, doi: 10.1007/s10853-020-05165-6.
181. T. Chowdhury, N. D'Souza, and D. Berman, "Electrospun Fe3O4-PVDF Nanofiber Composite Mats for Cryogenic Magnetic Sensor Applications," *Textiles*, vol. 1, no. 2, pp. 227–238, Jul. 2021, doi: 10.3390/textiles1020011.
182. P. Kaspar *et al.*, "Case Study of Polyvinylidene Fluoride Doping by Carbon Nanotubes," *Materials*, vol. 14, no. 6, p. 1428, Mar. 2021, doi: 10.3390/ma14061428.
183. H. Abdolmaleki and S. Agarwala, "PVDF-BaTiO3 Nanocomposite Inkjet Inks with Enhanced β-Phase Crystallinity for Printed Electronics," *Polymers (Basel)*, vol. 12, no. 10, p. 2430, Oct. 2020, doi: 10.3390/polym12102430.

 doi:10.20944/preprints202501.0023.v1

184. M. V. Arularasu, M. Harb, R. Vignesh, T. V. Rajendran, and R. Sundaram, "PVDF/ZnO hybrid nanocomposite applied as a resistive humidity sensor," *Surfaces and Interfaces*, vol. 21, p. 100780, Dec. 2020, doi: 10.1016/j.surfin.2020.100780.
185. S. Naz, A. Zameer, M. A. Z. Raja, and K. Muhammad, "Weighted differential evolution heuristics for improved multilayer piezoelectric transducer design," *Appl Soft Comput*, vol. 113, p. 107835, Dec. 2021, doi: 10.1016/j.asoc.2021.107835.
186. J. R. Mishra, S. K. Samal, S. Mohanty, and S. K. Nayak, "Polyvinylidene fluoride (PVDF)/Ag@TiO2 nanocomposite membrane with enhanced fouling resistance and antibacterial performance," *Mater Chem Phys*, vol. 268, p. 124723, Aug. 2021, doi: 10.1016/j.matchemphys.2021.124723.
187. A. C. Lopes, C. M. Costa, C. J. Tavares, I. C. Neves, and S. Lanceros-Mendez, "Nucleation of the Electroactive γ Phase and Enhancement of the Optical Transparency in Low Filler Content Poly(vinylidene)/Clay Nanocomposites," *The Journal of Physical Chemistry C*, vol. 115, no. 37, pp. 18076–18082, Sep. 2011, doi: 10.1021/jp204513w.
188. S. Guo, X. Duan, M. Xie, K. C. Aw, and Q. Xue, "Composites, Fabrication and Application of Polyvinylidene Fluoride for Flexible Electromechanical Devices: A Review," *Micromachines (Basel)*, vol. 11, no. 12, p. 1076, Dec. 2020, doi: 10.3390/mi11121076.
189. M. Sachin, R. Haridass, and B. T. S. Ramanujam, "Polyvinylidene fluoride (PVDF)-poly(methyl methacrylate) (PMMA)-expanded graphite (ExGr) conducting polymer blends: Analysis of electrical and thermal behavior," *Mater Today Proc*, vol. 28, pp. 103–107, 2020, doi: 10.1016/j.matpr.2020.01.353.
190. K. Pontes, T. Indrusiak, and B. G. Soares, "Poly(vinylidene fluoride-co-hexafluorpropylene)/polyaniline conductive blends: Effect of the mixing procedure on the electrical properties and electromagnetic interference shielding effectiveness," *J Appl Polym Sci*, vol. 138, no. 3, Jan. 2021, doi: 10.1002/app.49705.
191. Y. Zhang, X. Gu, C. Ni, F. Li, Y. Li, and J. You, "Improvement of PLLA Ductility by Blending with PVDF: Localization of Compatibilizers at Interface and Its Glycidyl Methacrylate Content Dependency," *Polymers (Basel)*, vol. 12, no. 8, p. 1846, Aug. 2020, doi: 10.3390/polym12081846.
192. D. Nudman, O. Weizman, E. Amir, and A. Ophir, "Development and characterization of expanded graphite filled-PET/PVDF blend: thermodynamic and kinetic effects," *Polym Adv Technol*, vol. 28, no. 5, pp. 590–599, May 2017, doi: 10.1002/pat.3855.
193. L. H. Gaabour and K. A. Hamam, "The Change of Structural, Optical and Thermal Properties of a PVDF/PVC Blend Containing ZnO Nanoparticles," *Silicon*, vol. 10, no. 4, pp. 1403–1409, Jul. 2018, doi: 10.1007/s12633-017-9617-y.
194. Y. Mallaiah, V. R. Jeedi, R. Swarnalatha, A. Raju, S. Narender Reddy, and A. Sadananda Chary, "Impact of polymer blending on ionic conduction mechanism and dielectric properties of sodium based PEO-PVdF solid polymer electrolyte systems," *Journal of Physics and Chemistry of Solids*, vol. 155, p. 110096, Aug. 2021, doi: 10.1016/j.jpcs.2021.110096.
195. A. M. Ismail and R. A. Nasr, "Structural characterization of <scp>PVDF</scp> / <scp>PVA</scp> polymer blend film doped with different concentration of <scp>NiO NPs</scp> for photocatalytic degradation of malachite green dye under visible light," *J Appl Polym Sci*, vol. 139, no. 13, Apr. 2022, doi: 10.1002/app.51847.
196. Ch. V. S. Reddy, Q.-Y. Zhu, L.-Q. Mai, and W. Chen, "Electrochemical studies on PVC/PVdF blend-based polymer electrolytes," *Journal of Solid State Electrochemistry*, vol. 11, no. 4, pp. 543–548, Apr. 2007, doi: 10.1007/s10008-006-0192-1.
197. R. Li *et al.*, "Polyamide 11/Poly(vinylidene fluoride) Blends as Novel Flexible Materials for Capacitors," *Macromol Rapid Commun*, vol. 29, no. 17, pp. 1449–1454, Sep. 2008, doi: 10.1002/marc.200800253.
198. S. S. Humbe, G. M. Joshi, R. R. Deshmukh, E. Dhanumalayan, and S. Kaleemulla, "Improved under damped oscillator properties of polymer blends for electronic applications," *Mech Time Depend Mater*, vol. 26, no. 1, pp. 119–132, Mar. 2022, doi: 10.1007/s11043-020-09478-6.
199. B. Lu, K. Lamnawar, A. Maazouz, and H. Zhang, "Revealing the dynamic heterogeneity of PMMA/PVDF blends: from microscopic dynamics to macroscopic properties," *Soft Matter*, vol. 12, no. 13, pp. 3252–3264, 2016, doi: 10.1039/C5SM02659H.

200. A. Tanaka, H. Sawada, and Y. Kojima, "Application of Poly(vinylidene fluoride) and Poly(methyl methacrylate) Blends to Optical Material," *Polym J*, vol. 22, no. 6, pp. 463–467, Jun. 1990, doi: 10.1295/polymj.22.463.
201. T. Ma *et al.*, "Preparation of PVDF based blend microporous membranes for lithium ion batteries by thermally induced phase separation: I. Effect of PMMA on the membrane formation process and the properties," *J Memb Sci*, vol. 444, pp. 213–222, Oct. 2013, doi: 10.1016/j.memsci.2013.05.028.
202. O. Guselnikova, J. Svanda, P. Postnikov, Y. Kalachyova, V. Svorcik, and O. Lyutakov, "Fast and Reproducible Wettability Switching on Functionalized PVDF/PMMA Surface Controlled by External Electric Field," *Adv Mater Interfaces*, vol. 4, no. 5, Mar. 2017, doi: 10.1002/admi.201600886.
203. P. Sengupta, A. Ghosh, N. Bose, S. Mukherjee, A. Roy Chowdhury, and P. Datta, "A comparative assessment of poly(vinylidene fluoride)/conducting polymer electrospun nanofiber membranes for biomedical applications," *J Appl Polym Sci*, vol. 137, no. 37, Oct. 2020, doi: 10.1002/app.49115.
204. J. N. Martins, M. Kersch, V. Altstädt, and R. V. B. Oliveira, "Electrical conductivity of poly(vinylidene fluoride)/polyaniline blends under oscillatory and steady shear conditions," *Polym Test*, vol. 32, no. 5, pp. 862–869, Aug. 2013, doi: 10.1016/j.polymertesting.2013.04.001.
205. X. Zhang, Y. Shen, Z. Shen, J. Jiang, L. Chen, and C.-W. Nan, "Achieving High Energy Density in PVDF-Based Polymer Blends: Suppression of Early Polarization Saturation and Enhancement of Breakdown Strength," *ACS Appl Mater Interfaces*, vol. 8, no. 40, pp. 27236–27242, Oct. 2016, doi: 10.1021/acsami.6b10016.
206. Surender Kumar Sharma, *Handbook of Materials Characterization*. Cham: Springer International Publishing, 2018. doi: 10.1007/978-3-319-92955-2.
207. V. R. Jeedi, E. L. Narsaiah, M. Yalla, R. Swarnalatha, S. N. Reddy, and A. Sadananda Chary, "Structural and electrical studies of PMMA and PVdF based blend polymer electrolyte," *SN Appl Sci*, vol. 2, no. 12, p. 2093, Dec. 2020, doi: 10.1007/s42452-020-03868-8.
208. F. Deeba, A. K. Gupta, V. Kulshrestha, M. Bafna, and A. Jain, "Investigations on dielectric properties of PVDF/PMMA blends," *Mater Today Proc*, vol. 66, pp. 3547–3552, 2022, doi: 10.1016/j.matpr.2022.06.417.
209. S. Mishra, R. Sahoo, L. Unnikrishnan, A. Ramadoss, S. Mohanty, and S. K. Nayak, "Enhanced structural and dielectric behaviour of PVDF-PLA binary polymeric blend system," *Mater Today Commun*, vol. 26, p. 101958, Mar. 2021, doi: 10.1016/j.mtcomm.2020.101958.
210. W. Dong, H. Hakukawa, N. Yamahira, Y. Li, and S. Horiuchi, "Mechanism of Reactive Compatibilization of PLLA/PVDF Blends Investigated by Scanning Transmission Electron Microscopy with Energy-Dispersive X-ray Spectrometry and Electron Energy Loss Spectroscopy," *ACS Appl Polym Mater*, vol. 1, no. 4, pp. 815–824, Apr. 2019, doi: 10.1021/acsapm.9b00061.
211. D. M. Correia *et al.*, "Influence of Cation and Anion Type on the Formation of the Electroactive β-Phase and Thermal and Dynamic Mechanical Properties of Poly(vinylidene fluoride)/Ionic Liquids Blends," *The Journal of Physical Chemistry C*, vol. 123, no. 45, pp. 27917–27926, Nov. 2019, doi: 10.1021/acs.jpcc.9b07986.
212. K. Ni *et al.*, "Preparation and properties of polyvinylidene fluoride dielectric nanocomposites for energy storage applications through synergistic addition of ionic liquid-modified graphene oxide nanosheets and functionalized barium titanate hybrid fillers," *Polym Compos*, vol. 45, no. 8, pp. 7102–7115, Jun. 2024, doi: 10.1002/pc.28252.
213. N. A. Shepelin *et al.*, "New developments in composites, copolymer technologies and processing techniques for flexible fluoropolymer piezoelectric generators for efficient energy harvesting," Apr. 01, 2019, *Royal Society of Chemistry*. doi: 10.1039/c8ee03006e.
214. Y. Huang *et al.*, "Enhanced piezoelectricity from highly polarizable oriented amorphous fractions in biaxially oriented poly(vinylidene fluoride) with pure β crystals," *Nat Commun*, vol. 12, no. 1, p. 675, Jan. 2021, doi: 10.1038/s41467-020-20662-7.
215. J.-Y. Ren *et al.*, "Enhanced Dielectric and Ferroelectric Properties of Poly(vinylidene fluoride) through Annealing Oriented Crystallites under High Pressure," *Macromolecules*, vol. 55, no. 6, pp. 2014–2027, Mar. 2022, doi: 10.1021/acs.macromol.1c02436.
216. K. Pilla, M. Neergat, and K. N. Jonnalagadda, "Strain and temperature induced phase changes in <scp>spin-coated PVDF</scp> thin films," *Journal of Polymer Science*, vol. 61, no. 11, pp. 1082–1096, Jun. 2023, doi: 10.1002/pol.20220688.

217. F. N. Mullaveettil, R. Dauksevicius, and Y. Wakjira, "Strength and elastic properties of 3D printed PVDF-based parts for lightweight biomedical applications," *J Mech Behav Biomed Mater*, vol. 120, p. 104603, Aug. 2021, doi: 10.1016/j.jmbbm.2021.104603.
218. Z.-Y. Cheng, T.-B. Xu, V. Bharti, S. Wang, and Q. M. Zhang, "Transverse strain responses in the electrostrictive poly(vinylidene fluoride–trifluorethylene) copolymer," *Appl Phys Lett*, vol. 74, no. 13, pp. 1901–1903, Mar. 1999, doi: 10.1063/1.123707.
219. H. Wang, Q. Z. Qiming Zhang, and L. E. C. Leslie Eric Cross, "A High Sensitivity, Phase Sensitive d 33 Meter for Complex Piezoelectric Constant Measurement," *Jpn J Appl Phys*, vol. 32, no. 9A, p. L1281, Sep. 1993, doi: 10.1143/JJAP.32.L1281.
220. R. Fu *et al.*, "A Tough and Self-Powered Hydrogel for Artificial Skin," *Chemistry of Materials*, vol. 31, no. 23, pp. 9850–9860, Dec. 2019, doi: 10.1021/acs.chemmater.9b04041.
221. S. Aghayari, "PVDF composite nanofibers applications," *Heliyon*, vol. 8, no. 11, p. e11620, Nov. 2022, doi: 10.1016/j.heliyon.2022.e11620.
222. F. Xiujuan, H. Longbiao, K. Triantafillos, N. Feng, Z. Bo, and Y. Ping, "Comparison between methods for the measurement of the D33 constant of piezoelectric materials COMPARISON BETWEEN METHODS FOR THE MEASURE-MENT OF THE D 33 CONSTANT OF PIEZOELECTRIC MATE-RIALS," 2018. [Online]. Available: https://www.researchgate.net/publication/326274919
223. X. Chen *et al.*, "Giant Electrostriction Enabled by Defect-Induced Critical Phenomena in Relaxor Ferroelectric Polymers," *Macromolecules*, vol. 56, no. 2, pp. 690–696, Jan. 2023, doi: 10.1021/acs.macromol.2c01952.
224. X. Chen *et al.*, "Relaxor ferroelectric polymer exhibits ultrahigh electromechanical coupling at low electric field," *Science (1979)*, vol. 375, no. 6587, pp. 1418–1422, Mar. 2022, doi: 10.1126/science.abn0936.
225. Z.-Y. Cheng *et al.*, "Transverse strain responses in electrostrictive poly(vinylidene fluoride-trifluoroethylene) films and development of a dilatometer for the measurement," *J Appl Phys*, vol. 86, no. 4, pp. 2208–2214, Aug. 1999, doi: 10.1063/1.371032.
226. T.-Bing. Xu, "Development of Electromechanical Devices based on Newly Developed Electroactive P(VDF-TrFE) polymer," The Pennsylvania State University, 2002. Accessed: Dec. 29, 2024. [Online]. Available: https://www.proquest.com/openview/9c2f4d8b211aa359eb7c083a1a7f95ad/1?pq-origsite=gscholar&cbl=18750&diss=y
227. T.-B. Xu, Z.-Y. Cheng, T. Mai, Yu Lu, and Q. M. Zhang, "Electromechanical coupling factor of electrostrictive P(VDF-TrFE) copolymer," in *2000 IEEE Ultrasonics Symposium. Proceedings. An International Symposium (Cat. No.00CH37121)*, IEEE, pp. 997–1000. doi: 10.1109/ULTSYM.2000.921492.
228. Y. Lin *et al.*, "Studies on the electrostatic effects of stretched PVDF films and nanofibers," *Nanoscale Res Lett*, vol. 16, no. 1, p. 79, May 2021, doi: 10.1186/s11671-021-03536-9.